AD-A038 160 NAVAL SEA SYSTEMS COMMAND WASHINGTON D C F/G 17/1
A METHODOLOGY FOR THE COMPARISON OF MODELS FOR SONAR SYSTEM APP--ETC(U)
DEC 76 R B LAUER, B SUSSMAN
UNCLASSIFIED NAVSEA-06H1/036-EVA/MOST- NL

1 OF 2
AD
A038160

SEA 06H1/036-EVA/MOST-10

12

9 December 1976

NAVSEA Panel On Sonar System Models

— POSSM —

IN SUPPORT OF

MOBILE SONAR TECHNOLOGY DEVELOPMENT

A METHODOLOGY FOR THE COMPARISON OF MODELS FOR SONAR SYSTEM APPLICATIONS

VOLUME I

NAVAL SEA SYSTEMS COMMAND
DEPARTMENT OF THE NAVY
WASHINGTON, D.C. 20362

SEA 06H1/036-EVA/MOST-10

12

9 December 1976

NAVSEA Panel On Sonar System Models

— POSSM —

IN SUPPORT OF

MOBILE SONAR TECHNOLOGY DEVELOPMENT

A METHODOLOGY FOR THE COMPARISON OF MODELS FOR SONAR SYSTEM APPLICATIONS

VOLUME I

NAVAL SEA SYSTEMS COMMAND
DEPARTMENT OF THE NAVY
WASHINGTON, D.C. 20362

PREFACE

The NAVSEA Panel on Sonar System Models (POSSM) is a joint effort of the Naval Underwater Systems Center (NUSC), the Naval Undersea Center (NUC), the Naval Research Laboratory (NRL), the Naval Coastal Systems Center (NCSL), and the Naval Ocean Research and Development Activity (NORDA), under the sponsorship of the Sonar Technology Office of the Naval Sea Systems Command (Task Area SF 52-552-701). Each of these organizations is represented in POSSM.

POSSM appreciates the continuing assistance of G. E. Miller of Arthur D. Little, Incorporated, during this project.

The work reported herein was completed before 1 January 1976; therefore, data conversion to metric units has not been made.

Authors:

Richard B. Lauer (NUSC)

Bernard Sussman (NUSC)

Released by:

F. R. DiNapoli (NUSC)
POSSM Chairman

Sponsoring Activity:

C. D. Smith
NAVSEA

A. P. Franceschetti
NAVSEA

POSSM Members

A. DiBonito (NUC)	T. Watson (NCSL)	H. Newman (NUSC)
E. Chaika (NUC)	K. V. Mackenzie (NORDA)	R. Lauer (NUSC)
R. McGirr (NUC)	H. Weinberg (NUSC)	W. Kuperman (NRL)

REPORT DOCUMENTATION PAGE		READ INSTRUCTIONS BEFORE COMPLETING FORM
1. REPORT NUMBER (14) NAV SEA-06H1/036-EVA/MOST-10	2. GOVT ACCESSION NO.	3. RECIPIENT'S CATALOG NUMBER
4. TITLE (and Subtitle) (6) A METHODOLOGY FOR THE COMPARISON OF MODELS FOR SONAR SYSTEM APPLICATIONS, VOLUME I		5. TYPE OF REPORT & PERIOD COVERED 6. PERFORMING ORG. REPORT NUMBER
7. AUTHOR(s) (10) Richard B. Lauer Bernard Sussman (16) F52552 NH		8. CONTRACT OR GRANT NUMBER(s) (17) SF 52-552-701
9. PERFORMING ORGANIZATION NAME AND ADDRESS Naval Underwater Systems Center New London Laboratory New London, Connecticut 06320		10. PROGRAM ELEMENT, PROJECT, TASK AREA & WORK UNIT NUMBERS A-301-81 (12) 149 p.
11. CONTROLLING OFFICE NAME AND ADDRESS Naval Sea Systems Command (SEA 06H1-4) Washington, D. C. 20362		12. REPORT DATE (11) 9 Dec[redacted] 1976 13. NUMBER OF PAGES 147
14. MONITORING AGENCY NAME & ADDRESS(if different from Controlling Office)		15. SECURITY CLASS. (of this report) UNCLASSIFIED 15a. DECLASSIFICATION/DOWNGRADING SCHEDULE

16. DISTRIBUTION STATEMENT (of this Report)

Approved for public release; distribution unlimited.

17. DISTRIBUTION STATEMENT (of the abstract entered in Block 20, if different from Report)

C0059372

18. SUPPLEMENTARY NOTES

19. KEY WORDS (Continue on reverse side if necessary and identify by block number)

Computer Programs	Sonar
Model Evaluation	Sonar Systems
Propagation Loss	Underwater Acoustics

A020672

20. ABSTRACT (Continue on reverse side if necessary and identify by block number)

A methodology is presented for making an optimum choice from several candidate models for a specific application. This is accomplished by providing information on several factors: accuracy, computer running time, computer storage required, ease of implementation, complexity of program execution, and available ancillary outputs. The assessment of accuracy is performed by means of quantitative comparisons with a standard. The method consists of obtaining differences between means of two data sets as a function of the

over

DD FORM 1 JAN 73 1473

391 345

20.
independent variable, followed by assigning numerical weighting factors to statistical measures of the differences. In order to illustrate the application of this method, comparisons are made of six transmission loss models available at the Naval Underwater Systems Center at this writing. The models are compared with one another with respect to the parameters given above, and the predictions are compared with a set of PARKA data for accuracy. In this process, numerical rankings are assigned to the models. However, this is done solely for the purpose of illustrating the method, and is not meant as an endorsement of any model. The methodology is in a state of evolution, and the final version may differ in detail from the one presented in this report.

TABLE OF CONTENTS

LIST OF ILLUSTRATIONS

LIST OF ILLUSTRATIONS (cont'd)

LIST OF TABLES

LIST OF TABLES (cont'd)

LIST OF TABLES (cont'd)

FOREWORD

The Naval Sea Systems Command Panel on Sonar Systems Models was chartered to make recommendations concerning the environmental acoustic (EVA) submodels such as propagation loss, reverberation and ambient noise to be used in NAVSEA sponsored sonar system programs.

The potential tactical sonar applications cover such a wide spectrum that it is unlikely that any single EVA submodel would be the optimum choice in all instances. It was thus decided that a matrix of information addressing those considerations which compose the model selection process be constructed for candidate EVA submodels. The analyst or user could then make the required trade-offs based on the quantitative matrix information and select the submodel best suited to his particular application. The methodology required to perform the objective model assessment is described in this volume and exemplified by extensive application to propagation loss submodels for a Pacific Ocean scenario. Future plans include the assessment of propagation loss submodels, in use at Navy laboratories and Fleet Numerical Weather Central, for other scenarios. The first of these, using Mediterranean Sea data, has been initiated. Later volumes will apply the assessment methodology to ambient noise and reverberation submodels.

Copies of this report can be obtained through Defense Documentation Center, Defense Supply Agency, Cameron Station, Alexandria, VA 22314.

C D Smith

C. D. SMITH, DIRECTOR
SONAR TECHNOLOGY OFFICE
06H1/036

A METHODOLOGY FOR THE COMPARISON OF MODELS FOR SONAR SYSTEM APPLICATIONS -- VOLUME I

INTRODUCTION

In the area of underwater acoustics the development of models in recent years has progressed rapidly. Although to the casual observer it would appear that many models exist which are purported to describe the same physical phenomenon and that, therefore, duplication of effort has been common, this is not the case. Rather, the variety of models arises from the choice of physical theories available to describe the phenomenon, assumptions involving a description of environmental conditions affecting the phenomenon, and method selected for a computer implementation of the process. The models which shall be examined here are those which generate transmission loss as a function of range. The various transmission loss models may be grouped in generic types as given in table 1. Within each type several models may exist which differ in their description and assumptions concerning environmental input parameters. Faced with a large number of models designed to describe the same phenomenon and with the requirement to select a single model for incorporation into an operational system or for the purposes of system design or research, one must find bases from which an optimum selection can be made. Factors which must be taken into account include the environments, modes of operation, and tactical situations over which the model must achieve a given level of performance. The decision

Table 1. Generic Types of Transmission Loss Models

A.	Semi-Empirical/Semi-Analytical Models
B.	Ray Theory Models with Corrections
C.	Normal Mode Theory Models
D.	Total Field Models
E.	Models with Range Dependent Inputs
F.	Generalized Ray Models
G.	Time Domain (Waveform Prediction) Models
H.	Exact Solutions

to select a model for inclusion into a given system or to be applied to a specific requirement will depend on a matrix for each candidate model such as that given in table 2. Such a matrix will be formed for transmission loss models available at the New London Laboratory of the Naval Underwater Systems Center (NUSC). Accuracy will be assessed quantitatively through comparisons with "standards" for selected cases. The accuracy required will, of course, depend on the application. The amount of computer time required to run a given sub-model is of concern due to the cost involved. Also, for certain applications such as a sonar trainer, a specific requirement of maximum allowable running time may be necessary. The amount of computer storage required is a critical factor; if the most accurate model requires more core than is available in the computer on which the program is to be run, that particular model would be useless. Ease of implementation is a factor which is reflected in terms of cost and time. Included here are issues such as the compatibility of computers and availability of a programmer intimately familiar with the given model. The complexity of program execution should vary with the application; thus, a program for shipboard use should be simple to operate and decisions concerning choice of inputs and outputs should be minimized or eliminated, if possible. A program intended for a research application should offer great flexibility in choice of inputs and outputs and would, therefore, be necessarily more complex. Often, a program can be made more efficient in terms of running time, core storage, or both, without affecting accuracy by making slight alterations to the program. Factors D, E, and F are largely dependent upon the extent to which and the clarity with which the various programs have been documented. For the specific transmission loss models constituting the study herein reported, available documentation is listed in the references. Finally, available ancillary information might include such data as arrival angle versus range or signal intensity as received by an array.

Table 2. Factors Influencing Model Selection

A.	Assessment of Accuracy
B.	Computer Running Time
C.	Amount of Computer Storage Required
D.	Ease of Implementation
E.	Complexity of Program Execution
F.	Ease of Effecting Slight Alterations to the Program
G.	Available Ancillary Information

The material presented below is intended to serve as an example of a matrix such as that of table 2. The most difficult portion of the matrix to complete is the assessment of accuracy. The usual method of graphically comparing outputs is a qualitative one and the conclusions obtained may be subjective. The approach applied here characterizes the data in terms of a mean and standard deviation, each of which is a function of the independent variable (e.g., range, azimuth or time).

Two or more data sets are then compared by statistical techniques yielding quantitative measures of agreement. Although the examples to be discussed specifically deal with transmission loss versus range, the applicability of the comparison method is not restricted to such data.

For the models constituting this study, running times are given with and without normalization for the number of points generated by each model. The amount of computer storage required is that for the models as they exist at NUSC and run on the Univac 1108 computer.

The comparisons herein reported were performed without interaction with any potential user and without regard to any particular operational system or other application. The comparisons were made for a selected set of cases and utilized a single sound speed profile and bottom type. In six of the cases examined, a model, the Fast Field Program (FFP), constituted the basis of comparison; in the remaining two cases, transmission loss data from the PARKA experiment as analyzed in American Standard one-third octave bands were compared with the outputs of models which assume the source to emit a continuous sinusoidal signal (with the exception of a simulated one-third octave prediction from the superposition of FFP outputs from CW sources within the band).

The examples selected and the comparisons performed have as their purpose the demonstration of a methodology for model selection. The models selected for this study were those readily available at NUSC and are optimized to varying degrees for running time and storage requirements. Only a single environmental scenario was examined and the actual data used in the comparisons might be considered too sparse for this process. Further, when outputs from models assuming CW sources are compared with one-third octave data, the results are open to interpretation. For these reasons, the results of this study do not constitute an endorsement of any model.

ENVIRONMENTAL INPUTS

Sound Speed Profile. The sound speed profile used in all listed models except the FFP is shown in figure 1. Figure 1A shows the complete profile, and figure 1B shows the profile to a depth of 2000 feet in greater detail. Also shown in this figure is a table of the values plotted in the curves. This profile is based on a profile measured during the PARKA exercise conducted in the Pacific Ocean during the period November-December 1969. The measured profile had additional points which were considered extraneous and were eliminated to produce the plotted profile.

The FFP utilized a 5-point approximation to the PARKA profile as given in figure 2. This approximation was made necessary by the manner in which the profile is used in FFP. The FFP model assumes that the medium is stratified as a function of depth and that within the J-th layer the sound speed is given by

$$c_J(z) = c_{J-1}(z_J)\exp\left[\pm(z-z_J)/H_J\right]$$

where J = 1, 2, 3,... and $c(z_1)$ is the sound speed at $z = z_1$ (the surface). The parameter H_J is a scale factor which will have a different magnitude in each layer. A condition related to the numerical procedures used in the FFP is that H_{max}/H_J be an integer, where H_{max} is the largest scale factor in absolute magnitude. These ratios are also related to the amount of computer storage required. Because of these last two factors, it is often impractical to fit a given sound speed profile arbitrarily closely for use in FFP.

An example of the effect of approximating the sound speed profile is to be seen by considering the deep portion of the profile as typically found in the Pacific. The profile usually exhibits a small amount of curvature, whereas its practical FFP version would be almost linear. The effect on the propagation loss of using the almost linear fit is to cause a systematic shift in the ranges at which the convergence zones will occur. Thus, the absolute differences between the FFP as run with a 5 point sound speed profile and other models run with the 29 point profile require careful scrutiny if an interpretation of the difference is required. However, all models compared with the FFP did utilize the 29 point profile; hence, the relative accuracy assessments between models constituting this study are based upon a common description of the sound speed environment.

Bottom Loss. Figure 3 shows bottom loss per bounce as a function of grazing angle, as used in all models except the FFP. The curve is constructed, assuming Rayleigh reflection, from parameters based upon NAVOCEANO data at 100 Hz. The FFP uses inputted bottom parameters directly to compute bottom loss. These bottom parameters are: density ρ_B, sound speed C_B, and attenuation coefficient α_B. The same parameters in the water, namely, ρ_W, C_W, and α_W are also required. The set of values used in all cases was:

$$\rho_B/\rho_W = 2.3$$
$$C_B = 5144 \text{ ft/sec}$$
$$C_W = 5088 \text{ ft/sec}$$
$$\alpha_B = 0.$$

The attenuation coefficient in the water used in the FFP is essentially that given by Thorp. The same bottom characteristics were used in all cases. Since bottom loss is known to be a frequency dependent parameter, the use of a single curve at 50, 500, and 2000 Hz based on data obtained for a frequency of 100 Hz would appear to be questionable. However, the authors were unable to locate bottom loss data at 50 and 400 Hz pertinent to the PARKA transmission loss data used in cases 7 and 8 and, therefore, the available data at 100 Hz were used. The use of these data at 2000 Hz in cases 1-6 is unrealistic but does not have a significant impact on the intent of this study, since the purpose is to demonstrate a methodology for the assessment of the relative accuracies of various models. The methodology certainly does not depend upon the choice of bottom loss parameters. Additionally, the comparison results should be fairly insensitive to the specific choice of bottom loss.

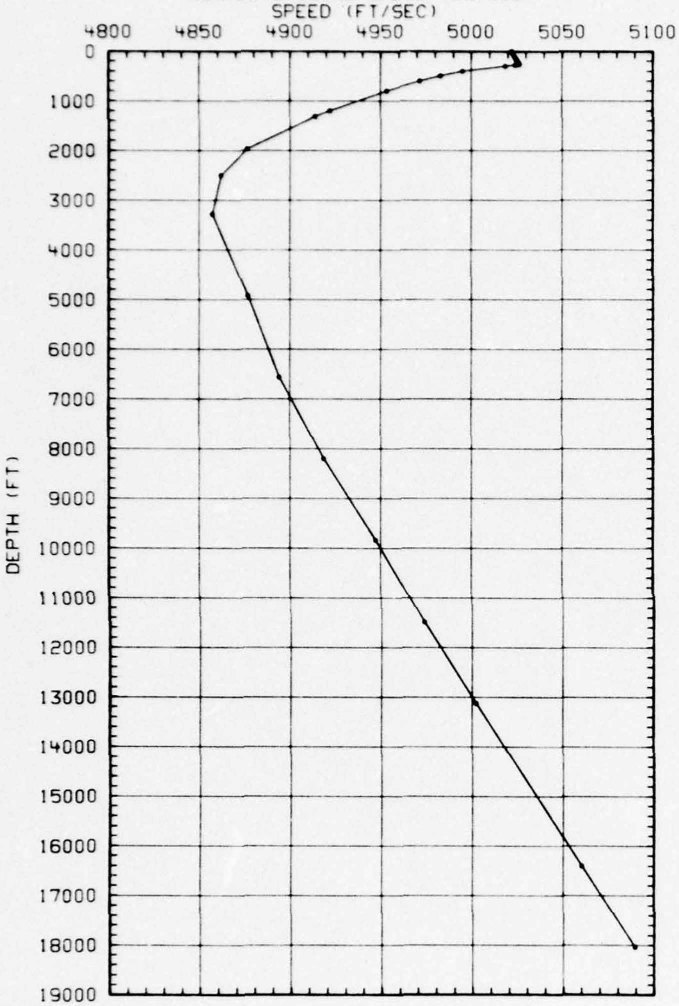

DEPTH	SPEED
0.0	5022.16
50.0	5022.98
100.0	5023.80
131.2	5024.32
164.0	5024.86
180.5	5025.13
200.0	5025.45
229.7	5025.94
246.1	5026.21
262.5	5026.49
278.9	5024.31
300.0	5018.86
400.0	4995.15
500.0	4983.04
600.0	4971.64
800.0	4953.36
1200.0	4922.25
1312.3	4913.92
1968.5	4876.22
2500.0	4861.85
3280.8	4857.19
4921.2	4876.77
6561.7	4894.17
8202.1	4918.48
9842.5	4947.26
11482.9	4973.59
13123.3	5002.03
16404.2	5060.11
18044.6	5089.60

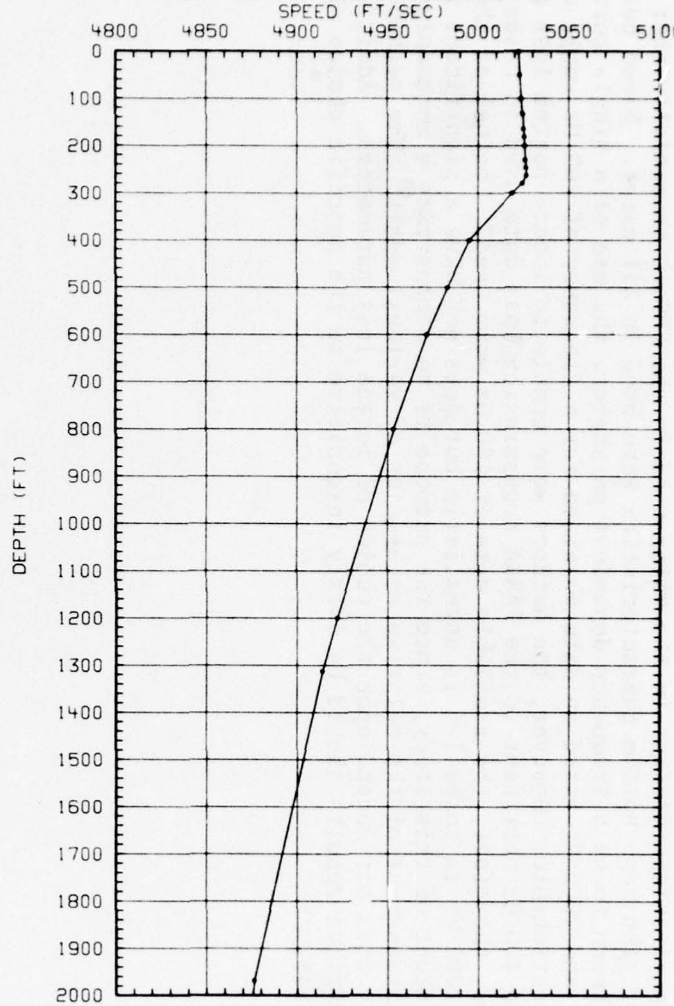

FIGURE 1

29-Point PARKA Sound Speed Profile

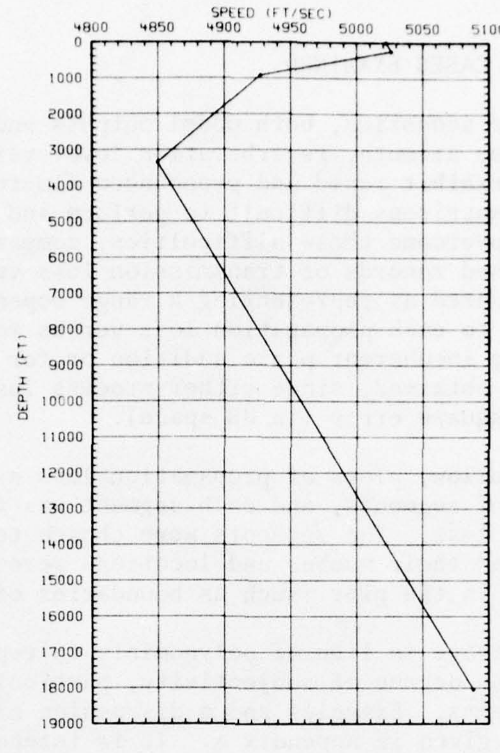

5-POINT PARKA SOUND SPEED PROFILE

FIGURE 2

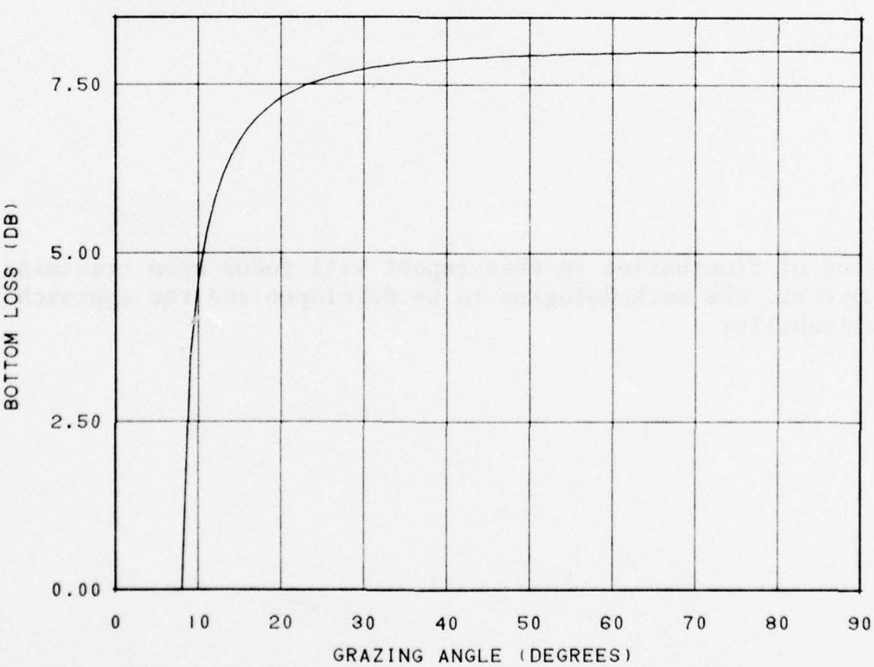

BOTTOM LOSS AS A FUNCTION OF GRAZING ANGLE

FIGURE 3

DESCRIPTION OF APPROACH AND CASES EXAMINED

Typically in underwater acoustics, both model outputs and experimental data (such as ambient noise versus azimuth, reverberation level versus time and transmission loss versus range) exhibit rapid and pronounced fluctuations.* The fluctuations make quantitative comparisons difficult to perform and even more difficult to interpret. In order to overcome these difficulties, comparisons can be made between, for example, smoothed records of transmission loss versus range. The smooth records can be considered as representing a range dependent mean. Accordingly, polynomials were fitted to each propagation loss versus range record (with the exception of those utilizing incoherent phase addition or for which a one-third octave simulated result was obtained, since either process leads to a smooth curve) so as to minimize the mean-square error (in dB space).

In the examples that follow, plots of propagation loss as a function of range were divided into a number of segments, and each segment was fitted with a polynomial of seventh degree or less. The segments were chosen to adequately represent the range dependent mean, and their number and locations were determined by significant features and changes in the plot (such as boundaries of convergence zones).

The use of a moving average in lieu of polynomials to represent the range dependent mean can reduce the degree of subjectivity, particularly that involved in dividing a record into segments. Examples and a discussion of the use of the moving average in this context are given in appendix A. It is intended in future investigations to use moving averages, rather than polynomials, for data smoothing.

---

*Further discussion of fluctuation in this report will focus upon transmission loss versus range. However, the methodologies to be developed and the approach taken have general applicability.

The comparisons constituting this study fall into two general groups: (I) FFP used as the basis of comparison for the models listed in table 3A; (II) data from the PARKA experiment used as the basis of comparison for the models listed in table 3B. The model listed in table 3B as FFP (1/3-Octave) produces an output which approximates* the process of 1/3-octave filtering of a broadband source.

Table 3A. Models Compared With The Fast Field Program (FFP)

CONGRATS V (Coherent Phase Addition)
CONGRATS V (Incoherent Phase Addition)
FACT (Coherent Phase Addition)
FACT (Incoherent Phase Addition)
NISSM II (Coherent Phase Addition)
NISSM II (Incoherent Phase Addition)
RAYMODE IV (Coherent Phase Addition)
RAYMODE IV (Incoherent Phase Addition)
RAYMODE X (Coherent Phase Addition)
RAYMODE X (Incoherent Phase Addition)

Table 3B. Models Compared With PARKA Data

CONGRATS V (Coherent Phase Addition)
CONGRATS V (Incoherent Phase Addition)
FACT (Coherent Phase Addition)
FACT (Incoherent Phase Addition)
FFP
FFP (1/3-Octave)
NISSM II (Coherent Phase Addition)
NISSM II (Incoherent Phase Addition)
RAYMODE IV (Coherent Phase Addition)
RAYMODE IV (Incoherent Phase Addition)
RAYMODE X (Coherent Phase Addition)
RAYMODE X (Incoherent Phase Addition)

*The 1/3-octave result is formed as follows: (1) FFP predictions are calculated at single frequencies across the one-third octave band (for the band of geometric mean frequency of 50 Hz, predictions were produced from 44 to 56 Hz at increments of 1 Hz; for the band of geometric mean frequency of 400 Hz, a prediction was produced every 10 Hz between 350 and 450 Hz); (2) the real and imaginary parts of the resulting complex pressures are averaged; (3) the resulting complex pressure is multiplied by its complex conjugate, and (4) 10 times the logarithm of the resulting product is obtained.

In all cases comparisons were performed to a range of 100 kyd. With the FFP as the standard of comparison six cases were examined, as shown in table 4A, consisting of three frequencies and two source/receiver depth combinations. As can be seen in figure 1, a surface duct extends to a depth of 280 feet. Cases 1-3, therefore, correspond to source and receiver being within this layer, whereas cases 4-6 correspond to source and receiver both being below the surface duct.

Table 4A. Parameters for Cases 1-6

Case No.	Frequency (Hz)	Source Depth (ft)	Receiver Depth (ft)
1	50	50	50
2	500	50	50
3	2000	50	50
4	50	500	300
5	500	500	300
6	2000	500	300

With PARKA data forming the basis of comparison, two cases were examined (table 4B). Case 7 has parameters identical with those of case 4. Case 8 differs from case 5 only in frequency, the difference being 100 Hz.

Table 4B. Parameters for Cases 7 and 8

Case No.	Frequency (Hz)	Source Depth (ft)	Receiver Depth (ft)
7	50	500	300
8	400	500	300

The quantitative comparisons in their most basic form are the graphical outputs giving the range dependent differences between smoothed data sets. For the cases and models constituting this study, 84 difference curves are generated. In order to more easily digest this information it is condensed and summarized in the form of tables. Toward this end, the data for each difference curve were divided into intervals of twenty kiloyards (in order to have a sufficient number of sample points for meaningful calculations of means and standard deviations), and the mean, μ, and standard deviation, σ, of the differences were calculated for each case within each

interval. Means and standard deviations of the differences were also calculated for the entire range interval (100 kiloyards) and for various combinations of cases: (A) cases 1-3 (source and receiver in the surface layer), (B) cases 4-6 (source and receiver below the layer), (C) cases 1-6, and (D) cases 7-8. Table 5 shows the number of points contained in each interval and in the entire 100 kyd for each model and for the PARKA data.

Table 5. Number of Sample Points for Models and PARKA Data

RANGE INTERVAL (kyd)	0-20	20-40	40-60	60-80	80-100	0-100
CONGRATS V	49	52	51	52	52	256
FACT	20	20	20	20	20	100
FFP (CW)	255	255	255	255	255	1275*
FFP (1/3-octave)	255	255	255	255	255	1275*
NISSM II	25	26	25	26	26	128
RAYMODE IV	20	20	20	20	20	100
RAYMODE X	40	40	40	40	40	200
PARKA (Case 7)	8	12	10	8	7	45
PARKA (Case 8)	6	8	6	12	7	39

*A record containing 4096 points is generated by the FFP. However, the first 100 kyd contain 1275 points.

DESCRIPTION OF MODELS

CONGRATS V - The CONGRATS V model expands the integral representation of the acoustic pressure into a geometric series, each term of which corresponds to a particular ray type. A careful evaluation of the pertinent quantities involved avoids problems associated with ordinary ray theory.

The Fast Asymptotic Coherent Transmission (FACT) Model[1,2,3] - The FACT model is a ray acoustic model which utilizes higher order theory for the solution in those areas in which the assumptions of ray acoustics lead to physically unrealizable solutions. Specifically, the infinite intensities resulting from geometric ray theory at caustics are disregarded. Instead, the acoustic field at caustics is evaluated using appropriate asymptotic expressions. The Clay-Tatro Model[4] is used for propagation in a surface duct. The FACT model has been developed and programmed to achieve minimum running time. The model development was sponsored by the Long Range Acoustic Propagation Project (LRAPP). Initially developed within several Navy and industrial laboratories, a preliminary version of the FACT model was turned over to the Acoustic Environmental Support Detachment where it was upgraded. On April 1, 1973, the Acoustic Environmental Modeling Coordinator, Dr. J. B. Hersey, designated the FACT model to be a new Navy Interim Standard Transmission Model for ocean environments which may be adequately described by a single sound speed profile and a flat bottom.

The Fast Field Program (FFP)[5] - The FFP applies Fast Fourier Transform methods to acoustic field theory. This model evaluates the exact integral solution to the wave equation, yielding propagation loss as a function of range. The FPP should be considered more accurate than many normal mode and ray theory solutions because, in general, these other methods represent approximate solutions or a part of the exact solution. It is for this reason that the FFP was chosen as the standard of comparison in cases 1-6. The FFP was developed at NUSC.

The Navy Interim Surface Ship Model II (NISSM II)[6] - NISSM II is designed to predict the performance of existing and proposed active sonar systems using ray tracing techniques. It is a full system performance model in that it calculates the reverberation field and includes a detection model. The propagation loss model in NISSM II consists of a continuous gradient ray theory model with higher order acoustic corrections. For cases of source and receiver in a surface duct, NISSM II calculates transmission loss from both ray theory and modified AMOS predictions, but uses the result giving the greatest loss. Since this model was designed to predict the performance of active sonar systems, its use in this study at frequencies such as 50 and 500 Hz may be somewhat inappropriate. NISSM II was sponsored by the Naval Sea Systems Command (Code 06H1) and was developed by NUSC and the Naval Undersea Center (NUC).

RAYMODE IV and RAYMODE X[7,8] - The RAYMODE models are wave propagation loss models which allow for the usual normal mode solution to be expanded in a ray path series. That is, the acoustic wave solution is converted into a set of integral solutions which can be identified as various ray paths. The RAYMODE models, therefore, allow for the exact normal mode wave solutions to be interpreted in terms of ordinary ray paths without the need to make the usual ray theory approximations.

RAYMODE X differs from RAYMODE IV in that it has incorporated advancements in analysis and computational techniques and is thus a more efficient model and more

accurate in calculating solutions to the governing integral representation of the physical process. The RAYMODE IV and RAYMODE X models were developed at NUSC.

ASSESSMENT OF ACCURACY

Usually, accuracy is assessed in a qualitative manner which consists of overplotting the various data sets and describing the agreement between them by terms such as good, fair, and poor. Of course, such terms are subjective and that which constitutes good agreement for one application may be poor agreement for another. When many data sets are being compared, the process of overplotting leads to confusion, especially when the further complication of several scenarios (such as differing sound speed profiles, bottom loss regimes, source/receiver depth combinations and frequencies) is considered. Also adding to the difficulty of making comparisons are the rapid fluctuations exhibited by various data sets, such as exemplified in figure 4. What is needed to ameliorate the situation described above is a method of comparing data sets that leads to meaningful quantitative results. Accordingly, a comparison approach was adopted in this investigation that produces outputs which form a hierarchical structure providing both quantitative measures sufficiently concise for the assessment of the relative accuracies of several candidate models for a given application and intermediate outputs from which the causes of discrepancies may be ascertained. The comparison approach consists of seven major steps:

(1) Fitting Polynomials to Raw Data Sets - This process eliminates the rapid fluctuations in each data set and thus permits a comparison of the data sets in terms of range dependent mean values. The procedure is to divide each data set into several range intervals and to fit a polynomial of appropriate degree in each interval. Figure 5 shows the result of this process as applied to the raw data of figure 4. Intervals are chosen on the basis of major significant features of the record such as the bottom bounce region and convergence zone. Features such as near field interference patterns are strongly affected by small changes in frequency, source or receiver depth, and sound speed. Such features are sensitive to model assumptions (e.g., a flat bottom and a sound speed field describable by a single profile) and the manner in which the model treats the sound speed data. For these reasons such features are averaged (c.f. figures 4 and 5).

The rapid fluctuations observed in transmission loss model outputs are due to constructive and destructive interference between two or more paths (or modes) resulting from coherent phase addition. Models which use incoherent phase addition tend to produce outputs essentially lacking in fine-scale fluctuations, although major features are largely retained. For this reason, outputs of models using incoherent phase addition are not smoothed by fitting polynomials.

(2) Calculation of Difference (in decibels) Between the Standard and Each Appropriately Smoothed Model Output as a Function of Range - For Cases 1-6, the standards are smoothed FFP outputs, the results of fitting polynomials to major features; for Cases 7-8, the standards are PARKA data. An example of a difference curve is shown in figure 6.

(3) Subdivision of the Difference of (2) into Range Intervals - The choice of five equal intervals of 20 kyd was made for this study. This choice ensures that each interval is large enough to contain sufficient points for the calculations of (4) to be of significance and small enough so that each interval contains no more than a single major feature. The number of sample points per interval is given in table 5 for each model and for the PARKA data.

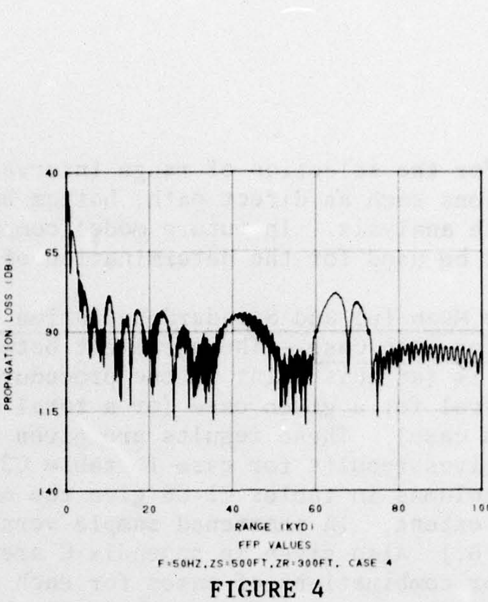

FIGURE 4

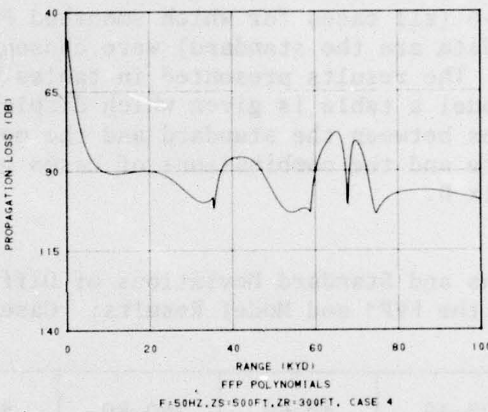

FIGURE 5

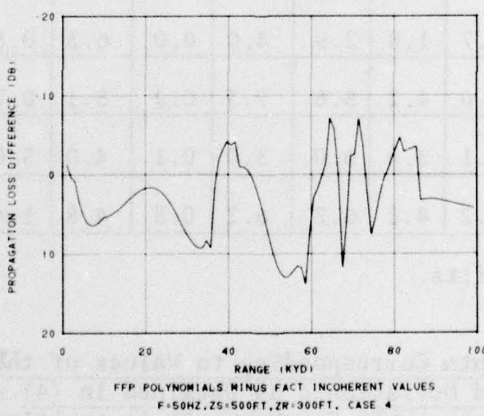

FIGURE 6

An alternative method for the selection of range intervals would be to divide the record according to regions such as direct path, bottom bounce, and convergence zone on the basis of ray path analysis. In future model comparisons the method given in this paragraph will be used for the determination of range intervals.

(4) Calculation of the Mean (μ) and Standard Deviation (σ) of Differences Within Each Range Interval for Each Case - The agreement between a given model output and a standard data set is (at this point in the procedure) represented by two numbers for each range interval for a given case (or a total of 10 numbers for the entire range extent for each case). These results are given in tables C1-C8 of appendix C, where table C1 gives results for case 1, table C2 gives results for case 2, etc. The last two columns in tables C1-C8 give the mean and standard deviation over the entire range extent. (A shortened sample version, selected from table C4, is shown as table 6.) Also given in appendix C are means and standard deviations of differences for combinations of cases for each range interval and for the entire range. The case combinations 1-3 (smoothed FFP the standard, source and receiver in the surface layer), 4-6 (smoothed FFP the standard, source and receiver below the surface layer), 1-6 (all cases for which smoothed FFP is the standard) and 7-8 (cases for which PARKA data are the standard) were chosen and correspond to tables C9-C12 respectively. The results presented in tables C1-C12 are also rearranged so that for each model a table is given which displays means and standard deviations of the differences between the standard and the model in question in all range intervals for each case and the combinations of cases given above. These results are found in appendix D.

Table 6. Means and Standard Deviations of Differences Between the FFP* and Model Results; Case 4

Range Interval (kyd)	0-20		20-40		40-60		60-80		80-100		0-100	
	μ	σ	μ	σ	μ	σ	μ	σ	μ	σ	μ	σ
CONGRATS V* (Coherent)	1.9	1.5	0.7	1.8	2.9	4.0	0.0	6.3	0.8	1.8	1.3	3.7
CONGRATS V (Incoherent)	4.3	2.3	4.0	4.2	5.6	7.3	0.4	5.1	0.7	2.8	3.0	5.1
FACT* (Coherent)	1.8	2.1	0.1	3.8	6.0	3.0	0.1	4.0	5.0	3.6	2.6	4.1
FACT (Incoherent)	3.7	2.2	4.2	4.2	6.2	6.2	0.5	4.8	1.4	3.3	3.2	4.8

*As smoothed by polynomial fits.

(5) Establishing Weights Corresponding to Values of the Absolute Value of the Mean $|\mu|$ and/or the Standard Deviation σ as Obtained in (4) - The set of weights used in this study is given in table 7. Here, it is tacitly assumed that all range intervals and cases are of equal importance. In general, weights would be assigned by a user in accordance with considerations such as tactical requirements and modes of operation. Thus, a user might apply more stringent weights in the convergence zone (i.e., the range interval between 60 and 80 kyd) for source and receiver below the surface layer at a frequency of 500 Hz (i.e., case 5) if his mission emphasized the importance of making detections for such a scenario.

Table 7. Weights Corresponding to Values of $|\mu|$ or σ

W	$\|\mu\|,\sigma$ (dB)
1	0.0-2.9
2	3.0-5.9
3	6.0-8.9
4	9.0-11.9
5	$\geq$12.0

(6) Determination of Measures of Accuracy by Summing the Weights* Corresponding to $\boxed{\mu}$ and σ in Each Range Interval for Each Case - At this point, the accuracy of each model is given by a single value in each range interval/case bin. The results of this process are given in appendix C in tables C13A-C13E and C14A-C14B. As an example, a shortened version of table C13D is given as table 8.

Table 8. Sum of Weights* Corresponding to Means and Standard Deviations** of Differences Between the Smoothed FFP and Model Results; Case 4

Range Interval (kyd)	0-20	20-40	40-60	60-80	80-100
CONGRATS V (Coherent)	2	2	3	3	2
CONGRATS V (Incoherent)	3	4	5	3	2
FACT (Coherent)	2	3	4	3	4
FACT (Incoherent)	3	4	6	3	3

* As defined in table 7.
** As given in table 6.

(7) Determination of Cumulative Measures of Accuracy by Averaging the Measures of Accuracy over all Range Intervals and Cases for Which a Given Standard was Used - (i.e., Cases 1-6 utilized FFP as the standard; Cases 7-8 utilized PARKA data as the standard). The cumulative accuracy measure provides a single number which may be used to compare the accuracies of several models. The user may establish an acceptable level for this measure; all models with cumulative measures of accuracy below this level would then be regarded as providing sufficiently accurate outputs.

The cumulative accuracy measure for each model resulting from comparison with smoothed FFP results is given in table 9. Two models are seen to be most accurate: RAYMODE X (coherent) and CONGRATS V (coherent). These are followed in accuracy by the incoherent versions of RAYMODE X and CONGRATS V and then FACT (coherent) and FACT (incoherent). The NISSM II and RAYMODE IV models, using either coherent or incoherent phase addition, are seen to be the least accurate models in comparison with the FFP. In general, the coherent versions of models compare more favorably with the FFP, as is to be expected (since the FFP uses coherent phase addition).

*From table 7.

Table 9. Cumulative Accuracy Measure* For Each Model Resulting From Comparison With Smoothed FFP Results

CONGRATS V (Coherent)	2.60
CONGRATS V (Incoherent)	2.90
FACT (Coherent)	2.97
FACT (Incoherent)	3.20
NISSM II (Coherent)	3.97
NISSM II (Incoherent)	4.03
RAYMODE IV (Coherent)	4.20
RAYMODE IV (Incoherent)	3.80
RAYMODE X (Coherent)	2.50
RAYMODE X (Incoherent)	2.73

*Weights of Tables C13A-C13E Averaged Over All Range Intervals

The cumulative accuracy measure for each model resulting from comparison with PARKA data is given in table 10. Here, four models are seen to be most accurate, namely, RAYMODE X (incoherent), CONGRATS V (coherent), CONGRATS V (incoherent) and RAYMODE IV (incoherent). The incoherent versions of models are seen to be more accurate than coherent versions in comparisons with PARKA data. The PARKA data are the result of processing the received signal in 1/3-octave filters and, therefore, represent averaging over frequency. The utilization of incoherent phase addition is also an averaging process. Both frequency and phase averaging result in smoothed outputs essentially lacking in rapid, large fluctuations. It is to be expected that such records will show better agreement than that between records which represent broadband results (i.e., 1/3-octave PARKA data) and narrowband results (i.e., coherent models assuming a CW source). To test the effect of comparing broadband (1/3-octave) and narrowband (CW) results as opposed to comparing two broadband outputs, the FFP was run as a CW and a 1/3-octave† model and each was compared with the 1/3-octave PARKA data. As expected, the FFP (1/3-octave) shows better agreement with the PARKA data.

†Using superposition of CW tonals across the 1/3 octave band.

Table 10. Cumulative Accuracy Measure* For Each Model Resulting From Comparison With PARKA data

CONGRATS V (Coherent)	2.6
CONGRATS V (Incoherent)	2.6
FACT (Coherent)	3.0
FACT (Incoherent)	2.9
FFP (CW)	3.1
FFP (1/3-Octave)	2.9
NISSM II (Coherent)	3.4
NISSM II (Incoherent)	2.8
RAYMODE IV (Coherent)	3.3
RAYMODE IV (Incoherent)	2.6
RAYMODE X (Coherent)	3.0
RAYMODE X (Incoherent)	2.5

*Weights of Tables C14A-C14B Averaged Over All Range Intervals

A REPRESENTATIVE EXAMPLE

Various features, choices, and conclusions relating to the graphs merit discussion. Case 4 is sufficiently representative so that most major points of interest are manifest. Figure IV-1A (of appendix B) shows a very complex interference pattern to a range of approximately 35 kyd followed by a large feature extending to 58 kyd at which point a double-lobe convergence zone (CZ) is found, finally followed by a fairly smooth structure between 75 and 100 kyd. This led to the representation of the range dependent mean by five polynomials as shown in figure IV-1B. It is this curve which constitutes the standard against which other models are compared for Case 4. The decision to utilize a single polynomial from 0 to 35 kyd is due to the unstable nature of the nearfield interference patterns as described above. However, if a user were to decide that features of this size are of significance, the use of up to 10 polynomials in this region would be indicated. The choice of a single polynomial fit to the FFP in this range interval led to smaller differences between the FFP and several models than would have resulted from a more complex representation. This was due to the lack of well defined features in many outputs (particularly when incoherent phase addition was utilized).

Figure IV-2A (showing CONGRATS V results) is sufficiently similar to the FFP output just discussed so that similar choices regarding polynomial fittings were made, resulting in figure IV-2B. In looking at the difference curve in figure IV-2C, sharp oscillations are observed between 60 and 80 kiloyards; these are due to a range discrepancy between the convergence zones predicted by the FFP and those predicted by CONGRATS V (coherent). When the mean and standard deviation of the difference curve are calculated in an instance such as this (i.e., range displacement of features which otherwise closely agree), it is found that the mean is nearly zero and the standard deviation is large. That this is indeed the case is seen in table C4 (of appendix C) for the CONGRATS V coherent model in the 60-80 kyd interval (μ = 0, σ = 6.3). Figure IV-2D shows the CONGRATS V incoherent output to have a single major feature, the convergence zone. This CZ is single lobed (unlike the FFP) but agrees quite well in range extent as measured at the 90 dB level; however, the "bottom bounce region" between 35 and 58 kyd in the FFP output is almost completely absent here. These factors explain the character of figure IV-2E.

FACT (coherent) output in figure IV-3A shows sufficient structure so that four polynomials were chosen to represent the mean (figure IV-3B). The very abrupt change in propagation loss at 86 kyd (a feature also seen in figure IV-3D and present in all FACT outputs), has been smoothed by the polynomial. The difference curve figure IV-3C shows a large error at 38 kyd; this is due to the bottom bounce region as predicted by FACT (coherent) occurring at larger ranges than predicted by FFP. In the range interval between 60 and 80 kyd, differences arise due to an extension of the CZ to shorter ranges by the FACT model as compared to FFP and to the absence of a deep notch in the CZ structure of the FACT output. FACT (incoherent) output, shown in figure IV-3D, shows the bottom loss feature to exhibit lower loss and to be found at greater range as compared with the FACT (coherent output). Differences from the FFP in figure IV-3E reflect these changes when compared with figure IV-3C.

Figures IV-4A, IV-4B, and IV-4C show, respectively, the NISSM II (coherent) output, a four polynomials fit to the output, and the difference between the FFP analytic fit and the NISSM II (coherent) analytic fit. The only area of large differences is the convergence zone region; NISSM II (coherent) gives a CZ which

lacks a deep notch, is narrower than the CZ of FFP, beginning at a greater range and terminating at a shorter range, and exhibits greater loss than the CZ of FFP. The NISSM II (incoherent) output of figure IV-4D shows a vestigial bottom bounce feature and a CZ somewhat broader (at the zone termination) as compared with the coherent results. The differences between the analytic fit to FFP and the NISSM II (incoherent) results are presented in figure IV-4E. The large differences between 50 and 60 kyd are due to the low losses of NISSM II (incoherent) in a region which for the FFP is between the end of the bottom bounce region and the start of the CZ.

The RAYMODE IV (coherent) output lacks clearly defined major features (see figure IV-5A). However, using the knowledge of major features from the standard (i.e., the analytic fit to the FFP), five polynomials were used to obtain the analytic fit to the RAYMODE IV (coherent) results, shown in figure IV-5B. Despite the choice of an analytic fit most faithful to the standard, the differences of figure IV-5C are seen to be large in all areas. The RAYMODE IV (incoherent) results (figure IV-5D) show a single major feature, the convergence zone, which is broader and shows greater loss than the FFP and lacks a deep notch. The nature of the CZ and the absence of a bottom bounce feature in the RAYMODE IV (incoherent) output accounts for the large differences observed between 40 and 80 kyd in figure IV-5E.

The RAYMODE X (coherent) output and the analytical fit (5 polynomials) to this output are shown in figures IV-6A and IV-6B, respectively. The only area of large differences between the FFP analytic fit and the RAYMODE X (coherent) analytic fit is in the convergence zone. The zone as given by RAYMODE X (coherent) is narrow, shows greater loss and has a poorly defined notch as compared with the FFP convergence zone, thus accounting for the differences in figure IV-6C. The RAYMODE X (incoherent) results of figure IV-6D show a convergence zone and no bottom bounce region. The resulting differences with respect to the analytic fit to the FFP are large, as shown in figure IV-6E.

As described above, the difference curves were subdivided into 20 kiloyard intervals and the mean (μ) and standard deviation (σ) of the differences were computed in each interval as well as for the entire 100 kiloyard range extent. Thus, the information contained in the 10 difference curves for Case 4 is condensed and presented in a single table, specifically table C4. Table 7, giving the weights to be used for different intervals of $|\mu|$ and σ was then applied to the results of table C4 resulting in the further condensation of information (table C13D). Finally, upon averaging these data with the data from Cases 1,2,3,5 and 6 over all ranges, the final result, that of table 9 is obtained.

The tables mentioned above are of primary use in comparing candidate models with a standard for an assessment of accuracy. Given that a specific model has achieved an overall cumulative measure of accuracy which is acceptable to the user (as obtained from table 9) it may be desired to focus upon the accuracy of this model for the various case/range interval combinations. Such results are found in appendix D (e.g., table D6-A for the RAYMODE X (coherent) model). From a table such as this, the accuracy of a model is revealed from the viewpoint of consistency. Also, case/range interval bins for which the model is not sufficiently accurate (according to criteria designated by the user) are readily identified.

COMPUTER RUN TIME REQUIREMENTS

Program running time is a factor that determines whether a program is suitable for a given application. For example, a transmission loss model to be used in a sonar trainer must be capable of producing a result in a matter of seconds; this is also true if such a model is utilized for sonar mode selection or tactical decision making. On the other hand, running time requirements can be significantly relaxed if the model is to be used for making predictions relating to sonar design concept formulation or evaluation and for other research oriented tasks.

The computer run times for the models as utilized in the comparison studies are given in tables 11A and 11B. It should be noted that models used in this study may not have been programmed to optimize running time. The running times are those obtained from executing the models as available at the Naval Underwater Systems Center on the UNIVAC 1108 computer. Table 11A gives the run times for each of the models as run on the UNIVAC 1108 computer without normalization based upon the number of points generated by the given model. Table 11B presents run times normalized to a prediction containing 100 points. This latter table was calculated since the run times are approximately proportional to the number of points generated by a model and, therefore, a direct comparison between the times listed in table 11A could be misleading. As presently programmed, the NISSM II and CONGRATS V models do not have the numbers of points per prediction as a user option; for these models the number of points is fixed at 128 and 256, respectively. This does not imply that these numbers cannot be changed or made user options, but rather that such changes would be made at a program level beyond that intended for the typical user. Despite the fact that the numbers of points per prediction are fixed for NISSM II and CONGRATS V and, hence, the running times given in table 11B are unachievable by these models as presently programmed, a normalized comparison was nonetheless deemed useful and, therefore, included.

For other models constituting the comparison study, the number of points per prediction is a user option up to a maximum allowable value; for FACT the maximum number of points is 250 and for RAYMODE IV and RAYMODE X a maximum of 400 points may be generated. As typically used, the FFP generates 8192 points of which 4096 are eliminated due to aliasing. Although the FFP may generate a prediction containing 2^M points, a choice of M which is small (e.g., M=7) may seriously affect the accuracy of the prediction and is not recommended.

To a certain degree, accuracy may be traded off against running time or, its counterpart, the number of points per prediction. Thus, had the models herein reported been run so as to produce the same number of points (implying the run times of table 11B) the results relating to accuracy might have been different.

A few comments related to the contents of table 11A are in order: (1) only the total run time was available for CONGRATS V. (2) The CONGRATS V run time includes an estimated 5 seconds required for plot related calculations. (3) For most of the models, the run time for Case 8 was unavailable. In such cases, a run time equal to that for Case 5 (the parameters of which are closest to Case 8) was assumed. (4) Only Case 7 and Case 8 were run using the FFP to construct a one-third octave prediction by averaging several CW predictions. Approximately 10 seconds should be added to the run times of each case for averaging of the components required for the final result.

The normalized computer run times as given in table 11B fall into three categories: Category I consists of those models for which the maximum time for any given case was less than or equal to four seconds and the total run time was less than 30 seconds; Category II for which individual case run times varied between 8 and 30 seconds and the total run time was between 1 and 2 minutes; Category III for which run times for individual cases varied between 6 seconds and 3 minutes and the total run time was greater than 5 minutes. The models fell into the three categories as follows:

I	FACT
	RAYMODE X
II	CONGRATS V
	NISSM II
	RAYMODE IV
III	FFP (CW)

FFP (1/3-octave) was not included in a category since the use of FFP in this manner represents a special application.

Table 11A. Computer Run Time

	CONGRATS V	FACT	FFP (CW)	FFP (1/3-Octave)	NISSM II	RAYMODE IV	RAYMODE X
Case 1	[a]	0:01.3	3:30.1	[d]	0:14.0	0:28.8	0:04.6
Case 2	[a]	0:01.1	6:08.0	[d]	0:12.6	0:27.1	0:04.7
Case 3	[a]	0:01.0	17:28.0	[d]	0:12.7	0:25.0	0:04.9
Case 4,7	[a]	0:01.3	3:39.0	44:28[d]	0:11.1	0:10.7	0:05.7
Case 5	[a]	0:01.3	27:37.4	[d]	0:11.0	0:09.4	0:07.9
Case 6	[a]	0:01.5	87:18.9	[d]	0:12.9	0:08.9	0:06.1
Case 8	[a]	0:01.3[c]	27:37.4[c]	112:21[d]	0:11.0	0:09.4[c]	0:08.1
Total (HR:MIN:SEC)	0:4:42.3[b]	0:0:08.8	2:53:18.8	2:36:49[d]	0:1:25.3	0:1:59.3	0:0:42.0

a. Not available.
b. Total CPU (Central Processing Unit) time, including plot time.
c. Not available. Running time for case 5 was used.
d. FFP (1/3-Octave) used only in cases 7 and 8. Values do not include required averaging time.

Table 11B. Computer Run Time Normalized to a 100 Point Prediction

	CONGRATS V	FACT	FFP (CW)	FFP (1/3-Octave)	NISSM II	RAYMODE IV	RAYMODE X
Case 1	[a]	0:01.3	0:06.6	[d]	0:10.9	0:28.8	0:02.3
Case 2	[a]	0:01.1	0:11.5	[d]	0:09.8	0:27.1	0:02.3
Case 3	[a]	0:01.0	0:32.8	[d]	0:09.9	0:25.0	0:02.5
Cases 4,7	[a]	0:01.3	0:06.8	1:23.4[d]	0:08.7	0:10.7	0:02.8
Case 5	[a]	0:01.3	0:51.8	[d]	0:08.6	0:09.4	0:04.0
Case 6	[a]	0:01.5	2:43.7	[d]	0:10.1	0:08.9	0:03.1
Case 8	[a]	0:01.3[c]	0:51.8[c]	3:30.7[d]	0:08.6	0:09.4[c]	0:04.0
Total (MIN:SEC)	1:50.3[b]	0:08.8	5:25.0	4:54.1[d]	1:06.6	1:59.3	0:21.0

a. Not available.
b. Total CPU (Central Processing Unit) time, including plot time.
c. Not available. Running time for case 5 was used.
d. FFP (1/3-Octave) used only in cases 7 and 8. Values do not include required averaging time.

STORAGE REQUIREMENTS

The UNIVAC 1108 storage requirements for the various models constituting this study are given in table 12. The reader is cautioned that models have been optimized in terms of storage requirements to varying degrees. The values in the table pertain to versions of the models available at the Naval Underwater Systems Center.

Table 12 is divided into two groups. The upper group, except as otherwise indicated, does not include the storage required for plot routines and plot related instructions. The values shown for NISSM II, while they do not include the storage required by the plot subroutines, do include storage for the plot instructions and buffer. The latter two account for approximately ten percent of the storage requirement of NISSM II. Storage requirements are not shown for the FFP (1/3-octave), inasmuch as it repeatedly uses the FFP in generating its predictions. The only available storage requirements for CONGRATS V included plot routines and these are shown in the lower group of table 12. A corresponding set of numbers is shown for NISSM II for comparison purposes.

The results of table 12 may be summarized by placing models into one of three categories:

Category I - Storage requirements between 8K and 16K locations;

Category II - Storage requirements between 16K and 32K locations;

Category III - Storage requirements between 32K and 64K locations.

The models fell into categories as follows:

I	RAYMODE X
	RAYMODE IV
II	FACT
III	NISSM II
	CONGRATS V
	FFP

Table 12. Storage Requirements

		CONGRATS V	FACT	FFP (CW)	FFP (1/3-oct)	NISSM II	RAYMODE IV	RAYMODE X
Without Plot Routines	Instructions	a	14,121	18,563	b	19,702[c]	8,959	8,532
	Data	a	7,734	33,009	b	16,680[c]	6,688	5,579
	Total	a	21,855	51,572	b	36,382[c]	15,647	14,111
Including Plot Routines	Instructions	20,129				21,037		
	Data	31,631				22,849		
	Total	51,760				43,886		

a. Not available.
b. Not applicable. The FFP (CW) is used repeatedly.
c. Includes plot related instructions.

EASE OF IMPLEMENTATION

The ease with which a program can be implemented on a given computer is revealed in a number of ways:

(1) Contact with the author or a cognizant individual or code with broad experience relating to the program is the most direct approach. For the programs used in this report, such a list of individuals and codes is given in table 13.

(2) Before consulting with the author of a program regarding its implementation on a given computer it is useful to know which computers already have the program running and for what type of machines minor program modifications will be required.

All transmission loss programs used in this report are written in FORTRAN and are easily adaptable to any computer with a FORTRAN compiler. Only slight modifications are sometimes required if the wordlength (in bits) of the prospective computer is different from that of the original.

A. FFP -- Following is a list of installations to which the FFP program has been sent, and, where known, the type of computer involved. It is presumed, but not known, that the FFP model has actually been implemented at these installations.

a) Honeywell, West Covina, CA. (IBM)
b) Acoustic Environmental Support Detachment (CDC)
c) Naval Intelligence Support Center, Suitland, MD. (Xerox Sigma)
d) Canadian Defence Establishment, Nova Scotia
e) Acoustic Research Laboratory, University of Texas (CDC 6600)

B. CONGRATS V -- Still in process of development.

C. FACT -- computers on which the FACT program has been implemented include:

CDC 1700, 3000 and 6000 series and CDC 7600
Honeywell Minicomputers
XDS-7
PDP-11, series
NOVA series

Program Requirements: 5 1/2 significant digits in the mantissa (floating point). This requirement is met by all 16-bit machines. Thus the program can be used directly on machines with 16-bit, floating point hardware (minor modifications are required for use on other than CDC-6000 series). The program can be modified for use on non-16-bit machines. Futher information can be obtained from NORDA, Code 32.

D. NISSM II -- This program has been implemented "all over the world on many different types of computers" according to Dr. H. Weinberg, author of the program. No record has been kept of the many places to which copies of the program have been sent. It can be used on any FORTRAN computer, with minor modifications required for non-36-bit machines.

E. RAYMODE IV -- In practice has been replaced by RAYMODE X.

F. RAYMODE X is available at the following facilities:

Facility	Computer
NUSC/NLL	UNIVAC 1108
Singer Corp., Silver Spring, MD.	UNIVAC 1108
NUC, San Diego, CA.	UNIVAC 1108
Edo Corp., College Point, NY.	UYK-20
NUSC/NLL	HP 9830
*NUSC/NLL	HP 9830
COMTHIRDFLT	HP 9830
COMCRUDESGRU TWO/DESDEVGRU	HP 9830
*USS MOINESTER (FF 1097)	HP 9830
**NUSC/NLL	DEC PDP 11
**USS CONNOLE (FF 1056)	DEC PDP 11

* Modified for shipboard use.
** SIMAS Version.

(3) For several reasons, one should be familiar with reference material regarding a given model before a commitment to program implementation is made. Accordingly, a list of references has been provided (see p. 49) for the transmission loss models used in this report. CONGRATS V is in the process of development and, therefore, no documentation is available.

Table 13. Points of Contact for Information Relating to Transmission Loss Models

I	CONGRATS V	:	Dr. H. Weinberg Code 314 New London Laboratory Naval Underwater Systems Center New London, CT. 06320 Tel. (203) 442-0771, Ext. 2589
II	FACT	:	Code 32 Naval Ocean Research and Development Activity National Space Technology Laboratories Bay St. Louis, MS. 39520
III	FFP	:	Dr. F.R. DiNapoli Code 3123 New London Laboratory Naval Underwater Systems Center New London, CT. 06320 Tel. (203) 442-0771, Ext. 2647
IV	NISSM II	:	Thelda Garret Code 314 New London Laboratory Naval Underwater Systems Center New London, CT. 06320 Tel. (203) 442-0771, Ext. 2991
V	RAYMODE IV	:	Dr. G. Leibiger Code 222 New London Laboratory Naval Underwater Systems Center New London, CT. 06320 Tel. (203) 442-0771, Ext. 2221
VI	RAYMODE X	:	Same as RAYMODE IV (above).

COMPLEXITY OF PROGRAM EXECUTION

The complexity of program execution is best revealed by listing the inputs required in order to run the program. Programs differ widely in their degree of complexity; this largely reflects the number of decisions left under the user's control. For example, in a program utilizing ray theory, required inputs include the total angular extent of rays emanating from the source and the angular difference between adjacent rays. These inputs are best decided independent of the user in applications such as transmission loss computations for use aboard ship or in a sonar trainer. On the other hand, it is advantageous to allow these inputs to be under user control if the program is to be used in a Navy R&D laboratory where requirements are likely to be variable, or if the program is to be used in making predictions for sonar systems, existing and proposed, or if the environmental scenarios may have unusual aspects. Thus, the desirable level of complexity is dependent upon the application. Following are the input requirements for the models constituting this study.

A. CONGRATS V - Input requirements are identical to those for NISSM II (see below).

B. FACT - As described in reference 2, "THE CARD INPUTS TO LOSS ARE DETAILED IN THE COMMENTS WITHIN THAT PROGRAM, AND REPEATED HERE FOR REFERENCE PURPOSES."

CARD		DATA	FORMAT
1		TITLE	8A10
	(EOF ENDS RUN)		
2		N,IL,IB,IW,IPL,IAR	6I5
3A,B,...		Z(I),C(I) (I=1,N)	8F10.2
	OR	D(I),T(I),S(I)	3(F8.2,F6.2,F6.2)
4		NR,ORNMI	I5,5X,F10.2
5		F(I) (I=1,6)	6F10.2
6		S,R,JC(I) (I=1,6)	2F10.2,6I5

(EOF ENDS RUN)

(S.GE. 10E6 GOES BACK TO READ CARD 1)

FACTTL CALLED TO COMPUTE LOSSES

LOSSES PRINTED AND/OR PLOTTED

(GOES TO READ CARD 6)

- -

N IS NO. OF PROFILE POINTS 2.LE. (ABS(N)).LE. 50

*FOR N POSITIVE, PROFILE IS INPUT DIRECTLY IN DEPTH, VELOCITY PAIRS, 4/CARD. A VELOCITY .LT. 3000 IS USED AS AN INDICATOR OF METRIC INPUT (M,M PER S). BOTH DEPTHS + VELOCITIES ARE CONVERTED TO ENGLISH UNITS (FT,FT PER SEC).

*FOR N NEGATIVE, PROFILE IS INPUT AS DEPTH, TEMP., SALINITY TRIPLETS, 3/CARD. METRIC UNITS ARE ASSUMED (M,CENT,PPT). WILSONS FORMULA IS USED TO COMPUTE VELOCITIES, DEPTHS + VELOCITIES ARE THEN CONVERTED TO ENGLISH UNITS.

*THE INPUT PROFILE IS ALWAYS PRINTED, IF CALCULATIONS + CONVERSIONS ARE REQUIRED, THE RESULTING VALUES ARE ALSO PRINTED.

*THE BOTTOM DEPTH IS ALWAYS Z(N)

IL IS THE INDEX OF THE MIXED LAYER DEPTH IN THE INPUT PROFILE (SEPARATE COMPUTATIONS ARE THEN PERFORMED FOR A SURFACE DUCT OF THIS DIMENSION AND NO RAYS ARE TRACED IN THE DUCT). EITHER 1 OR 0 CAN BE USED TO INDICATE THAT NO LAYER IS PRESENT. 0 .LE. IL .LE. (ABS(N)). IL = (ABS(N)) INDICATES THAT A HALF-CHANNEL CONDITION IS PRESENT AND THAT THE ROUTINE HFCHTL (NORMALLY USED ONLY FOR ASRAP) SHOULD BE USED.

IB IS THE BOTTOM TYPE

A NEGATIVE VALUE INDICATES THAT THE USER WILL SUPPLY A BOTTOM LOSS FUNCTION, AND MODIFY FUNCTION BOTTOM TO CALL THE REPLACEMENT FOR THE DEFAULT FUNCTION BTMLOS.

1-9 INDICATES FNWC BOTTOM LOSS FUNCTIONS

IW IS THE WAVE HEIGHT IN FEET

IPL IS THE PRINT/PLOT INDICATOR

0.. PRINT ONLY (DB. LOSS VS. RANGE)

1.. PAGE PLOT ONLY (DB. LOSS VS. RANGE, 1 PAGE/FREQUENCY)

2.. PRINT AND PLOT (=0 PLUS 1)

-1.. PAGE PLOT ONLY (DB. LOSS VS. RANGE, ALL FREQS. ON SAME PLOT)

-2.. PRINT AND PLOT (=0 PLUS -1)

IAR IS THE ARRIVAL CALCULATION INDICATOR

0 .. NO ARRIVALS

1.. ARRIVAL ANGLES VS. RANGE CALCULATED AND PLOTTED

NR IS THE NUMBER OF RANGE POINTS 1 .LE. NR .LE. 250

DR IS THE INCREMENTAL (AND FIRST) RANGE IN N.MI.

F(I) ARE THE FREQUENCIES - UP TO SIX - IN HERTZ

S IS THE SOURCE DEPTH IN FEET.

R IS THE RECEIVER DEPTH IN FEET.

*IF EITHER SOURCE OR RECEIVER DEPTH IS OUTSIDE THE PROFILE LIMITS (LESS THAN ZERO OR GREATER THAN Z(N)) THE SOURCE OR RECEIVER IS BOTTOMED.

JC(I) ARE THE COHERENCY INDICATORS, AND CORRESPOND TO THE F(I)S 1-TO-1

0 = SEMI-COHERENCE

1 = INCOHERENCE

2 = FULL COHERENCE

*THE VALUES OF JC(I) ARE NORMALLY LEFT BLANK TO INDICATE THAT SEMI-COHERENCE IS TO BE USED FOR ALL FREQUENCIES."

C. FFP

Card No.	Column Nos.	Field Symbol	Format
1	1-72	TITLE	18A4
		An alpha-numeric title specified by the user.	
2	1-10	F (frequency Hz)	E10.4
	11-20	CO (surface velocity) ft/sec.	"
	21-30	ZZR (receiver depth) ft.	"
	31-40	ZZS (source depth) ft.	"
	41-42	LAYER (number of water layers)	"
	43-44	IGO = 0 1 RUN	
		$\neq 0$ loop program to card 2	I2
3	1-20	Z(I+1) (layer depths) ft.	E20.8
	21-40	AAH(I) (H_j for J^{th} layer)	"

The information on this set of cards is obtained from subroutine PROFIT. The number of cards in the set corresponds to LAYER.

Card No.	Column Nos.	Field Symbol	Format
4	1-10	RO (starting point in range, ft.) arbitrary	E10.8
	11-20	PRATIO (density of first bottom layer/density of water)	"
	21-23	M size of FFP (2^M=N)	I2
	23-24	LPRINT = 1 additional checkout prints = 2 normal print output	"
	25-26	LDELTA should always be set = 1	"
5	1-5	IP number of times the FFT is collapsed, IP = 1 no collapsing	I5

The quantity $N=2^M$ is the size of the FFT used in the program (i.e., the total number of range points at which predictions for propagation loss will be obtained of which only the first N/2 values are to be considered valid due to aliasing). Most computers have a maximum array size (e.g., on the NUSC UNIVAC 1108 this is

8192 or M=13). The FFP is dimensioned to this maximum size.

In some instances it is necessary to include more samples than can be accommodated by the maximum array size allowed to achieve an accurate answer.* This is accomplished by utilizing a collapsing technique. The input parameter which controls this option is IP. If IP=1, N samples will be transformed resulting in N answers for propagation loss versus range. If IP is set greater than 1, then in effect IP*N samples will be transformed, again resulting in N answers. This technique can be of great advantage when the FFP is run on computers with limited memory location. If for example the maximum allowed array size is 1024 and it is determined that 16,384 samples are required then IP should be set to 5.

The FFP program automatically sets $\Delta\xi$, the spacing between input samples, equal to the reciprocal of H_{max}, a scale factor used in the process of fitting the sound speed profile. The important information in the integration process is found for the values of ξ smaller than the wave number corresponding to the slowest sound speed, C_{min}, associated with the problem. Then

$$\xi_{max} = 2\pi f/C_{min} + 10\ \Delta\xi .$$

The last term is added as an insurance factor. The smallest wave number, ξ_{min}, considered is then determined by a choice for N and IP according to

$$\xi_{min} = \xi_{max} - (IP*N-1)*\Delta\xi$$

6	1-10	AKI (sound speed in first bottom layer, ft/sec)	E10.4
	11-20	AK (sound speed in second bottom layer, ft/sec)	"
	21-30	ALPHAB (attenuation in both bottom layers, dB/ft)	"
	31-40	DENSR (density in first bottom layer/density in second bottom layer)	"
	41-50	THICK (thickness of first bottom layer, ft)	"

* If N is not chosen sufficiently large, the answers will be in error from the source up to some range which is difficult to determine beforehand. If a question exists about the size of N, the program can be rerun with N doubled, and the new results examined at the close ranges to see if they have significantly changed. With a little experience the user can easily determine whether N is too small, since then the results at the close ranges will yield uncharacteristically high propagation loss values whereas for slightly larger ranges the values of propagation loss will be reasonable.

This last card gives the information about the ocean bottom. It is assumed that a two layered bottom is sufficiently general. Additional layers can be added with a minor change in subroutine BOTTOM. If AK1=AK2 and DENSR=1 the two layered bottom reduces to a semi-infinite bottom.

The program provides N answers for propagation loss at the ranges

$$r_m = r_o + (m-1)\,\Delta r \qquad m=0,1,2...,N-1.$$

Only the first N/2 are considered valid due to aliasing. The spacing between points, Δr is automatically determined

$$\Delta r = \frac{2\Pi}{N\Delta\xi} = \frac{2\Pi}{N} H_{max}$$

where $\Delta\xi$ in an increment of wavelength (i.e., the resolution Δr is proportional to the inverse of the record length in wavelengths).

D. NISSM II - Table 14 (table 7 of reference 6) is a sample deck which will result in the production of a sound speed profile, ray diagram, and transmission loss for two target depths. Included in reference 6 is a table citing default values for the various parameters required by the NISSM II program. Card formats are also given as are options relating to input tables such as attenuation coefficient vs. frequency. Since NISSM II is a system performance model, input tables describing variables such as transmitter response and volume scattering strength are provided for as are parameters such as bandwidth, pulse length and target strength. As demonstrated by the sample deck of table 14 it is not necessary to specify system variables for the computation of transmission loss versus range. The length and complexity of the inputs required by NISSM II (necessitated by its being a system performance model) preclude a complete listing of input variables, options and card formats. These are described in detail in reference 6.

Table 14. Input Deck for Computing Propagation Loss versus Range

```
Δ XQT NISSM2
COMMENT

                        TYRRHENIAN SEA-JUNE 1969

Δ EOF
RANGE AXIS                              0.00      55.0      11.0     KYD
DEPTH AXIS                              0.0    10000.0       5.0     FT
VELOCITY AXIS                           1.50       1.56      6.0     KM/S
VELOCITY PROFILE
FT            DEG F       /1000                39.5
0.0           71.8        38.25
16.0          71.3        38.24
25.0          70.8        38.23
50.0          70.7        38.20
65.0          70.6        38.16
100.0         62.5        38.11
150.0         60.2        38.06
175.0         58.0        38.00
200.0         57.6        38.00
300.0         56.9        38.09
400.0         57.2        38.29
500.0         57.4        38.38
1500.0        57.2        38.62
2500.0        56.5        38.55
4000.0        56.0        38.48
6000.0        56.0        38.40
9840.0        56.0        38.40
Δ EOF
BOTTOM DEPTH                           9840.0 FT
BOTTOM LOSS                               3.0 MGS
FREQUENCY                                3.55 KCPS
SONAR DEPTH                              16.0 FT
MAXIMUM RANGE                            55.0 KYD
SONAR TILT ANGLE                          5.0 DEG
SONAR RESPONSE
DEG          DB
    -90.0     18.0
    -16.0     18.0
    -15.0     14.6
    -14.0     16.1
    -13.0     17.4
    -12.0     15.8
    -11.0     13.2
    -10.0     11.0
    - 9.0      8.8
    - 8.0      7.0
    - 7.0      5.2
    - 6.0      3.6
```

Table 14 (Cont'd). Input Deck for Computing Propagation Loss versus Range

```
      - 5.0      2.3
      - 4.0      1.0
      - 3.0      0.5
      - 2.0      0.2
      - 1.0      0.1
        0.0      0.0
        2.0      0.2
        3.0      0.4
        5.0      1.0
        7.0      2.4
        8.0      3.3
        9.0      4.7
       10.0      5.8
       11.0      6.8
       12.0      7.9
       13.0      9.0
       14.0     10.4
       15.0     12.2
       16.0     13.9
       17.0     15.8
       18.0     18.0
       90.0     18.0
Δ EOF
PROCESS
0.0        20.0     1.0        DEG           2        2        4        4
Δ EOF
RANGE AXIS                     35.0     55.0      4.0      KYD
PROPAGATION LOSS AXIS          40.0    140.0      5.0      DP
MINIMUM RANGE                      35.0 KYD
TARGET DEPTH                       25.0 FT
PROCESS
Δ EOF
TARGET DEPTH                      150.0 FT
PROCESS
Δ EOF
END
Δ FIN
```

E. RAYMODE IV and RAYMODE X - The input requirements for the execution of RAYMODE IV and RAYMODE X are:

a. one card read by format 12A6 followed by
b. a NAMELIST deck called INPUTS.

a. The alphanumeric card is used to title the case. Any comment should be centered within the first 72 columns for best results. If no such title is desired, insert blank card.

b. The NAMELIST data deck is easy to work with when running more than one case. For a new case, the user needs to input only those values different from previously assigned values. Variables may be read in any order and need not be in special fields or on separate cards.

The minimum input information to be supplied by the user consists of:

1) sound velocity profile
2) depth of source and receiver
3) frequency
4) bottom loss table (loss vs. grazing angle) <u>or</u> MGS province number
5) wind speed
6) source beam specified by deviation loss table
7) receive beam specified by deviation loss table
8) range limits and range spacing for propagation loss computations
9) number of ray cycles required for bottom bounce propagation loss computations
10) number of ray cycles required for non-bottom bounce propagation loss computations (e.g., surface duct or convergence zone)

A discussion of the particular input variables are listed in table 15 on page 40. Each variable is typed according to the name rule. Arrays are distinguished by the subscript (I).

Starred entries in the table specify a number of program control variables selectable by the user for special applications. If the user is not sufficiently familiar with the program to assign values to these inputs, he may rely on the default values automatically assigned by the program during execution, which are suitable for almost all cases. A method for estimating the parameter values in 9) and 10) above are given at the end of this discussion. It should be noted that the program can easily be made to assign these values internally, thus relieving the user of this task. (The latter approach has been employed in the adaptation of RAYMODE X to the Optimum Mode Selection (OMS) System for the AN/BQQ-6 sonar.)

Table 15. Definition of RAYMODE X Input Variables

a. ξ_{min},	ALPHANUMERIC HEADING CARD
b. $INPUT$	(NAMELIST name in columns 2 - 8).
N =	No. of points in sound velocity profile, $2<N\leq 50$.
Z(I) =	Depth entries from surface to bottom in ft or yds.
C(I) =	Velocity entries in ft/sec or yd/sec to correspond to depth units <u>or</u> temperature in ^{o}F. A profile may be made up of a mixture of velocity and temperature entries. The depths for any profile involving BT data should be in ft and any included velocities in ft/sec. The program converts each profile to yds and yds/sec. It is better to input all new Z and C arrays than to modify a profile in a previous case.
*SALNTY =	Salinity in 0/00 for conversion of temperatures to sound speed (default 35).
NU =	Index of source depth, $2\leq NU<N$.
MU =	Index of receiver depth, $2\leq MU<N$. Source and receiver depth must be included in the profile.
F =	Frequency in Hz.
MGSOP =	MGS bottom loss province, $0\leq MGSOP\leq 9$ (default 0).
ITAB =	No. of pts in input bottom loss table, $0\leq ITAB\leq 50$ (default 0).
THETA(I) =	Angles in deg. for bottom loss table from 0^{o} to ANGLE.
BL(I) =	Bottom losses in $dB\geq 0$. Set MGSOP = 0 when an input bottom loss table is desired.
R =	Range minimum in yds, R>0.
RMAX =	Range minimum in yds, $RMAX\geq R$.
DELTAR =	Range increment in yds, DELTAR>0. Maximum no. of ranges = 400.
WS =	Wind speed in kts (default 0).
IDL =	No. of pts in source deviation loss table, $0\leq IDL\leq 50$ (default 0).

Table 15. (Cont'd). Definition of RAYMODE X Input Variables

THEDA(I)	=	Angles in deg. for source deviation loss tables to be supplied from -ANGLE to ANGLE.
DL(I)	=	Source deviation losses in dB ≥ 0 corresponding to THEDA(1) angles.
JDL	=	No. of pts in receiver deviation loss table, $0 \leq$ JDL ≤ 50 (default 0).
THEDA2(I)	=	Angles in deg. for receiver deviation loss table to be supplied from -ANGLE to ANGLE.
DL2(I)	=	Receiver deviation losses in dB ≥ 0 corresponding to THEDA2(1) angles. *IDL or JDL = 0 indicates an omni-directional source or receiver.*
*ABL	=	Provides variation to MGS bottom loss curves by adding (B*ABL) dB to MGS curves. $0 \leq$ ABL ≤ 2 (default 0).
LAMDA	=	Maximum no. of ray cycles for propagation modes other than bottom bounce, LAMDA ≥ 0.
LAMDAB	=	Maximum no. of ray cycles for bottom bounce. LAMDA = 0 indicates direct path modes.
*ANGLE	=	Positive and negative ray angular limits in deg, 0^{o} ANGLE 90^{o} (default 60^{o}).
*NL	=	No. of pts in ray tables, $2 <$ NL ≤ 25 (default 10).
*MØ	=	Mode cutoff for mode summation method, $3 \leq$ MØ ≤ 25 (default 10).
*NKEXP	=	Interpolation spacing control within ray tables, $1 \leq$ NKEXP ≤ 4 default 2).
$END		(NAMELIST deck end in columns 2 - 5).

*Starred inputs are defaulted to values adequate for most conditions. In general, they need not be changed.

A good estimate of LAMDA is

LAMDA = IFIX(RMAX/RC)+1

where RC is the smallest average cycle range of surface duct SD (if any) or convergence zone CZ ray paths (if any). That is, the number of ray cycles should be sufficiently large to reach the maximum range selected.

An overly large LAMDA will give accurate results but will cost some execution time due to increased testing; the program does not waste time by computing ray effects beyond the desired RMAX. Since the program runs in considerably less than a minute per case generally, this is not a real problem. A value of LAMDA too small, however, will result in poor overall propagation loss, since not enough ray cycles will have been included.

Similarly LAMDAB may be estimated using RC associated with the smallest bottom bounce angle. This will be roughly the same as the RC for CZ if CZ exists.

Examples of RC:

For CZ in Atlantic or Pacific, RC$\sim$70 kyd.
For CZ in Mediterranean, RC$\sim$35 kyd.
Average SD might be RC$\sim$10 kyd.

The plot of source angle versus range will show the user if LAMDA and LAMDAB are adequate, since these plots must show ray path contributions out to the maximum range (RMAX).

These two inputs have been maintained in order to give the user versatility in looking at various paths. As mentioned earlier, for general propagation loss comparisons the calculations of LAMDA and LAMDAB could be handled by the program.

An example of a RAYMODE X deck for a run producing transmission loss versus range outputs for three cases (source depth = 500 ft, receiver depth = 300 ft, frequency = 400, 500, 2000 Hz) is given in table 16.

Table 16. Sample Multicase Run Stream Table

```
@DATA,L JP*DATA
DATA T7 RL70-5 08/12-07:45:22
                                   PARKA DATA
        $INPUTS
         N=29,
         Z(1)=0.,50.,100.,131.2,164.,180.5,200.,229.1,246.1, 262.5,
         278.9,360.,400.,500.,600.,800.,1200.,1312.3,1968.5,2500.,
         3280.8,4921.2,6561.7,8202.1,9842.5,11482.9,13123.3,16404.2,
         18044.6,
         C(1)=5022.17,5022.99,5023.81,5024.33,5024.87,5025.14, 5025.46,
         5025.95,5026.22,5026.5,5024.32,5018.87,4995.16,4983.05,4911.65,
         4953.37,4922.25,4913.93,4876.22,4861.85,4857.19,4876.77,4894.18,
         4918.49,4947.27,4913.6,5002.04,5000.12,5089.61,
         NU=14,  MU=12,  F=50.,  MGSOP=2,
         R=1000.,  RMAX=260000.,  DELTAR=1060.,  WS=10.,
         NL=25,  MO=10,  LAMDA=5,  LAMDAB=5,  PLOTOP=0,  PLOTT=0,  PLOTCZ=0,
        $END
                                   PARKA DATA
        $INPUTS
         F=400.,
        $END
                                   PARKA DATA
        $INPUTS
         F=500.,
        $END
                                   PARKA DATA
        $INPUTS
         F=2000.,
        $END
END DATA.

@XQT TEN*RAYMOD.RAMODXA
```

ANCILLARY INFORMATION

All model programs provide information other than propagation loss as a function of range. Such information could be useful to a potential customer and is given below:

A. FFP -- Provides the beamformer output, as a function of angle, for a horizontal or vertical linear array.

B. CONGRATS V -- This program is still in the process of development. It is intended to be a generic program of very general application. Included in the available output will be

a) complete ray tracing
b) reverberation as a function of time for a given source-receiver configuration
c) Eigenray solutions
d) Sorting of the eigenrays by angle
e) Six curve fits for sound-speed profiles

It is anticipated that additional features will be implemented.

C. FACT -- Gives angle of arrival for rays arriving at angles within $\pm 25^{o}$.

D. NISSM II -- Plots Available

Velocity versus Depth
Ray Diagram
Propagation Loss versus Range for Specific Target Depth
Reverberation versus Time
- Surface Reverberation
- Bottom Reverberation
- Volume Reverberation
- Total Reverberation

Signal Excess versus Range
Probability of Detection versus Range

Printed Output Available -- Tables

Ray printout at points along the ray:
Range, Depth, Angle (deg), Arc Length, Travel Time, Propagation Loss (dB)

Eigenray printout:
Range, Sonar Angle, Target Angle, Arc Length, Travel Time (sec), Propagation Loss (dB), Phase (deg)

Propagation Loss versus Range {Random Phase Addition; Coherent Phase Addition}

Reverberation versus Time {Surface, Bottom, Volume, Total}

Signal Excess versus Range
Probability of Detection versus Range.

E. Raymode IV -- Raymode X has replaced this model in actual use.

F. Raymode X -- Information obtainable from Raymode X in addition to propagation loss versus range includes:

a. A 2-page input plot which includes plots of the entire profile and an enlarged near-surface profile plus curves of bottom loss vs. grazing angle, surface loss vs. grazing angle, and beam deviation loss vs. angle relative to beam MRA (Maximum Response Axis) if they are being used.

b. Plots of course angle vs. range and receiver angle vs. range for each separate propagation path.

c. A plot of travel time vs. range for each separate propagation path.

d. Travel time differences between multipaths given with respect to an assigned path time reference.

SUMMARY AND CONCLUSIONS

One of the difficult choices facing the sonar systems engineer or underwater acoustician is which among many possible models to use for a given application. Many factors enter into such a decision: (1) Accuracy, (2) Running Time, (3) Computer Storage Required, (4) Ease of Implementation, (5) Complexity of Program Execution, (6) Ease of Effecting Slight Alterations to the Program, and (7) Available Ancillary Information. If information relating to these factors were readily available the selection of a model could be performed with a minimum of effort and a maximum of confidence. An attempt has been made in this report to supply such information for a specific type of model (transmission loss) for the purpose of determining the difficulty in amassing such knowledge and to determine if the resultant of such an effort does indeed optimize the model selection process. Accordingly, transmission loss models available at the Naval Underwater Systems Center were examined in terms of the aforementioned factors. The models were CONGRATS V, FACT, NISSM II, RAYMODE IV and RAYMODE X and they were run using both coherent and incoherent phase addition. Eight cases were examined; in the first six the Fast Field Program (FFP) was the standard of comparison and (1/3-octave) PARKA data was the standard for the remaining two cases. In all cases a single sound speed profile appropriate to the PARKA data was used in producing model outputs. The first six cases are for frequencies of 50, 500 and 2000 Hz with source and receiver (1) both in a surface duct and (2) both below the surface layer. The last two cases have both source and receiver below the layer and the frequencies are 50 and 400 Hz. (In the last two cases the FFP was included among the models in two forms; first, under the normal assumption of an infinitely long CW source and, secondly, assuming a 1/3-octave source with a flat spectrum over the band.)

In the assessment of accuracy, coherent models were compared quantitatively in terms of their range dependent mean levels (as obtained through polynomial fits). Incoherent models yield outputs essentially lacking in rapid fluctuations and hence were compared to the standard without further smoothing (as was also the case for the 1/3-octave FFP output). The approach used provides the information required to determine the accuracies of two or more models from a small number of quantitative measures and also provides intermediate products useful in the analysis of discrepancies between a given model and the standard. For the cases listed above, two models achieved essentially equal overall accuracy and, therefore, share a first place standing in accuracy - CONGRATS V and RAYMODE X. This should not be interpreted as meaning that other models are not sufficiently accurate for specific applications - this issue is to be decided by the user.

Computer run times were normalized to account for differences in numbers of points generated by each model. The models exhibiting the shortest run times were FACT and RAYMODE X. It must be recognized that programs have been optimized for short running times to varying degrees. The results obtained do not imply that slower programs cannot be so optimized. These same general comments can also be made in regard to computer storage requirements. In the cases examined above, the models which required the least storage (excluding storage required for plot routines) were RAYMODE IV and RAYMODE X.

Ease of implementation of a given program on a specific computer is a factor not directly addressed in this report. Although the number of different computers on which a program has successfully been run is an indicator, it can be misleading for those programs which have been recently developed or are still in the development

stage. Another indirect manner in which ease of implementation may be assessed is through available documentation. Accordingly a list of references has been provided (see p. 49). Of perhaps primary assistance to a user in determining ease of implementation is access to the author(s) of a given program (or people completely acquainted with the program). To this end, a list of such personnel has been included (see p. 30).

The complexity of program execution is well revealed by providing the input card deck required to run the program with appropriate definitions, default values and explanations of the meaning of various parameters and guidance relating to their selection. Such information has been provided in the body of this report to a limited extent. In this context, "user's guides" can be most valuable and the reader is referred to the list of references. The desirability of a given input deck depends upon its requirements vis-a-vis the requirements for a given application. The degree of concordance between desired and actual complexity of program execution must be assessed by the user.

It is quite possible that a program is "almost right" for a given application and that slight alterations are required. Even given a program listing, effecting a slight alteration may be complex and involve several subroutines. For this reason, consultation with the author of a program (or a person fully cognizant of all programming details) is recommended. Once again the reader is directed to the list on page 30.

Ancillary information may be desirable or not depending on the application. Some models provide only transmission loss versus range. Others are components of a complete systems model and, thus, can provide a variety of information such as reverberation level vs. time, probability of detection vs. range, etc. A list of available ancillary information for each model is to be found on pages 44-45.

In attempting to provide information relating to the factors needed for an intelligent choice of a model for a given application various conclusions can be drawn: (1) The quantitative method of accuracy assessment utilized leads to results easily interpreted by a user in terms of an accuracy requirement. Although the use of several polynomials requires somewhat subjective decisions with regard to identifying significant features in a data record and breaking up this record accordingly, an examination of the results reveals this problem to be of minor significance (i.e., different choices would have negligible effects on final results). Nonetheless, future smoothing of records with rapid fluctuations will be done using moving averages, thereby obtaining greater objectivity. (2) The choice of weighting factors to be utilized in the quantitative assessment of model accuracy is best determined by the user based upon system parameters, environmental scenarios and tactical constraints. (3) The standard(s) of comparison must be of significance to the user. (4) A sufficient number of environmental situations must be treated for the final results to lead to a valid choice of a "best" model for a specific application.

The matrix of information provided for the various candidate models should lead to model selection for various applications in a more optimal fashion than has been heretofore possible. The matrix presented and applied to transmission loss models in this report is general in its nature and the same techniques can be applied to any type of model.

It should be stressed that the methodology described in this report is still in a state of evolution. Some changes to be introduced in furture analyses - - the use of sliding averages instead of polynomials for smoothing and the determination of range intervals on the basis of physical features of the acoustic path - - have already been mentioned. Other possible changes, such as the use of higher statistical moments, will also be considered.

REFERENCES

1. C. W. Spofford, "The FACT Model, Vol. I" (U) Acoustic Environmental Support Detachment, Maury Center for Ocean Science, Office of Naval Research MC Report 109, November, 1974 (UNCLASSIFIED).

2. C. L. Baker and C. W. Spofford, "The FACT Model, Vol. II" (U) Acoustic Environmental Support Detachment, Office of Naval Research, AESD Technical Note TN-74-04, December, 1974 (UNCLASSIFIED).

3. F. R. DiNapoli and D. Ryan, "Implementation of the FACT Model on the NUSC UNIVAC 1108," NUSC Technical Memorandum TA11-3-74, 10 January 1974 (UNCLASSIFIED).

4. C. S. Clay, "Sound Transmission in a Half Channel and Surface Duct," Technical Notes on Sound Propagation in the Sea, Vol. 2, Meteorology International, Inc., Project M-153, Monterey, California, August 1968.

5. F. R. DiNapoli, "Fast Field Program for Multi-Layered Media," NUSC Technical Report 4103, 26 August 1971 (UNCLASSIFIED).

6. H. Weinberg, "Navy Interim Surface Ship Model (NISSM) II," NUC Technical Publication 372 and NUSC Technical Report 4527, 14 November 1974 (UNCLASSIFIED).

7. G. A. Leibiger, "A Combined Ray Theory-Normal Mode Approach to Long Range, Low Frequency Propagation Loss Prediction," (U) NUSC Technical Memorandum PA3-0109-71, 13 August 1971 (CONFIDENTIAL).

8. D. F. Yarger, "A User's Guide for the RAYMODE X Propagation Loss Program," NUSC Technical Memorandum No. PA32-10-76, 9 August 1976 (UNCLASSIFIED).

APPENDIX A

AVERAGING: DECIBELS VERSUS PRESSURE

In all the analyses described in this report smoothing of propagation loss data was accomplished by operating on values expressed in decibels. Smoothing of data expressed in terms of physical parameters such as acoustic intensity (pressure squared) and acoustic pressure was undertaken for comparison purposes. Two smoothing functions were used: polynomials and sliding averages. In each case the decibel (dB) values were converted to the "physical" parameters; these were then smoothed and the resultant values reconverted to decibels. Case 4 (source depth = 500 ft., receiver depth = 300 ft., frequency = 50 Hz) data were chosen for these calculations. The results are described in what follows.

POLYNOMIALS

The Case 4 FFP propagation loss values, PL, expressed in decibels were converted to the parameter A*, proportional to acoustic pressure, by means of

$$A = \text{antilog } (PL/20).$$

The set A was then subdivided into the same five groups as the original data, and a best fit polynomial for each group was found. The values obtained from the polynomials were then reconverted to decibels by means of the inverse of the relation given above. However, some of the values of A determined by the polynomials were negative. Specifically, the first ten values (corresponding to the ten smallest values of range) and eight values at ranges in the vicinity of 70 kyd were negative. An attempt to use acoustic intensity (or pressure squared) as the parameter in this comparison failed for the same reason. Since pressure squared cannot be negative, the parameter A, proportional to pressure, was used instead. Since a logarithm of a negative number is not real, it was decided to ignore these 18 negative numbers in all further data processing. The remaining dB values are shown plotted in figure A3. Figures A1 and A2 show, respectively, the original FFP data and the polynomial approximations obtained from the original dB values.

A comparison of the pertinent figures will show that the polynomials fit to the data expressed in decibels give a much better approximation to the original data than the "A polynomials". Thus the "A polynomials" show marked distortion in the bottom bounce region (ranges between 35 and 65 kyd) and in both sections of the convergence zone (ranges between 60 and 75 kyd). The "dB polynomials", on the other hand, show good agreement with the original data throughout the whole curve. This is to be expected. For, whatever physical reason one may have for converting the data to other units prior to processing, mathematically one would expect better agreement with the original data when the approximating function uses the original data rather than "converted" data.

SLIDING AVERAGES

The sliding averages were formed as follows: the arithmetic mean of propagation loss values 1 to n was found. The process was repeated for points 2 to n+1,

*From $PL = 20 \log(P/P_o)$, one gets $A = P/P_o = \text{antilog } (PL/20)$. Thus A is the ratio of the acoustic pressure at the receiver to the index pressure.

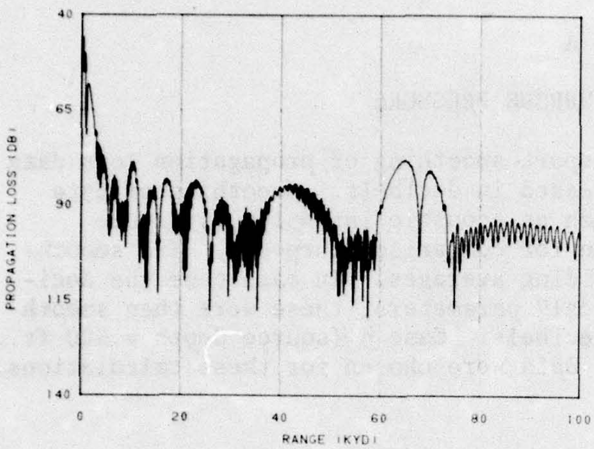

FFP VALUES

F=50HZ,ZS=500FT,ZR=300FT, CASE 4

FIGURE A1

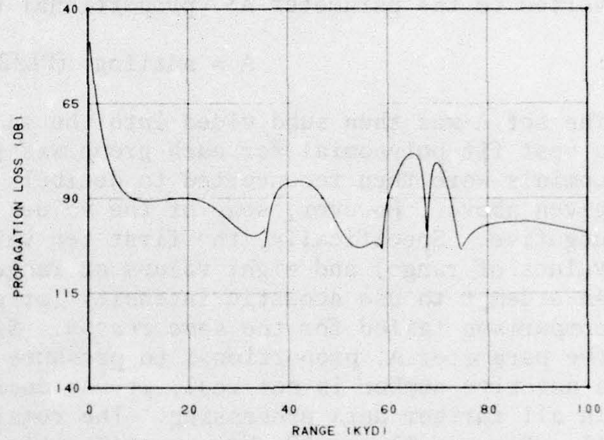

SEVENTH DEGREE POLYNOMIALS COMPUTED USING DB VALUES

FFP, 50,500,300, CASE 4

FIGURE A2

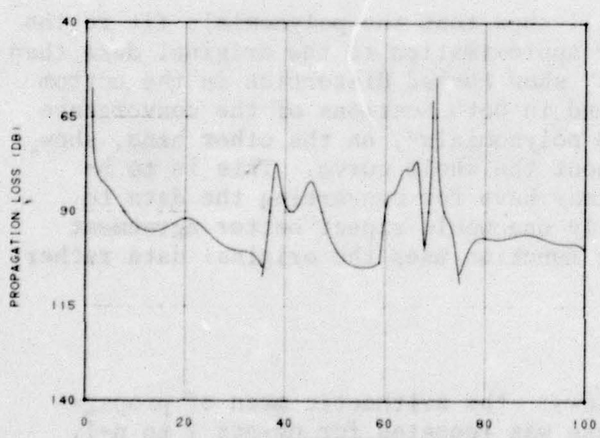

SEVENTH DEGREE POLYNOMIALS COMPUTED USING PRESSURES

FFP, 50,500,300, CASE 4

FIGURE A3

then for 3 to n+2, etc., until all available sets of n points had been used. The range corresponding to the first set of n points was the largest listed range that was equal to or less than the mean of the first n ranges. Successive listed ranges were then associated with averages of successive groups of points. Models used were FFP and coherent values of NISSM II for Case 4. The averaging process was applied to the dB values of propagation loss, PL, and to a parameter B, proportional to acoustic pressure squared, where

$$B = \text{antilog } (PL/10).$$

The averaged values of B were then reconverted to decibels. The parameter n (the number of points in each set) was assigned values so that averaging would take place successively over range intervals of 2, 4 and 8 kyd for the NISSM II model. For the FFP, choices of n of 30, 50, 100, and 200 points correspond to averaging over ranges of 2.35, 3.92, 7.84, and 15.69 kyd. The sets of averaged points were plotted as a function of the respective ranges.

The results obtained with the FFP and NISSM II models are shown in figures A4-A11 and A12-A18, respectively. Figure A4 shows the result of "pressure-squared" averaging of the FFP with the number of points involved in the average equal to 30; figure A5 shows the corresponding result for "decibel averaging". The figure sets (A6,A7), (A8,A9), and (A10,A11) present similar results for n equal to 50, 100, and 200 points, respectively. Figure A12 shows the original NISSM II coherent results for case 4. Figures A13-A18 show the results of averaging these data over the range intervals of 2, 4, and 8 kyd. Once again, both "decibel averaging" and "pressure-squared averaging" were performed.

Reference to the figures will show that both types of averaging have the predictable effect of eliminating much of the "fine structure" of the original data, and also of "compressing" the data - that is, both high and low spikes are clipped. However, "pressure square averaging" also has the effect of broadening the (reduced) spikes. The broadening is proportional to n, the range interval used in the averaging. This is explained by the fact that a difference of several dB between neighboring points is magnified manyfold when the values are expressed as pressure squares. Thus in the latter unit the spike will dominate the n groups of values in which it appears, thus broadening the spike. This broadening effect on the individual spikes in turn causes a narrowing of both the bottom bounce zone (30 to 55 kyd range) and the convergence zone (60 to 75 kyd) by prolonging the effect of the spikes into these regions. This broadening is largely absent in "dB averaging". If n is so chosen that averaging is over a large range interval, then the features of the original curve are completely lost in "pressure averaging" -- as in figures A10 and A11, in which the range interval is almost 16 kyd.

Here too, processing the original data yields better results than conversion of data prior to processing. "dB averaging" retains the major features of the original curve, while "pressure square averaging" distorts these features, and, if the averaging interval is large enough, these features are completely lost.

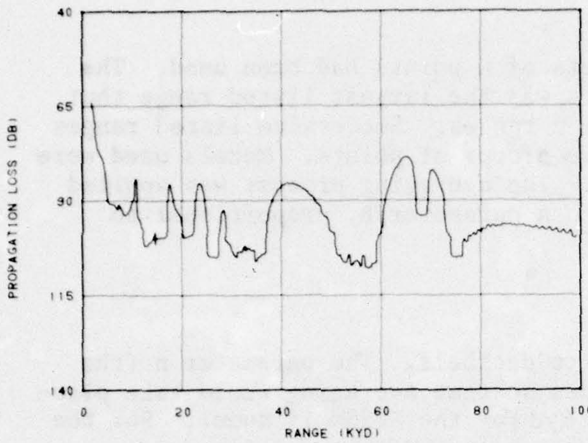

PROPAGATION LOSS COMPUTED BY AVERAGING PRESSURE-SQUARES
FFP, 50,500,300, CASE 4
NUMBER OF POINTS AVERAGED = 30

FIGURE A4

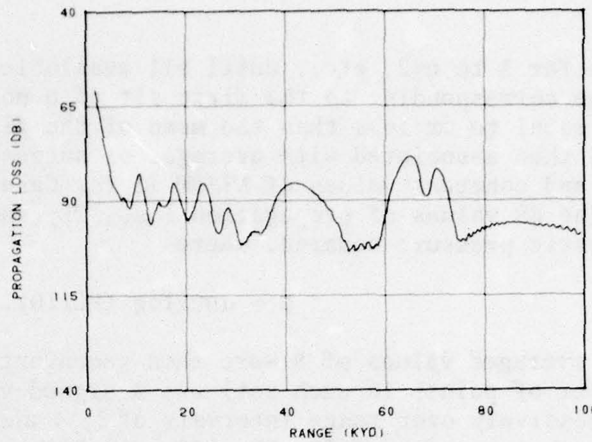

PROPAGATION LOSS COMPUTED BY AVERAGING DB'S
FFP, 50,500,300, CASE 4
NUMBER OF POINTS AVERAGED = 30

FIGURE A5

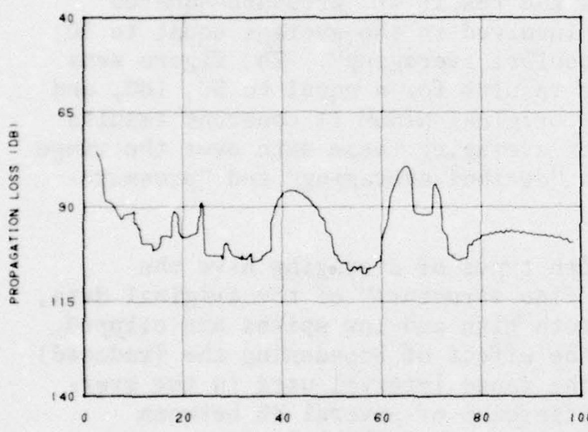

PROPAGATION LOSS COMPUTED BY AVERAGING PRESSURE-SQUARES
FFP, 50,500,300, CASE 4
NUMBER OF POINTS AVERAGED = 50

FIGURE A6

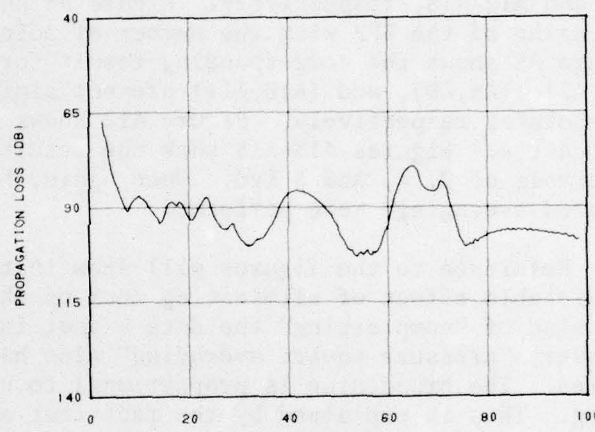

PROPAGATION LOSS COMPUTED BY AVERAGING DB'S
FFP, 50,500,300, CASE 4
NUMBER OF POINTS AVERAGED = 50

FIGURE A7

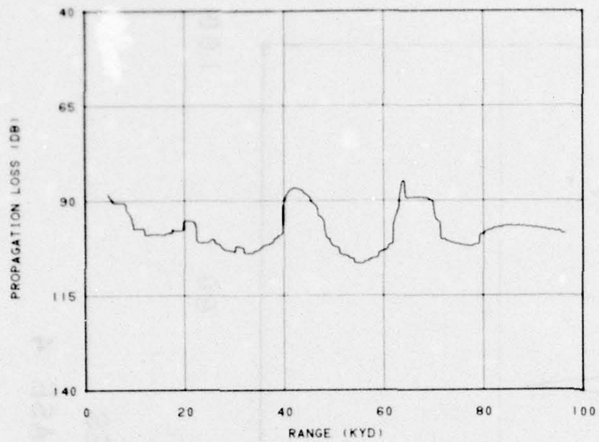

PROPAGATION LOSS COMPUTED BY AVERAGING PRESSURE-SQUARES
FFP, 50,500,300, CASE 4
NUMBER OF POINTS AVERAGED = 100

FIGURE A8

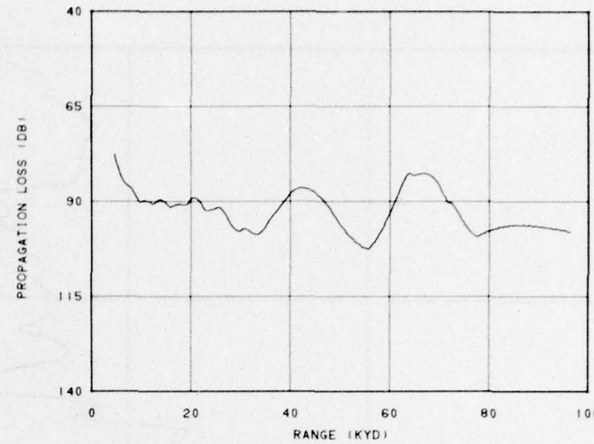

PROPAGATION LOSS COMPUTED BY AVERAGING DB'S
FFP, 50,500,300, CASE 4
NUMBER OF POINTS AVERAGED = 100

FIGURE A9

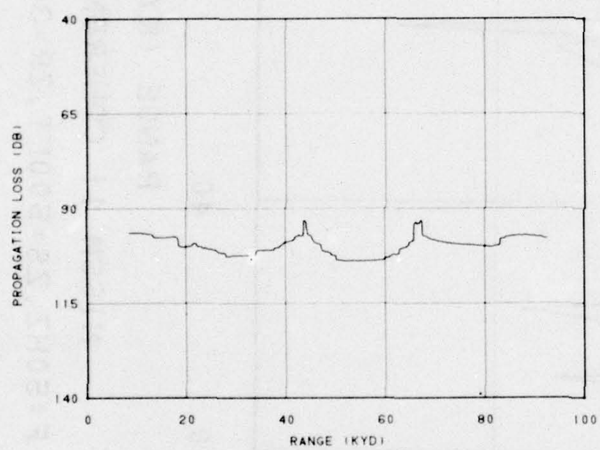

PROPAGATION LOSS COMPUTED BY AVERAGING PRESSURE-SQUARES
FFP, 50,500,300, CASE 4
NUMBER OF POINTS AVERAGED = 200

FIGURE A10

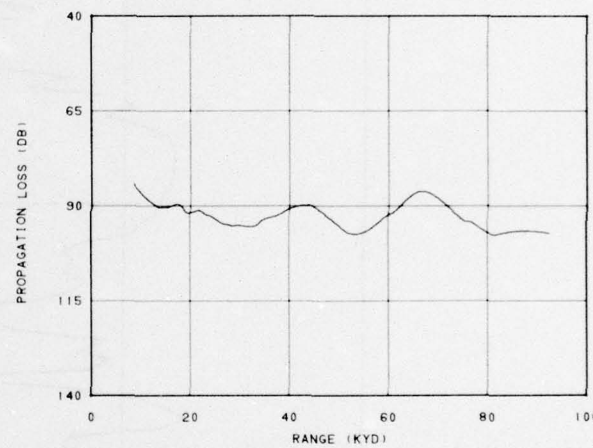

PROPAGATION LOSS COMPUTED BY AVERAGING DB'S
FFP, 50,500,300, CASE 4
NUMBER OF POINTS AVERAGED = 200

FIGURE A11

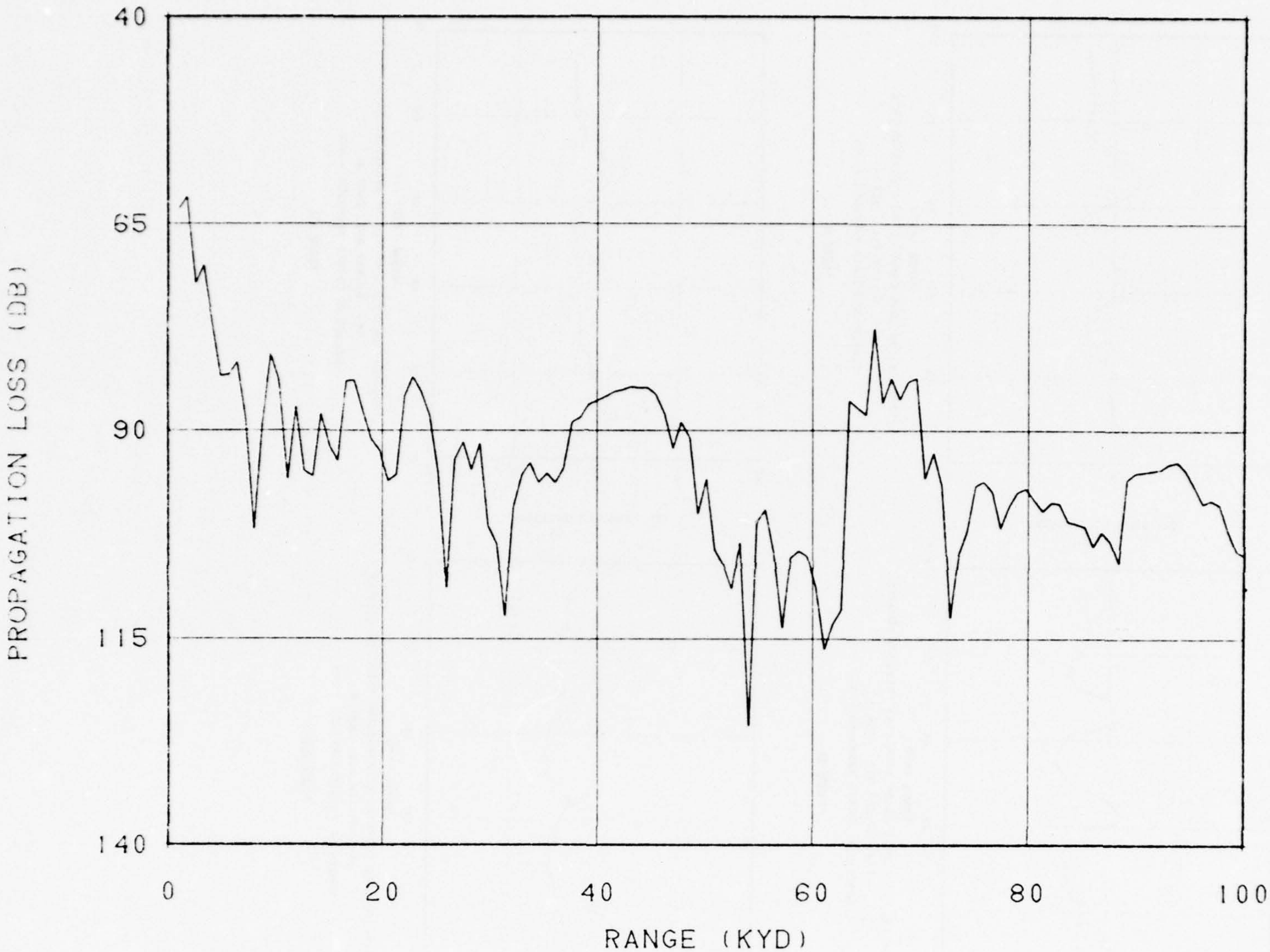

NISSM II COHERENT VALUES

F=50HZ,ZS=500FT,ZR=300FT, CASE 4

FIGURE A12

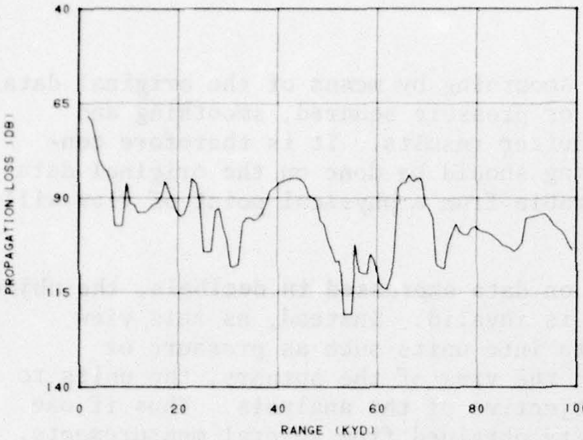

PROPAGATION LOSS COMPUTED BY AVERAGING PRESSURE-SQUARES
NISSM II COHERENT, CASE 4
NUMBER OF POINTS AVERAGED = 3

FIGURE A13

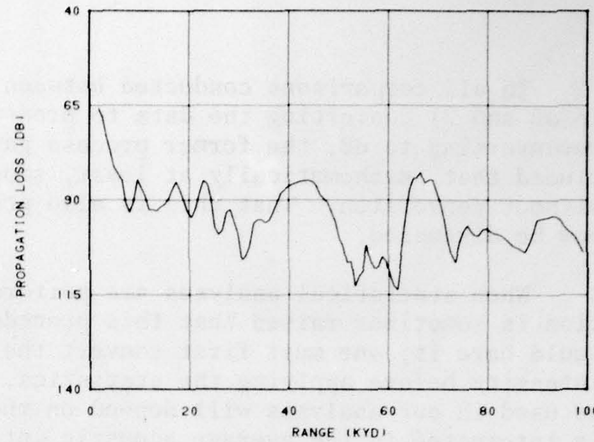

PROPAGATION LOSS COMPUTED BY AVERAGING DB'S
NISSM II COHERENT, CASE 4
NUMBER OF POINTS AVERAGED = 3

FIGURE A14

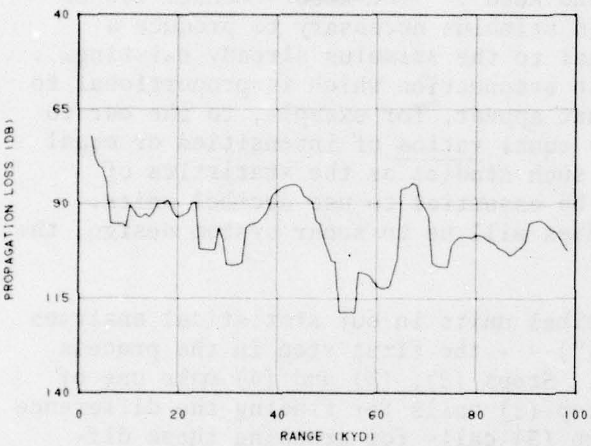

PROPAGATION LOSS COMPUTED BY AVERAGING PRESSURE-SQUARES
NISSM II COHERENT, CASE 4
NUMBER OF POINTS AVERAGED = 5

FIGURE A15

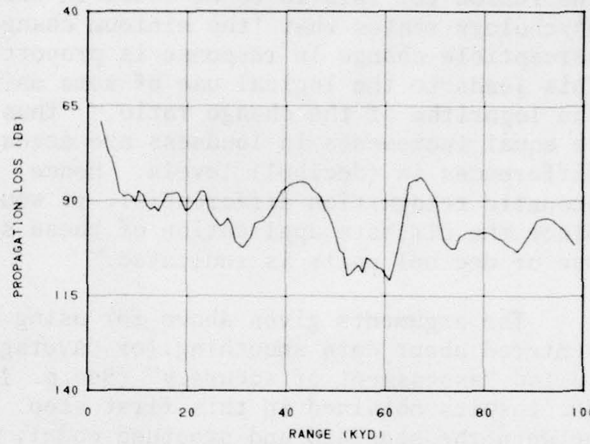

PROPAGATION LOSS COMPUTED BY AVERAGING DB'S
NISSM II COHERENT, CASE 4
NUMBER OF POINTS AVERAGED = 5

FIGURE A16

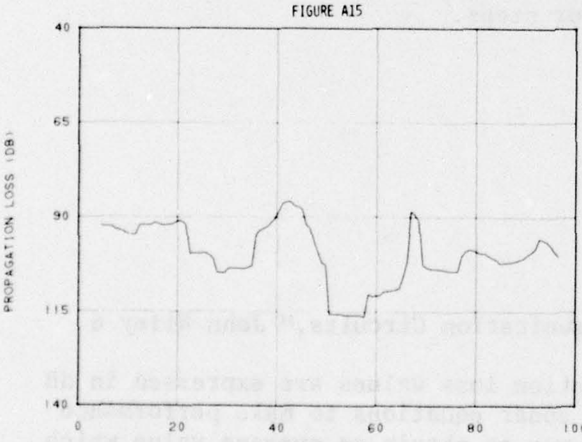

PROPAGATION LOSS COMPUTED BY AVERAGING PRESSURE-SQUARES
NISSM II COHERENT, CASE 4
NUMBER OF POINTS AVERAGED = 10

FIGURE A17

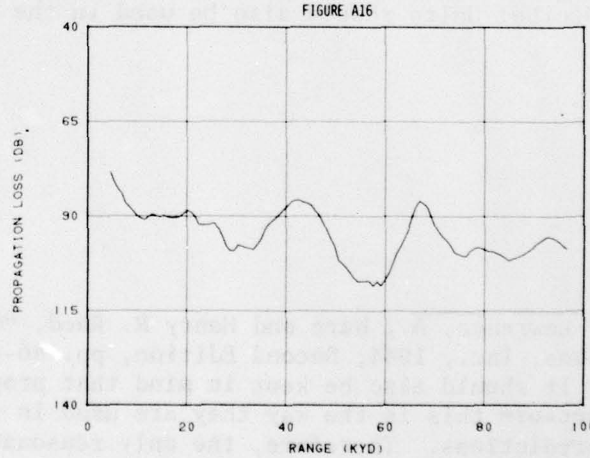

PROPAGATION LOSS COMPUTED BY AVERAGING DB'S
NISSM II COHERENT, CASE 4
NUMBER OF POINTS AVERAGED = 10

FIGURE A18

In all comparisons conducted between 1) smoothing by means of the original data in dB and 2) converting the data to pressure or pressure squared, smoothing and reconverting to dB, the former process gave better results. It is therefore concluded that, mathematically at least, smoothing should be done on the original data without conversion. That this is also preferable from a physical point of view will now be discussed.

When statistical analyses are performed on data expressed in decibels, the objection is sometimes raised that this procedure is invalid. Instead, as this view would have it, one must first convert the data into units such as pressure or intensity before applying the statistics. In the view of the authors, the units to be used in our analysis will depend on the objective of the analysis. Thus if one is interested in the average acoustic intensity obtained from several measurements, averaging of decibel units is incorrect. However, if one is dealing with the response of a human operator to acoustic waves, use of decibel units is correct. The reason for this is to be found in Ware and Reed*: "The Weber-Fechner law of phychology states that 'the minimum change in stimulus necessary to produce a perceptible change in response is proportional to the stimulus already existing. . . This leads to the logical use of some unit in attenuation which is proportional to the logarithm of the change ratio." Thus what appear, for example, to the ear to be equal increments in loudness are actually equal ratios of intensities or equal differences in (decibel) levels. Hence, in such studies as the statistics of acoustic recognition differential, it would be essential to use decibel units. Since the ultimate application of these studies will be to sonar system design, the use of decibel units is indicated.†

The arguments given above for using decibel units in our statistical analyses centered about data smoothing (or "averaging") - - the first step in the process called "assessment of accuracy" (See p. 14). Steps (2), (3) and (4) make use of the results obtained in this first step. Step (2) calls for finding the difference between the standard and smoothed model; step (3) calls for grouping these differences; and step (4) calls for finding μ and σ for each group. Since it was shown that the use of decibel units in step (1) is called for, it follows that decibel units should also be used in the other steps.

---

* Lawrence, A., Ware and Henry R. Reed, "Communication Circuits," John Wiley & Sons, Inc., 1944, Second Edition, pp. 46-47.

† It should also be kept in mind that propagation loss values are expressed in dB because this is the way they are used in the sonar equations to make performance predictions. Therefore, the only reasonable way to obtain an average value which is representative of the individuals in the group is to compute the average in dB.

POLYNOMIALS VERSUS SLIDING AVERAGES*

Of the two types of smoothing used so far in these studies, sliding averages, for an appropriate value of N, yield a closer approximation to the original data than do polynomials. In the former, while rapid fluctuations are smoothed out, slower fluctuations are retained. This tends to retain many details of the original data, including some unwanted ones. Polynomials as used in these studies, on the other hand, have smoothed out all but major features of the original data. One reason for this is that when the data were subdivided into groups for polynomial approximation, each group usually included many more points than were included in the groups used in sliding averages. Increasing the size of the group in the latter process tends to distort the original curve unduly. Mathematically, polynomials can be stored as a set of coefficients, something which cannot be done with sliding averages. On the other hand, the polynomial method requires the making of choices in the process of subdividing the data into sets, whereas this is avoided if sliding averages are used. After considering all the factors discussed above, it was decided to use sliding averages for data smoothing in future analyses.

---

* Processing in decibel units is assumed in this section.

APPENDIX B

Appendix B contains all figures pertaining to the quantitative assessment of accuracy. Each figure is designated by a roman numeral, an arabic numeral and a letter (e.g., V-3C). The roman numeral gives the case (i.e., roman numeral V corresponds to Case 5). Arabic numerals denote the various models, as follows:

1 - FFP

2 - CONGRATS V

3 - FACT

4 - NISSM II

5 - RAYMODE IV

6 - RAYMODE X

For roman numerals I-VI and arabic numeral 1, the letter A gives the raw model output while B gives the analytical fit. For roman numerals I-VI and arabic numerals 2-6, the letters designate the following:

A - Raw Model Output (Coherent Phase Addition)

B - Analytical Fit to (A)

C - FFP Analytical Fit Minus (B)

D - Raw Model Output (Incoherent Phase Addition)

E - FFP Analytical Fit Minus (D)

For roman numerals VII and VIII and for all arabic numerals with the exception of 1, the letters designate the following:

A - PARKA Experimental Data and Raw Model Output (Coherent Phase Addition)

B - PARKA Experimental Data and the Analytical Fit to the Model

C - PARKA Experimental Data Minus the Analytical Fit to the Model

D - PARKA Experimental Data and Raw Model Output (Incoherent Phase Addition)

E - PARKA Experimental Data Minus the Incoherent Model Output

For 1 (i.e., the FFP) these letter designations hold upon replacement of the phrases "Coherent Phase Addition" and "Incoherent Phase Addition" by "CW" and "1/3-Octave", respectively.

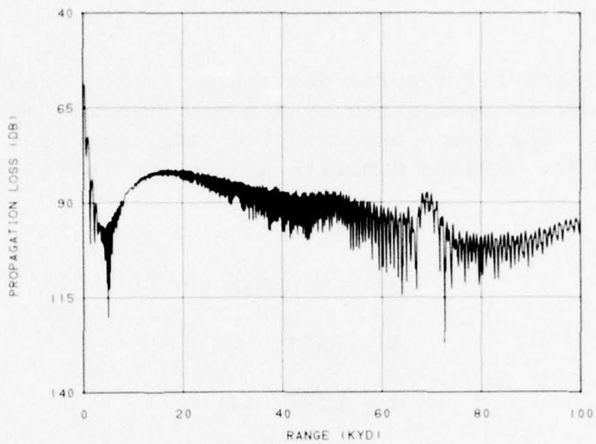

(I-1A) FFP

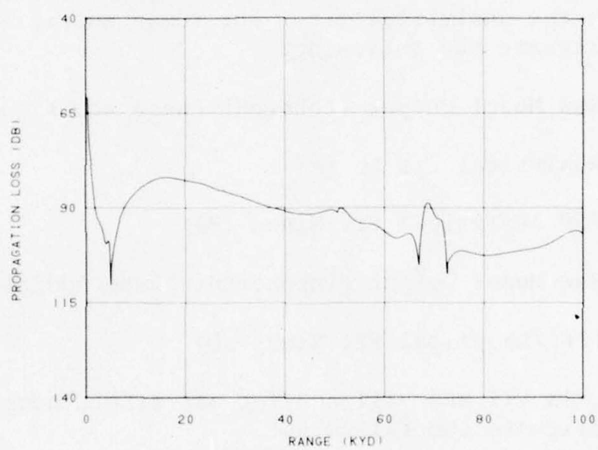

(I-1B) ANALYTICAL FIT TO FFP

FIGURE I-1

FFP RESULTS

CASE I:
FREQUENCY = 50 HERTZ
SOURCE DEPTH = 50 FEET
RECEIVER DEPTH = 50 FEET

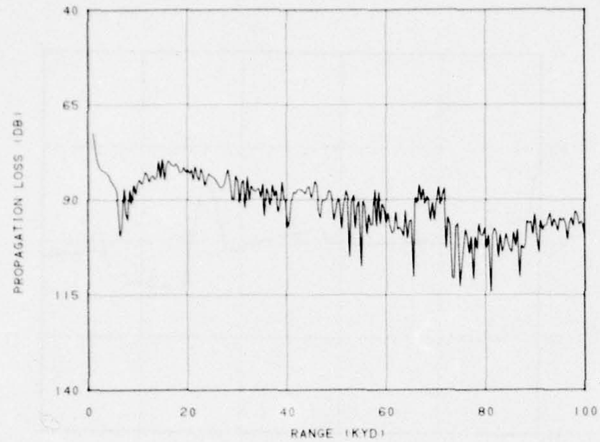

(I-2A) CONGRATS V (COHERENT)

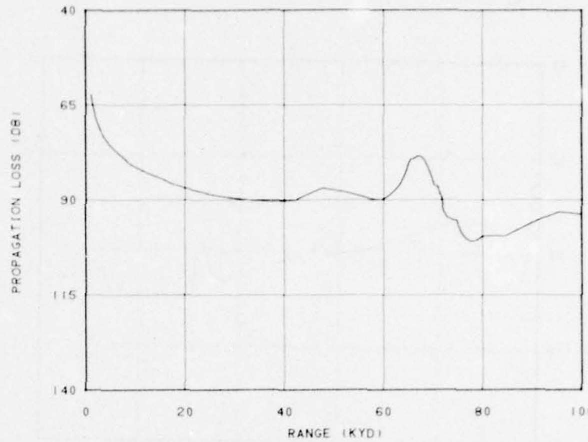

(I-2D) CONGRATS V (INCOHERENT)

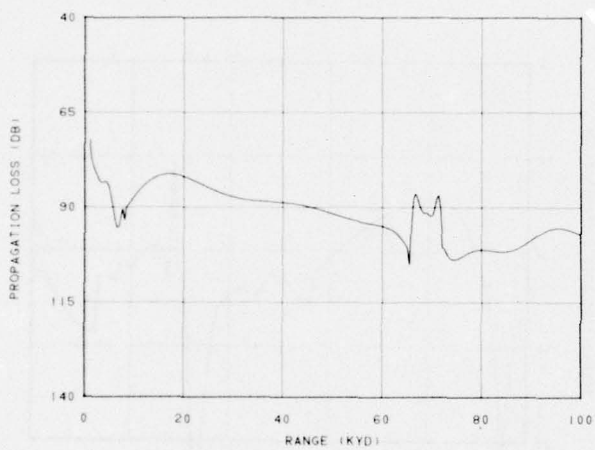

(I-2B) ANALYTICAL FIT TO CONGRATS V (COHERENT)

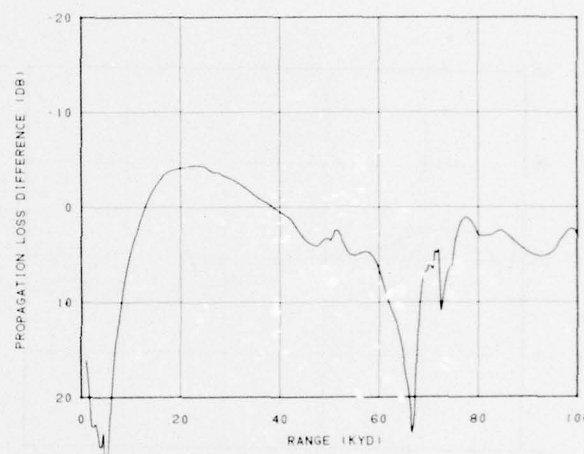

(I-2E) FFP ANALYTICAL FIT MINUS CONGRATS V (INCOHERENT)

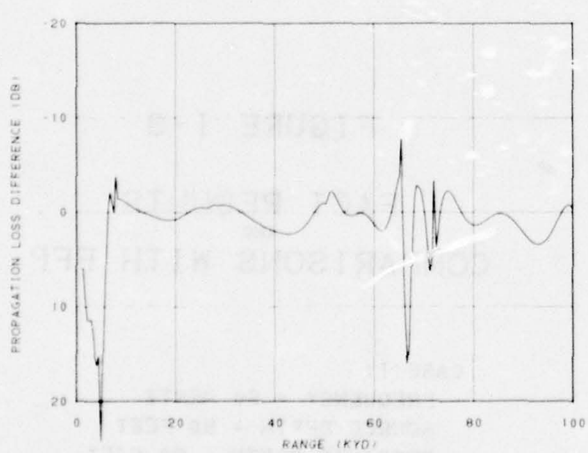

(I-2C) FFP ANALYTICAL FIT MINUS CONGRATS V (COHERENT) ANALYTICAL FIT

FIGURE I-2

CONGRATS V RESULTS
AND
COMPARISONS WITH FFP

CASE I:
FREQUENCY = 50 HERTZ
SOURCE DEPTH = 50 FEET
RECEIVER DEPTH = 50 FEET

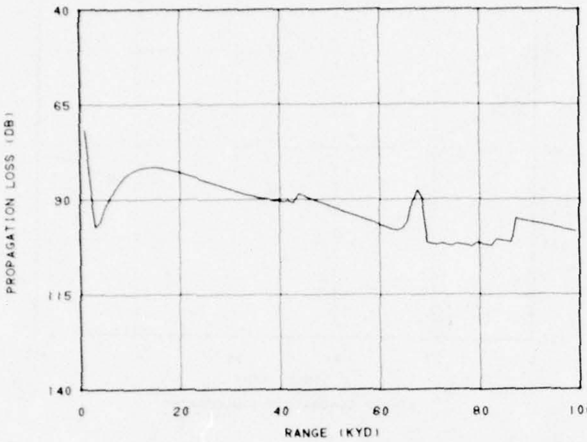

(I-3A) FACT (COHERENT)

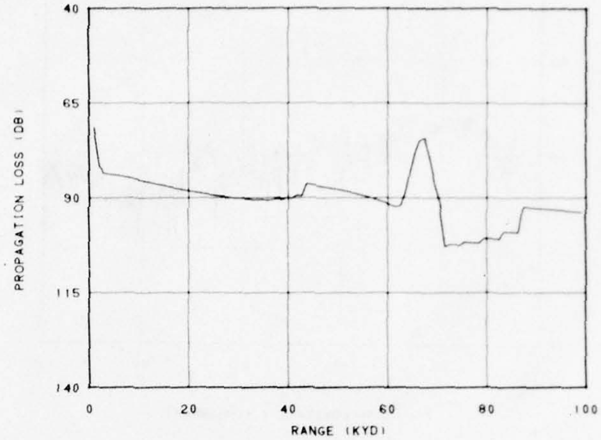

(I-3D) FACT (INCOHERENT)

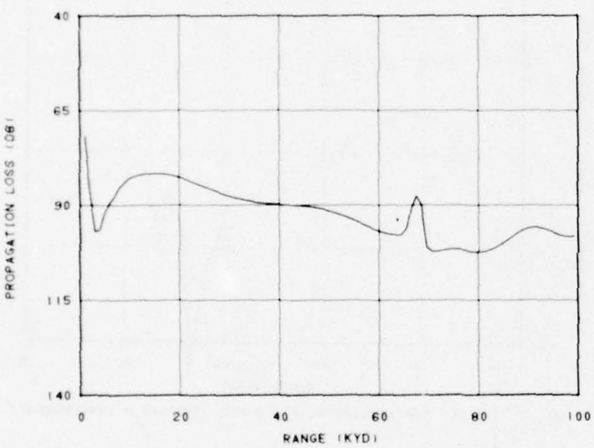

(I-3B) ANALYTICAL FIT TO FACT (COHERENT)

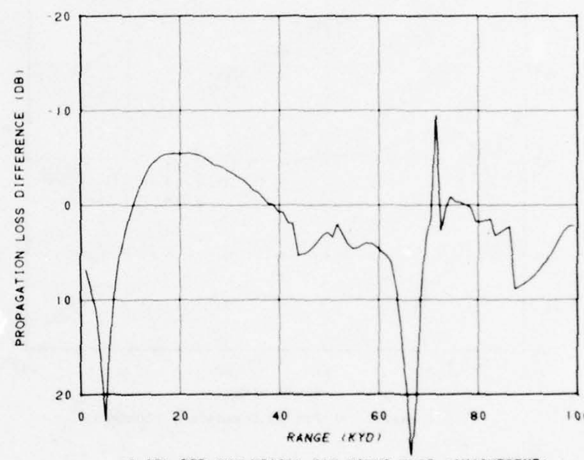

(I-3E) FFP ANALYTICAL FIT MINUS FACT (INCOHERENT)

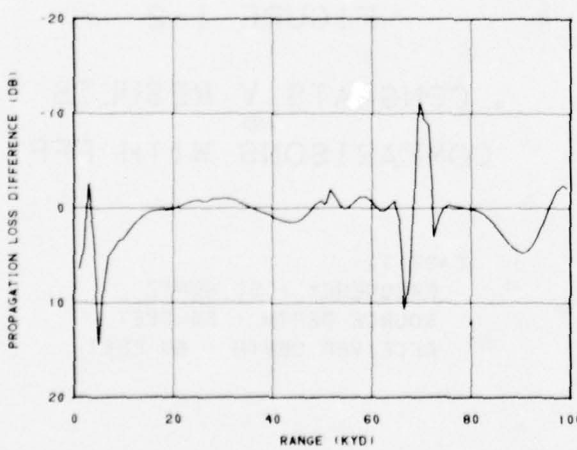

(I-3C) FFP ANALYTICAL FIT MINUS FACT (COHERENT) ANALYTICAL FIT

FIGURE I-3

FACT RESULTS AND COMPARISONS WITH FFP

CASE I:
FREQUENCY = 50 HERTZ
SOURCE DEPTH = 50 FEET
RECEIVER DEPTH = 50 FEET

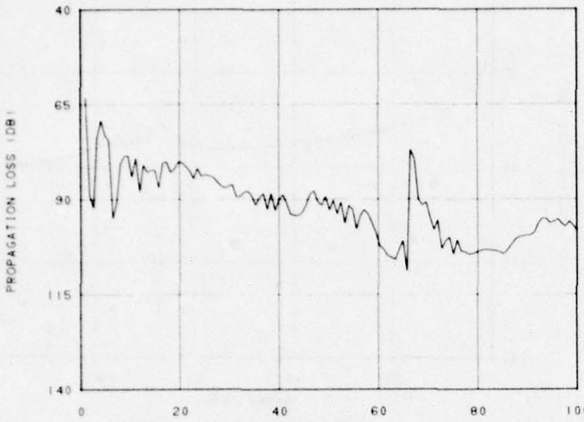

(I-4A) NISSM II (COHERENT)

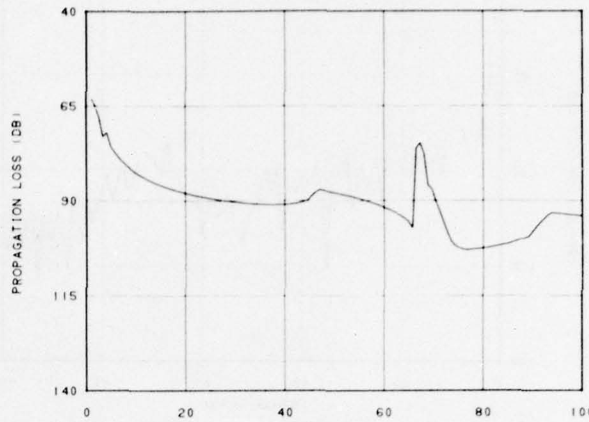

(I-4D) NISSM II (INCOHERENT)

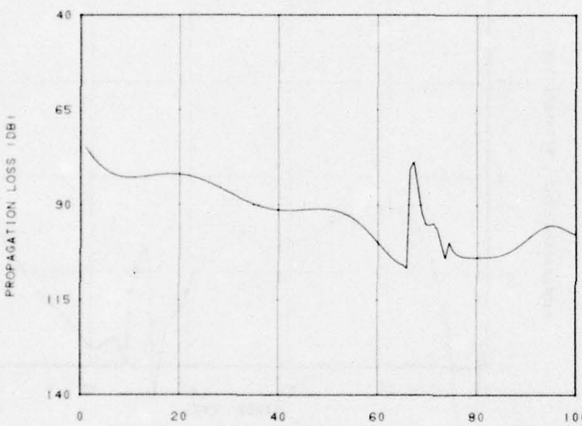

(I-4B) ANALYTICAL FIT TO NISSM II (COHERENT)

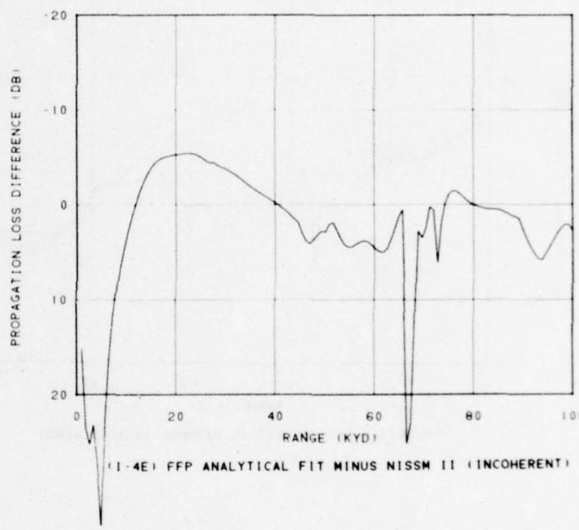

(I-4E) FFP ANALYTICAL FIT MINUS NISSM II (INCOHERENT)

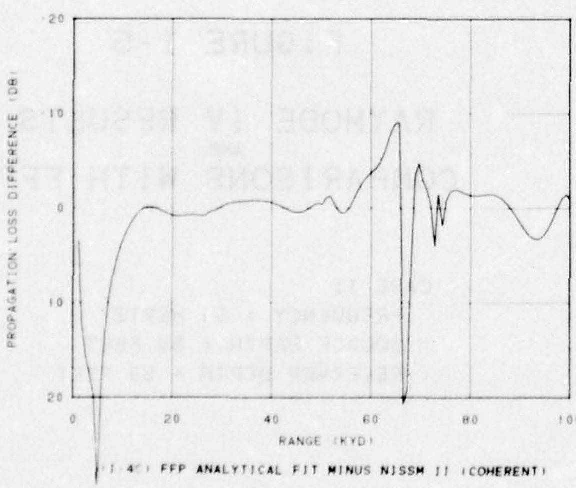

(I-4C) FFP ANALYTICAL FIT MINUS NISSM II (COHERENT)

ANALYTICAL FIT

FIGURE I-4

NISSM II RESULTS
AND
COMPARISONS WITH FFP

CASE I:
FREQUENCY = 50 HERTZ
SOURCE DEPTH = 50 FEET
RECEIVER DEPTH = 50 FEET

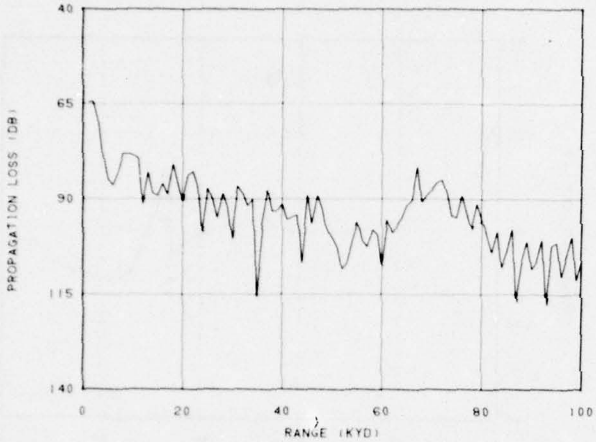

(I-5A) RAYMODE IV (COHERENT)

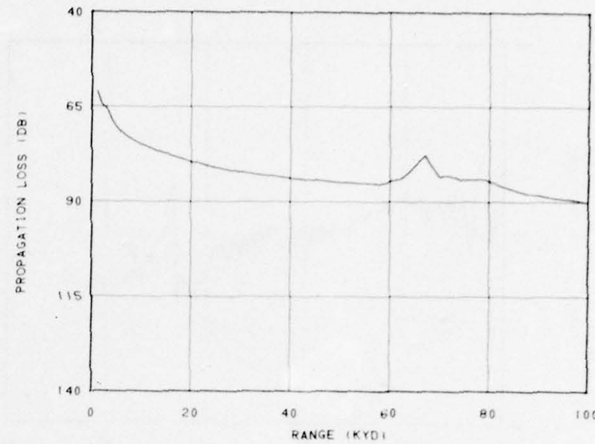

(I-5D) RAYMODE IV (INCOHERENT)

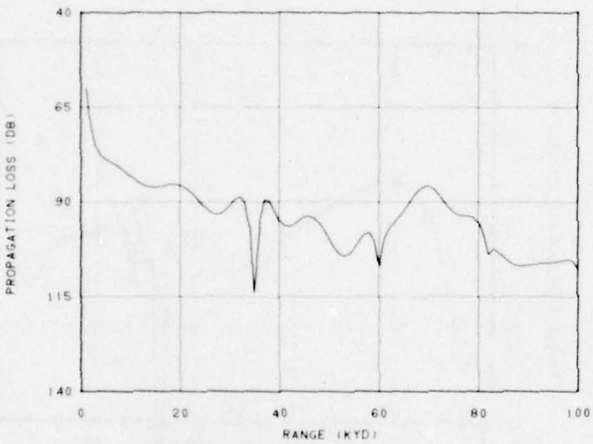

(I-5B) ANALYTICAL FIT TO RAYMODE IV (COHERENT)

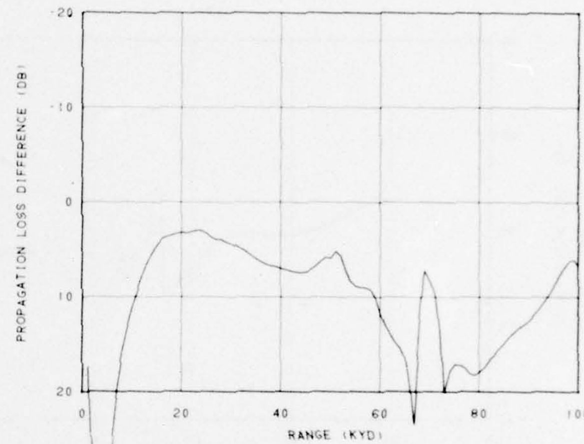

(I-5E) FFP ANALYTICAL FIT MINUS RAYMODE IV (INCOHERENT)

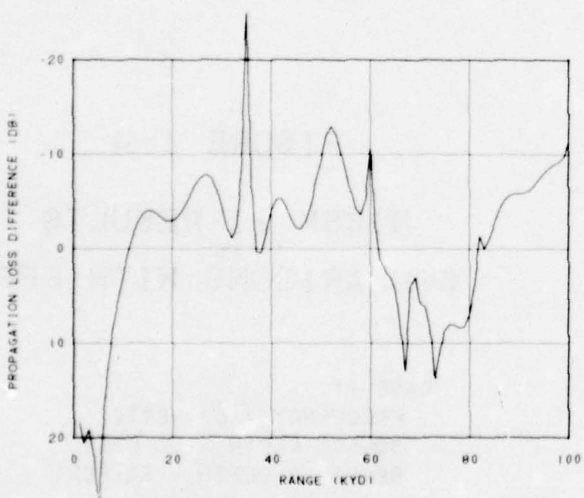

(I-5C) FFP ANALYTICAL FIT MINUS RAYMODE IV (COHERENT)
ANALYTICAL FIT

FIGURE I-5

RAYMODE IV RESULTS
AND
COMPARISONS WITH FFP

CASE I:
FREQUENCY = 50 HERTZ
SOURCE DEPTH = 50 FEET
RECEIVER DEPTH = 50 FEET

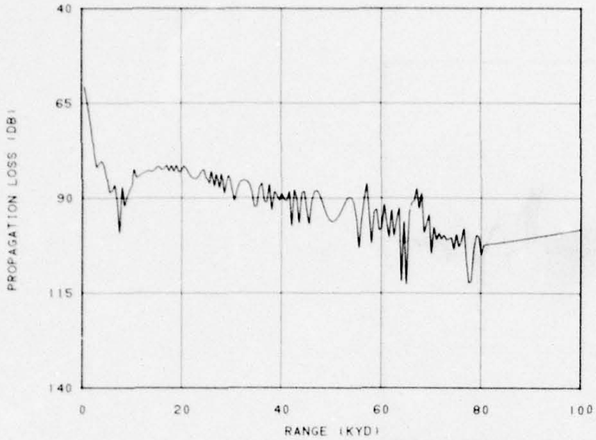

(I-6A) RAYMODE X (COHERENT)

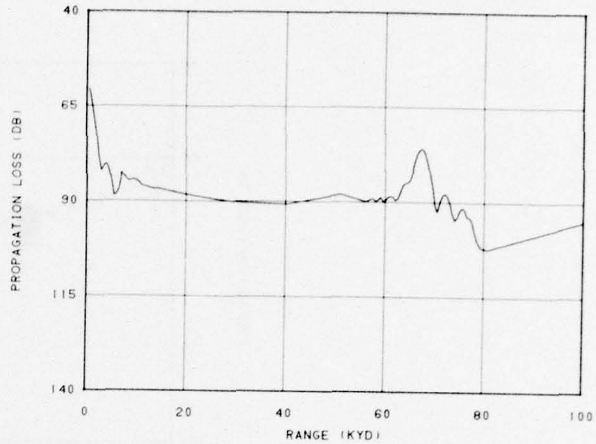

(I-6D) RAYMODE X (INCOHERENT)

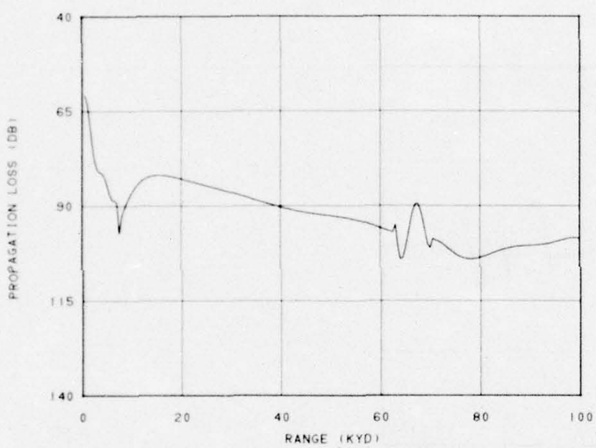

(I-6B) ANALYTICAL FIT TO RAYMODE X (COHERENT)

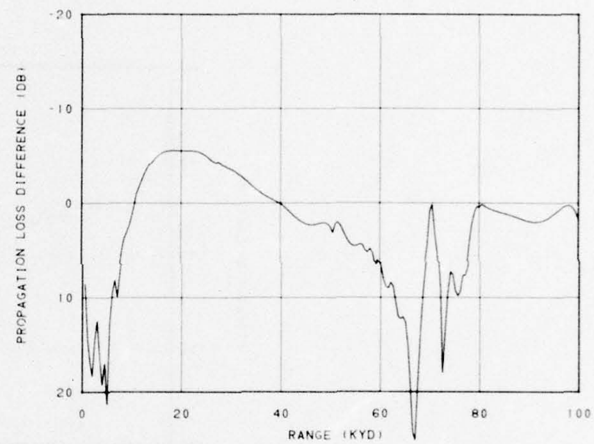

(I-6E) FFP ANALYTICAL FIT MINUS RAYMODE X (INCOHERENT)

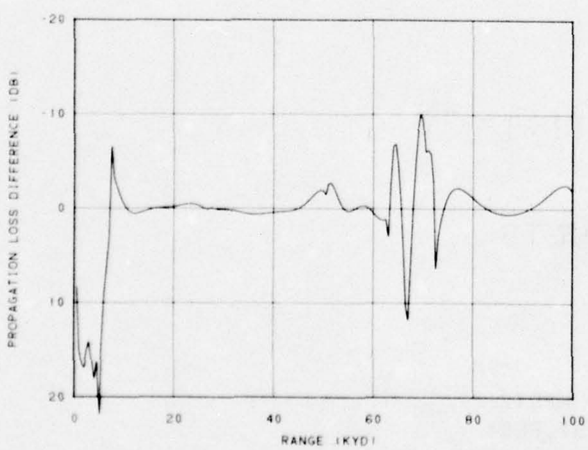

(I-6C) FFP ANALYTICAL FIT MINUS RAYMODE X (COHERENT) ANALYTICAL FIT

FIGURE I-6

RAYMODE X RESULTS
AND
COMPARISONS WITH FFP

CASE I:
FREQUENCY = 50 HERTZ
SOURCE DEPTH = 50 FEET
RECEIVER DEPTH = 50 FEET

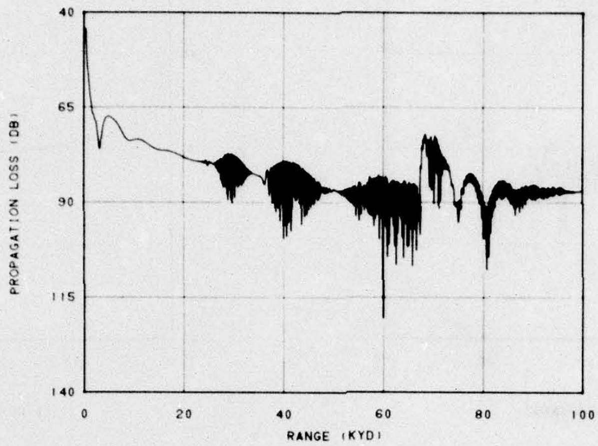

(II-1A) FFP

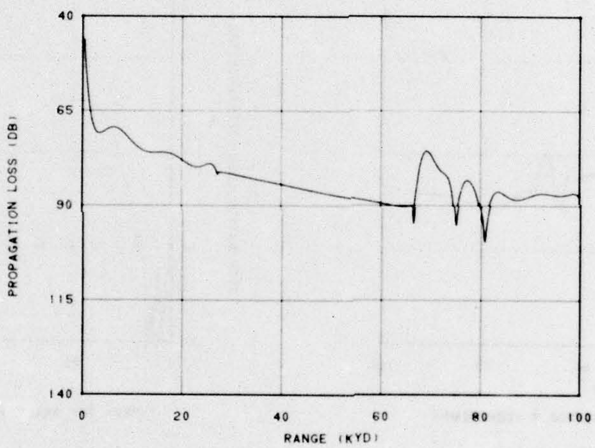

(II-1B) ANALYTICAL FIT TO FFP

FIGURE II-1

FFP RESULTS

CASE II:
FREQUENCY = 500 HERTZ
SOURCE DEPTH = 50 FEET
RECEIVER DEPTH = 50 FEET

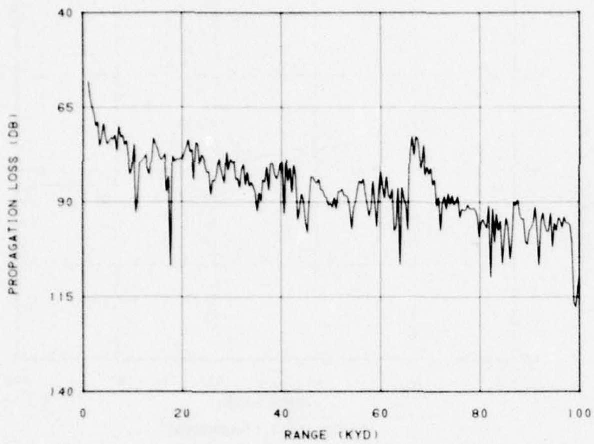

(II-2A) CONGRATS V (COHERENT)

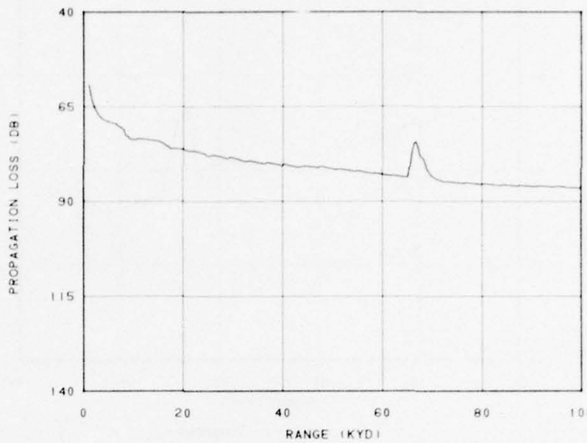

(II-2D) CONGRATS V (INCOHERENT)

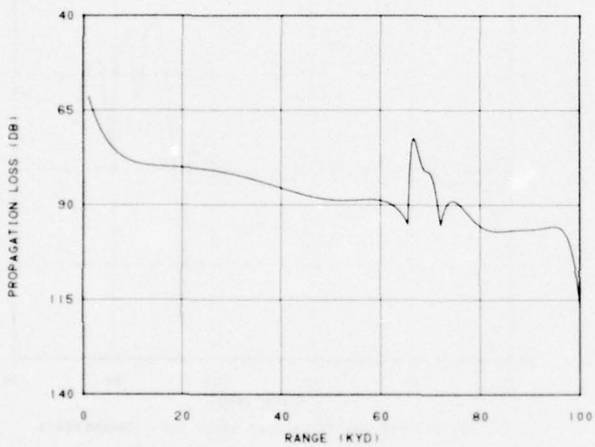

(II-2B) ANALYTICAL FIT TO CONGRATS V (COHERENT)

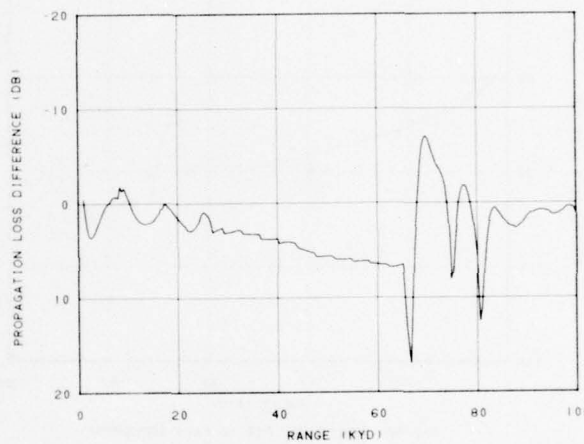

(II-2E) FFP ANALYTICAL FIT MINUS CONGRATS V (INCOHERENT)

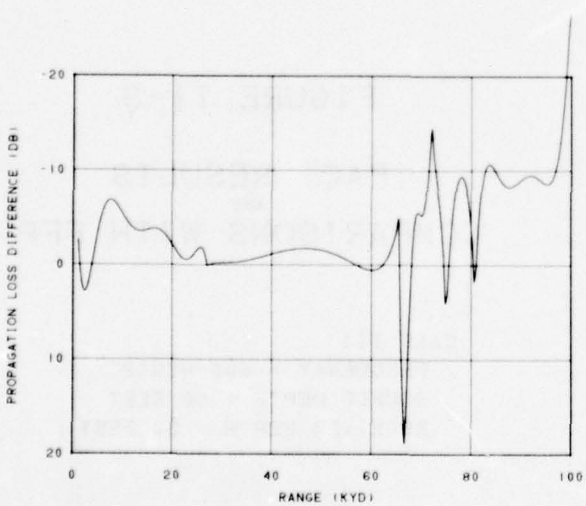

(II-2C) FFP ANALYTICAL FIT MINUS CONGRATS V (COHERENT) ANALYTICAL FIT

FIGURE II-2

CONGRATS V RESULTS
AND
COMPARISONS WITH FFP

CASE II:
FREQUENCY = 500 HERTZ
SOURCE DEPTH = 50 FEET
RECEIVER DEPTH = 50 FEET

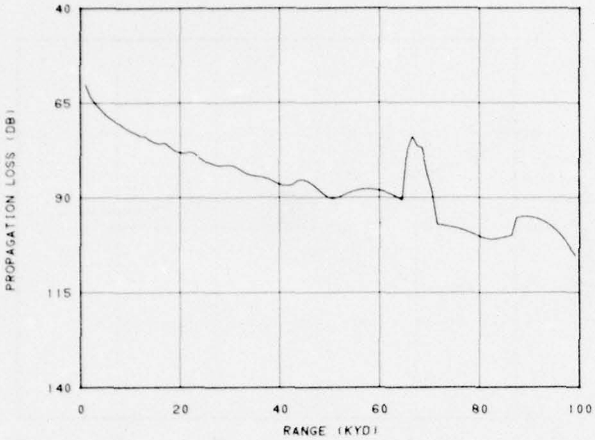

(II-3A) FACT (COHERENT)

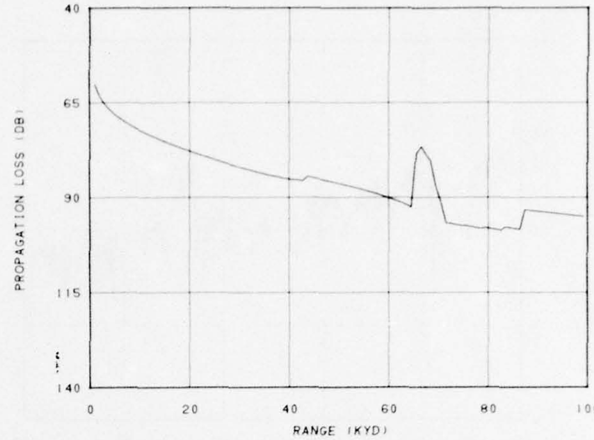

(II-3D) FACT (INCOHERENT)

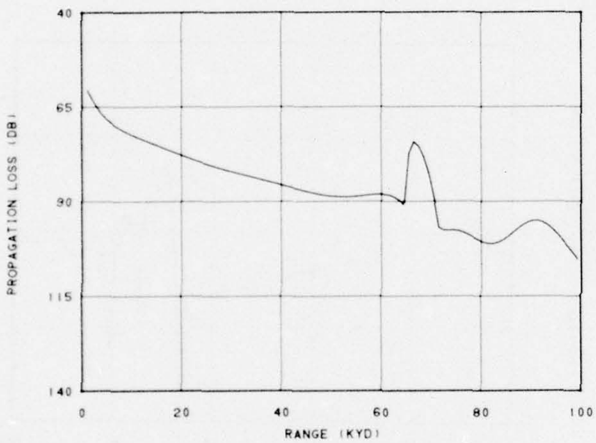

(II-3B) ANALYTICAL FIT TO FACT (COHERENT)

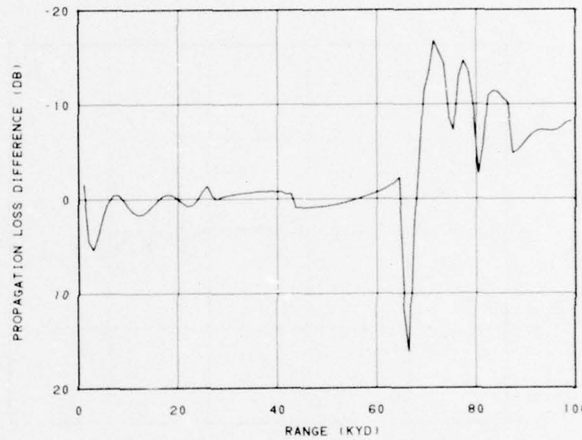

(II-3E) FFP ANALYTICAL FIT MINUS FACT (INCOHERENT)

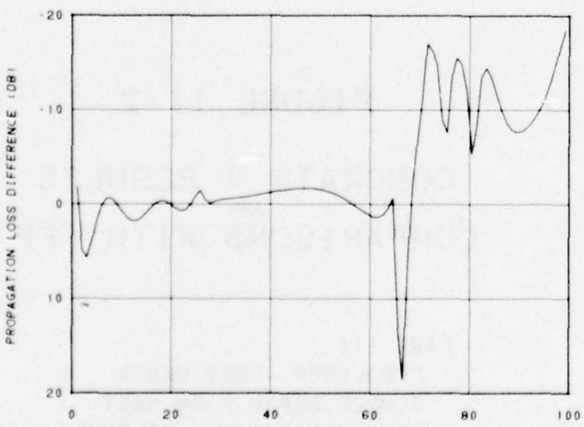

(II-3C) FFP ANALYTICAL FIT MINUS FACT (COHERENT) ANALYTICAL FIT

FIGURE II-3

FACT RESULTS
AND
COMPARISONS WITH FFP

CASE II:
FREQUENCY = 500 HERTZ
SOURCE DEPTH = 50 FEET
RECEIVER DEPTH = 50 FEET

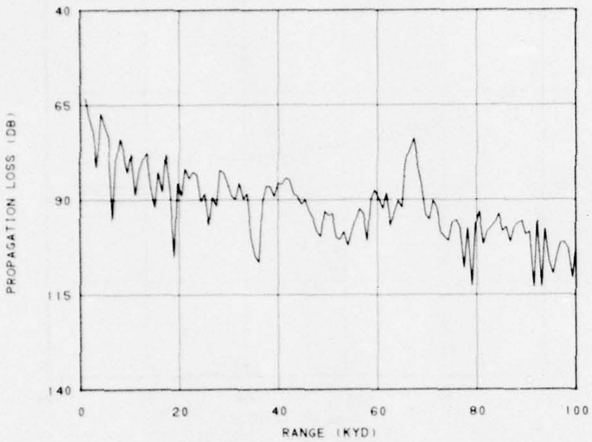

(II-4A) NISSM II (COHERENT)

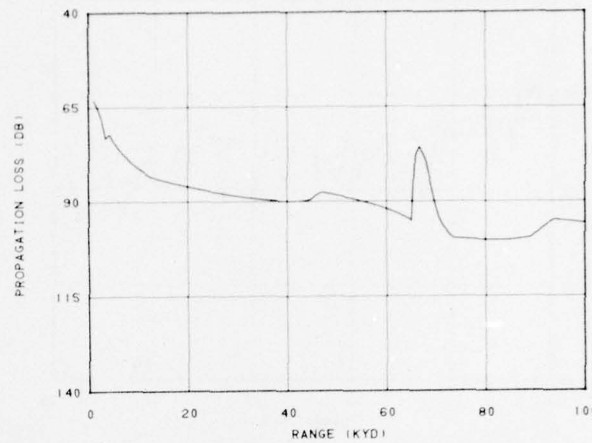

(II-4D) NISSM II (INCOHERENT)

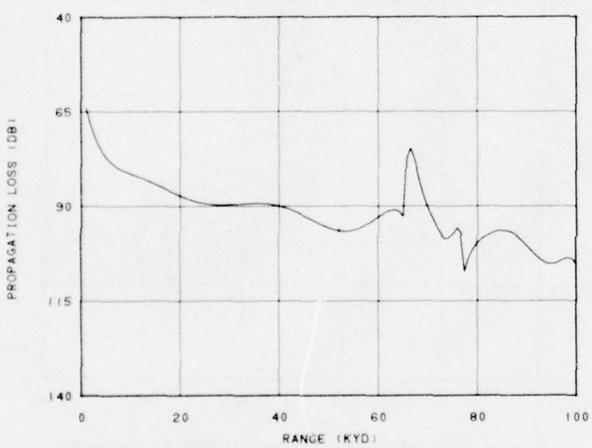

(II-4B) ANALYTICAL FIT TO NISSM II (COHERENT)

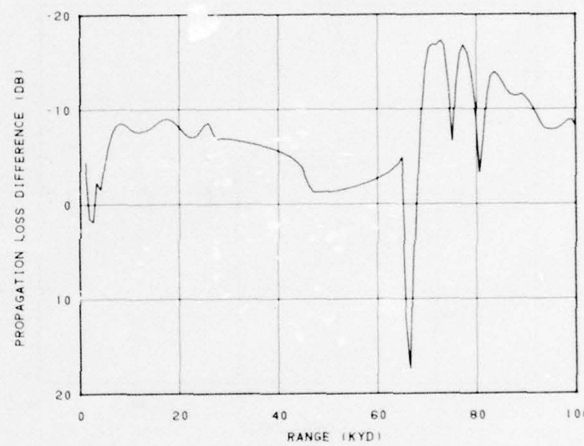

(II-4E) FFP ANALYTICAL FIT MINUS NISSM II (INCOHERENT)

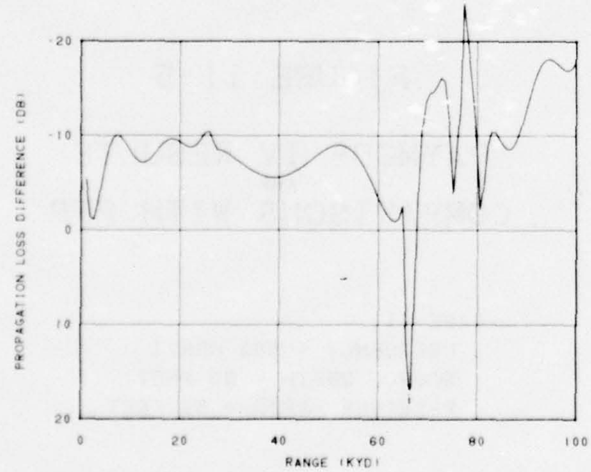

(II-4C) FFP ANALYTICAL FIT MINUS NISSM II (COHERENT) ANALYTICAL FIT

FIGURE II-4

NISSM II RESULTS AND COMPARISONS WITH FFP

CASE II:
- FREQUENCY = 500 HERTZ
- SOURCE DEPTH = 50 FEET
- RECEIVER DEPTH = 50 FEET

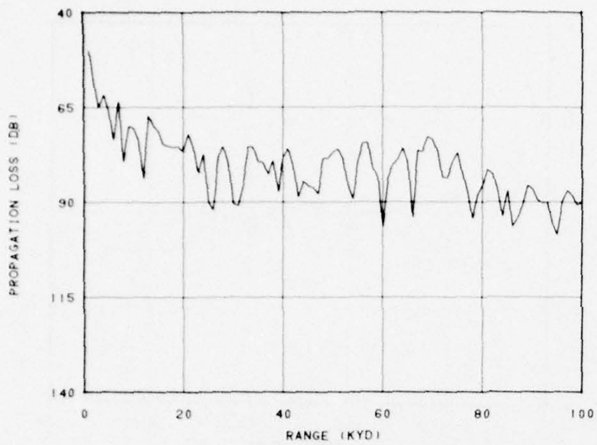

(II-5A) RAYMODE IV (COHERENT)

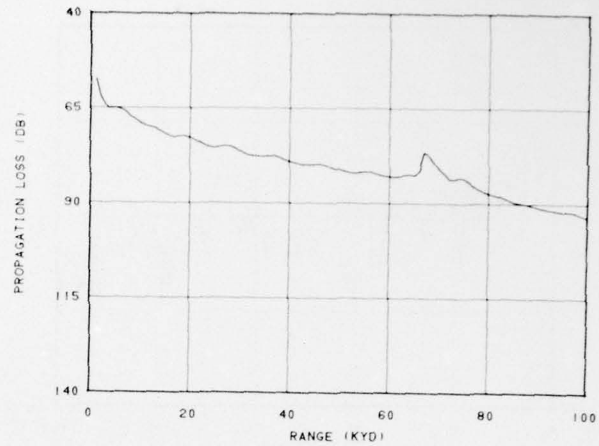

(II-5D) RAYMODE IV (INCOHERENT)

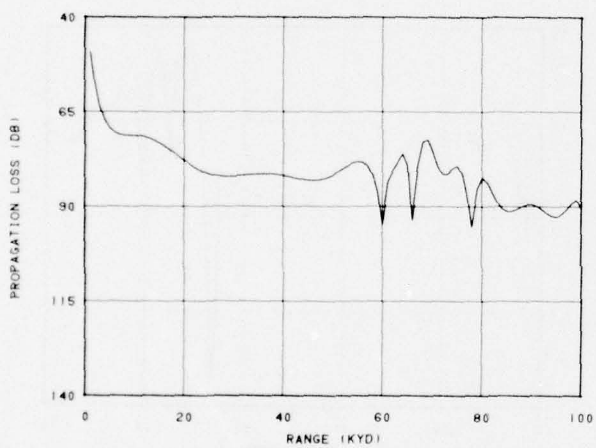

(II-5B) ANALYTICAL FIT TO RAYMODE IV (COHERENT)

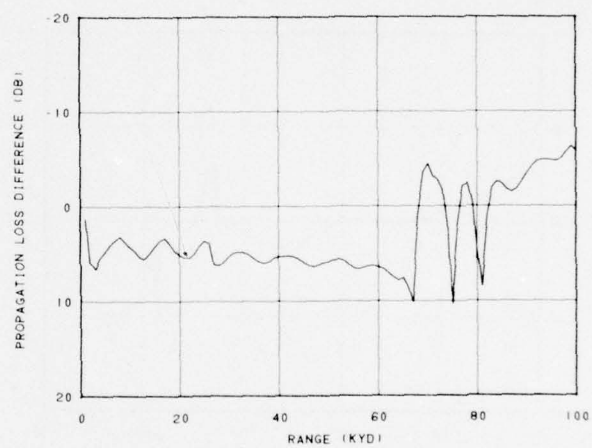

(II-5E) FFP ANALYTICAL FIT MINUS RAYMODE IV (INCOHERENT)

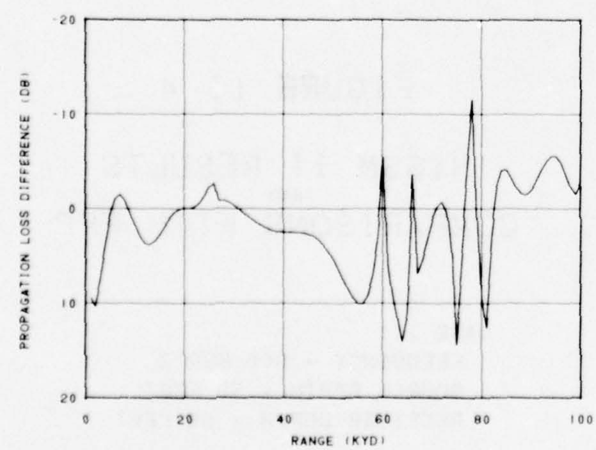

(II-5C) FFP ANALYTICAL FIT MINUS RAYMODE IV (COHERENT) ANALYTICAL FIT

FIGURE II-5

RAYMODE IV RESULTS
AND
COMPARISONS WITH FFP

CASE II:
FREQUENCY = 500 HERTZ
SOURCE DEPTH = 50 FEET
RECEIVER DEPTH = 50 FEET

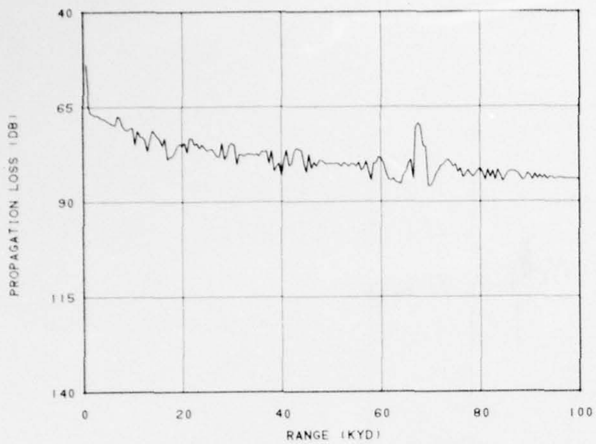

(II-6A) RAYMODE X (COHERENT)

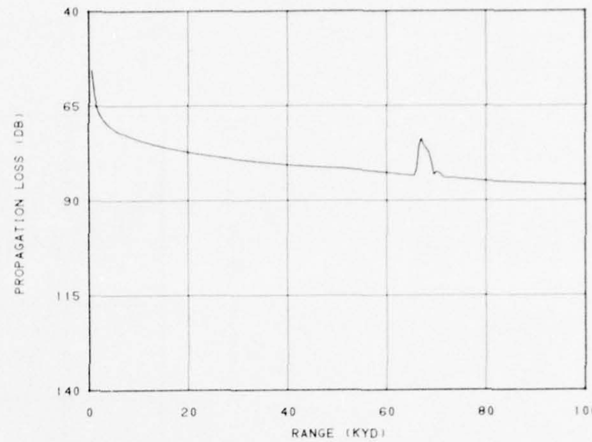

(II-6D) RAYMODE X (INCOHERENT)

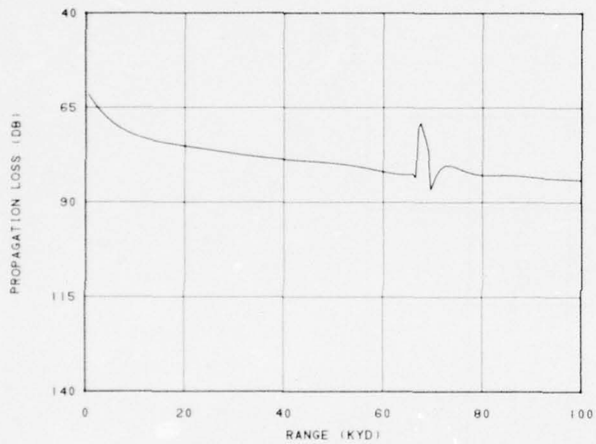

(II-6B) ANALYTICAL FIT TO RAYMODE X (COHERENT)

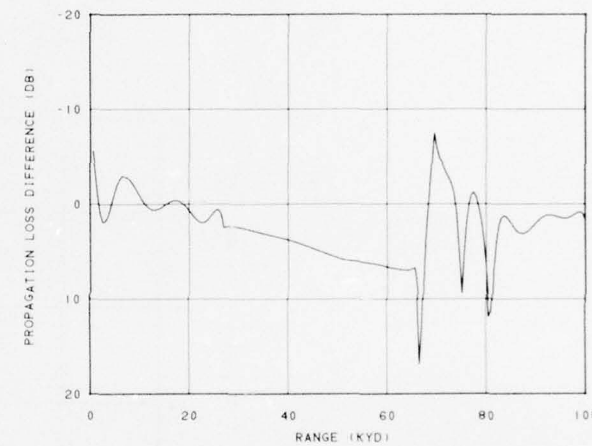

(II-6E) FFP ANALYTICAL FIT MINUS RAYMODE X (INCOHERENT)

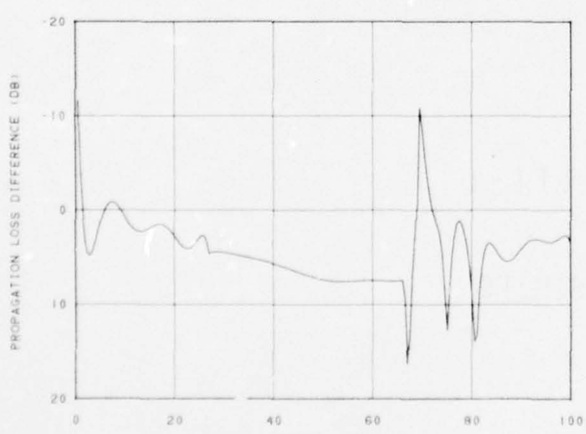

(II-6C) FFP ANALYTICAL FIT MINUS RAYMODE X (COHERENT) ANALYTICAL FIT

FIGURE II-6

RAYMODE X RESULTS
AND
COMPARISONS WITH FFP

CASE II:
FREQUENCY = 500 HERTZ
SOURCE DEPTH = 50 FEET
RECEIVER DEPTH = 50 FEET

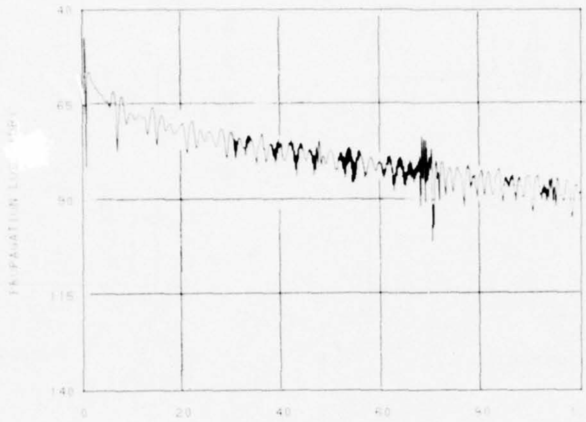

(III-1A) FFP

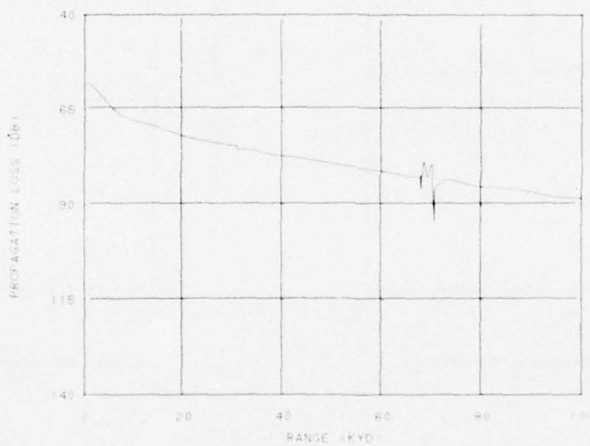

(III-1B) ANALYTICAL FIT TO FFP

FIGURE III-1

FFP RESULTS

CASE III:
FREQUENCY = 2000 HERTZ
SOURCE DEPTH = 50 FEET
RECEIVER DEPTH = 50 FEET

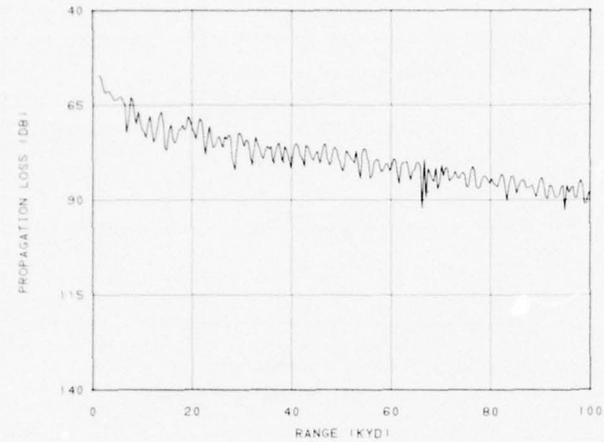

(III-2A) CONGRATS V (COHERENT)

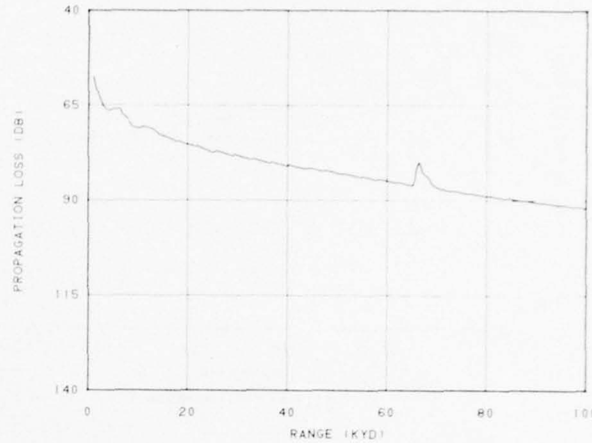

(III-2D) CONGRATS V (INCOHERENT)

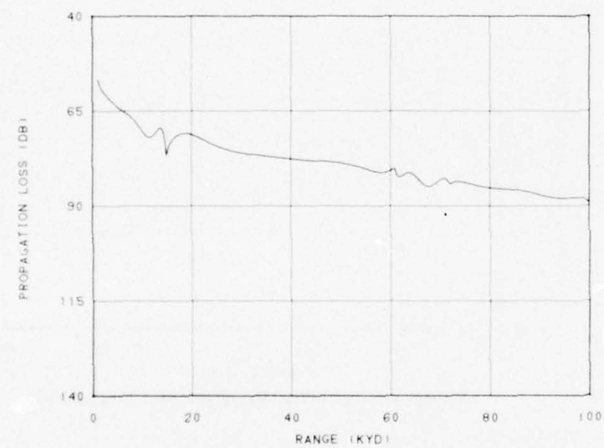

(III-2B) ANALYTICAL FIT TO CONGRATS V (COHERENT)

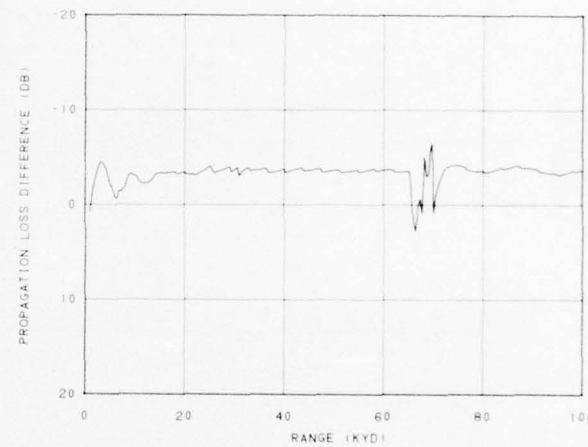

(III-2E) FFP ANALYTICAL FIT MINUS CONGRATS V (INCOHERENT)

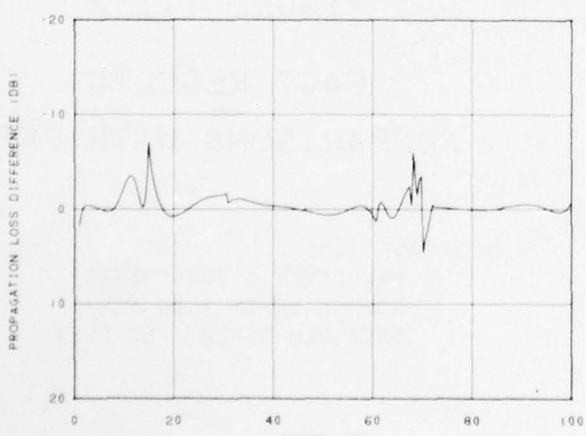

(III-2C) FFP ANALYTICAL FIT MINUS CONGRATS V (COHERENT) ANALYTICAL FIT

FIGURE III-2

CONGRATS V RESULTS
AND
COMPARISONS WITH FFP

CASE III:
FREQUENCY = 2000 HERTZ
SOURCE DEPTH = 50 FEET
RECEIVER DEPTH = 50 FEET

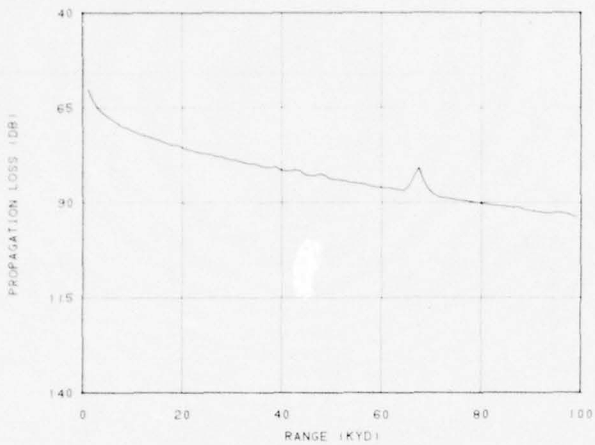

(III-3A) FACT (COHERENT)

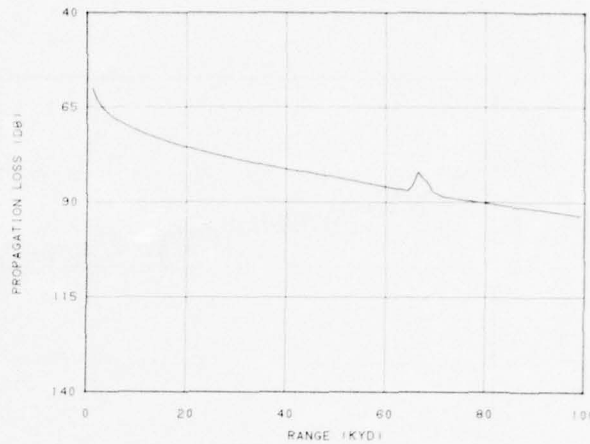

(III-3D) FACT (INCOHERENT)

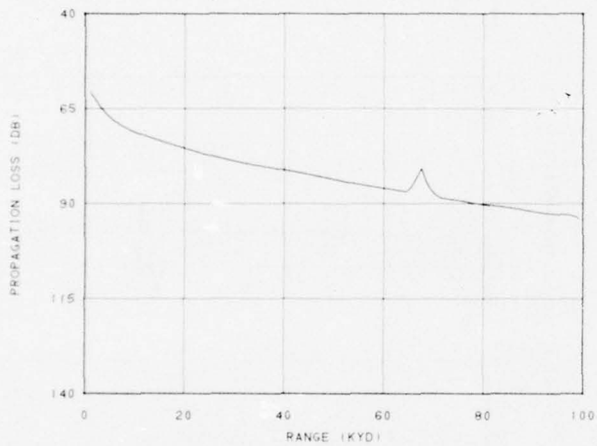

(III-3B) ANALYTICAL FIT TO FACT (COHERENT)

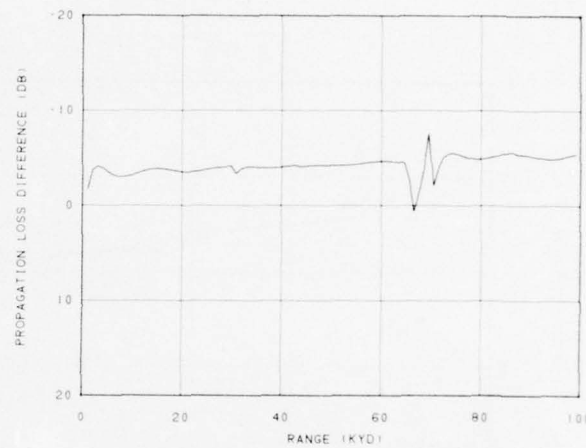

(III-3E) FFP ANALYTICAL FIT MINUS FACT (INCOHERENT)

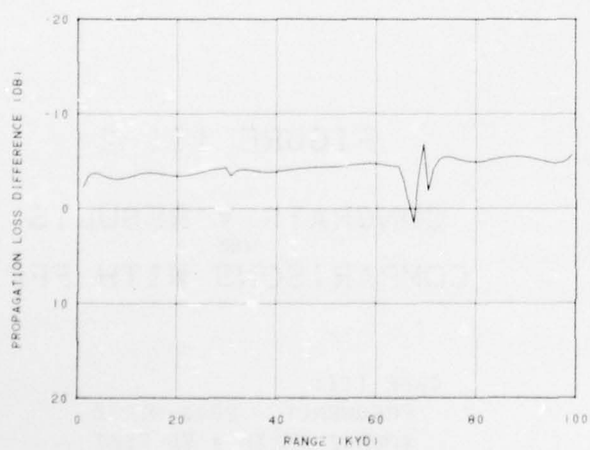

(III-3C) FFP ANALYTICAL FIT MINUS FACT (COHERENT) ANALYTICAL FIT

FIGURE III-3

FACT RESULTS
AND
COMPARISONS WITH FFP

CASE III:
FREQUENCY = 2000 HERTZ
SOURCE DEPTH = 50 FEET
RECEIVER DEPTH = 50 FEET

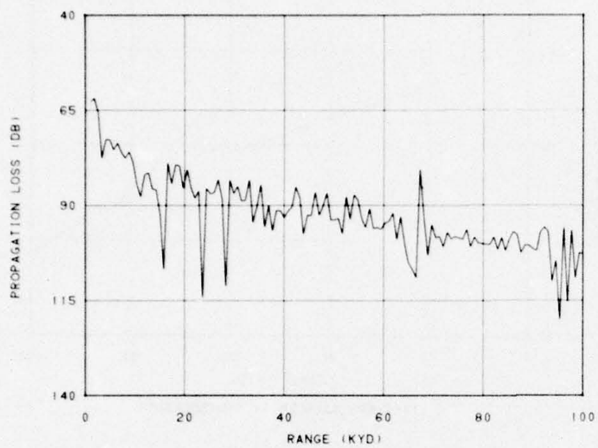

(III-4A) NISSM II (COHERENT)

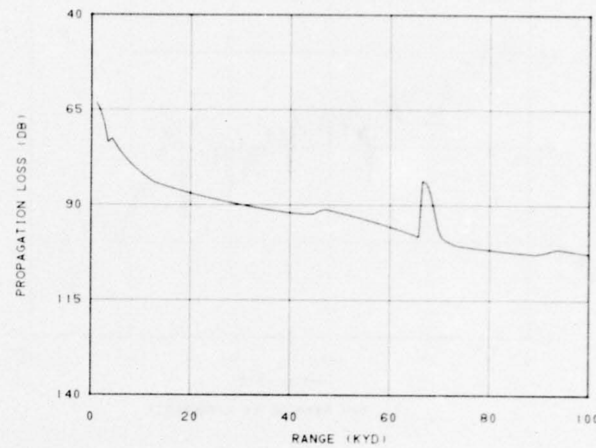

(III-4D) NISSM II (INCOHERENT)

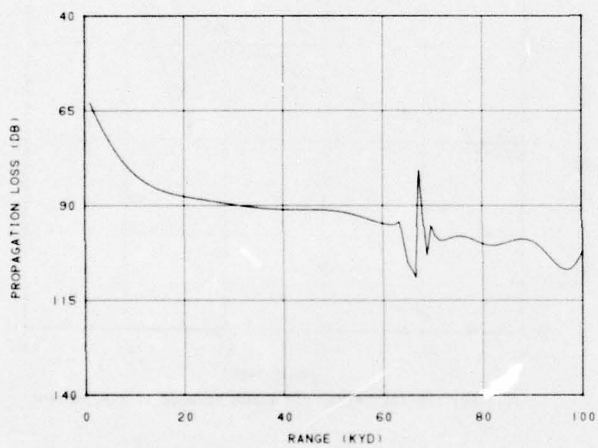

(III-4B) ANALYTICAL FIT TO NISSM II (COHERENT)

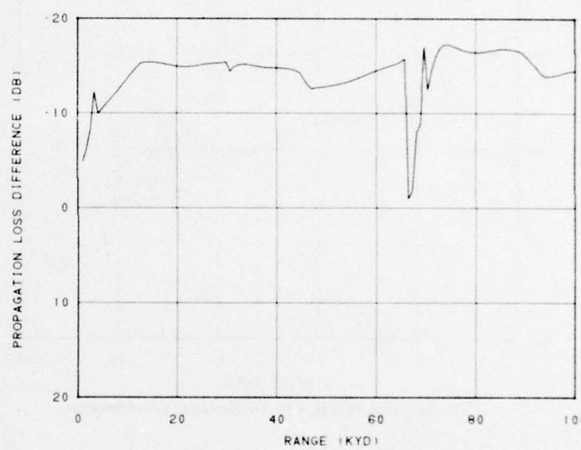

(III-4E) FFP ANALYTICAL FIT MINUS NISSM II (INCOHERENT)

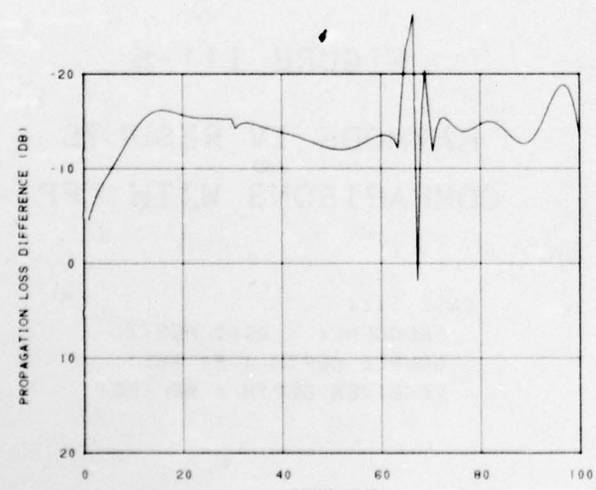

(III-4C) FFP ANALYTICAL FIT MINUS NISSM II (COHERENT) ANALYTICAL FIT

FIGURE III-4

NISSM II RESULTS
AND
COMPARISONS WITH FFP

CASE III:
FREQUENCY = 2000 HERTZ
SOURCE DEPTH = 50 FEET
RECEIVER DEPTH = 50 FEET

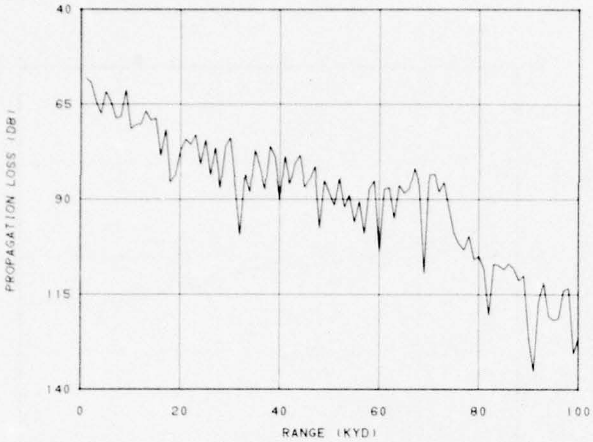

(III-5A) RAYMODE IV (COHERENT)

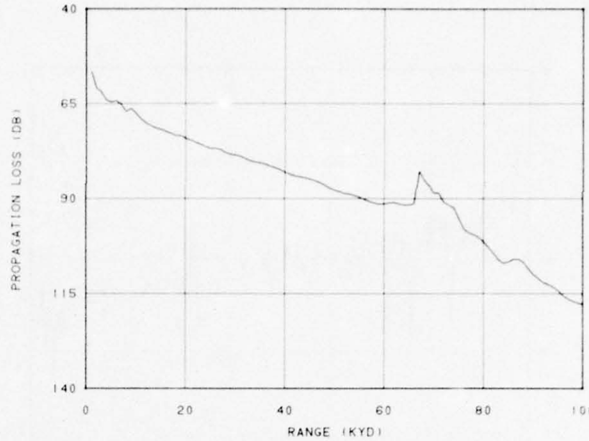

(III-5D) RAYMODE IV (INCOHERENT)

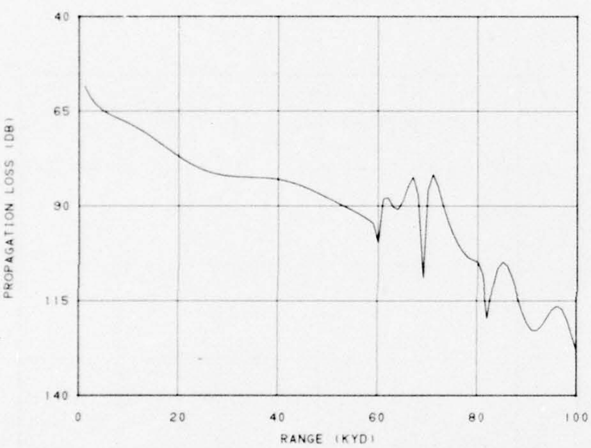

(III-5B) ANALYTICAL FIT TO RAYMODE IV (COHERENT)

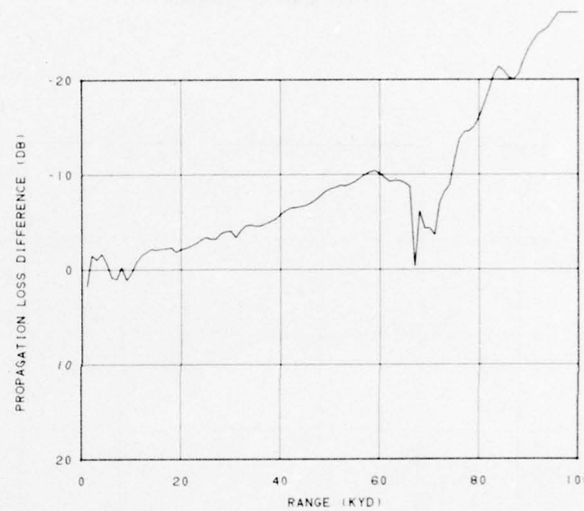

(III-5E) FFP ANALYTICAL FIT MINUS RAYMODE IV (INCOHERENT)

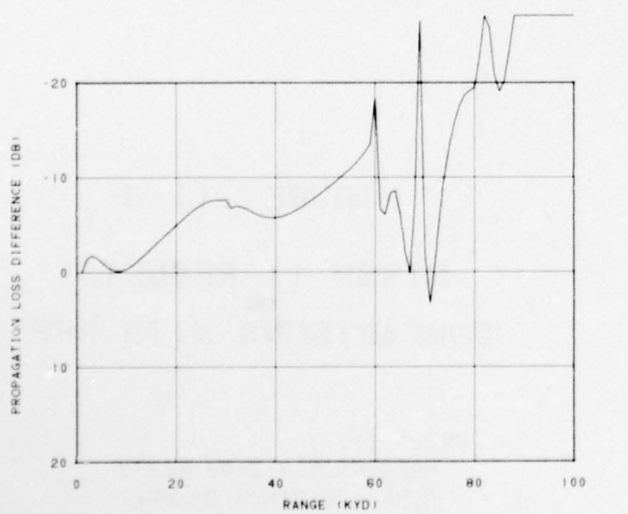

(III-5C) FFP ANALYTICAL FIT MINUS RAYMODE IV (COHERENT) ANALYTICAL FIT

FIGURE III-5

RAYMODE IV RESULTS AND COMPARISONS WITH FFP

CASE III:
- FREQUENCY = 2000 HERTZ
- SOURCE DEPTH = 50 FEET
- RECEIVER DEPTH = 50 FEET

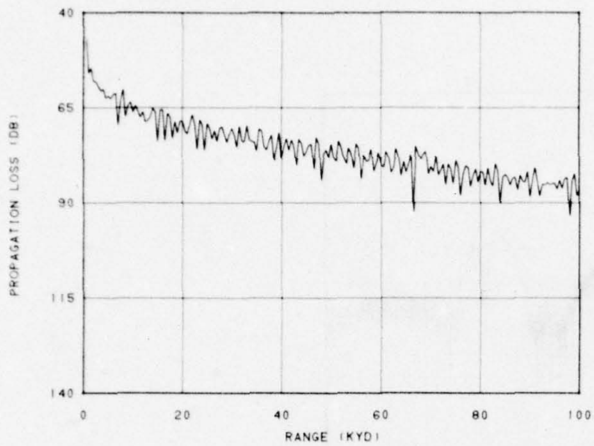

(III-6A) RAYMODE X (COHERENT)

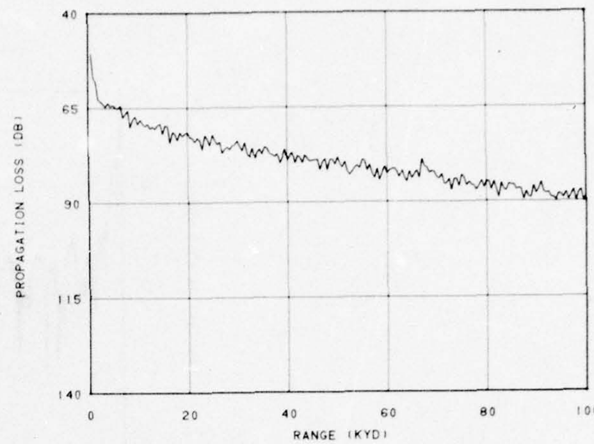

(III-6D) RAYMODE X (INCOHERENT)

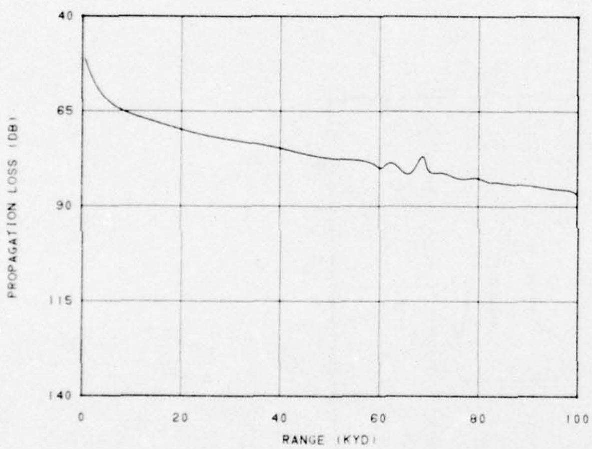

(III-6B) ANALYTICAL FIT TO RAYMODE X (COHERENT)

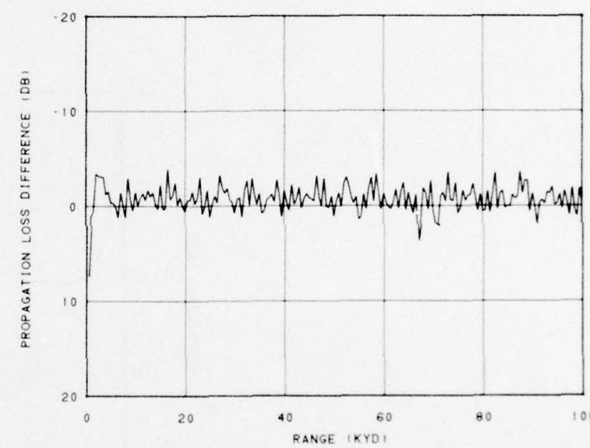

(III-6E) FFP ANALYTICAL FIT MINUS RAYMODE X (INCOHERENT)

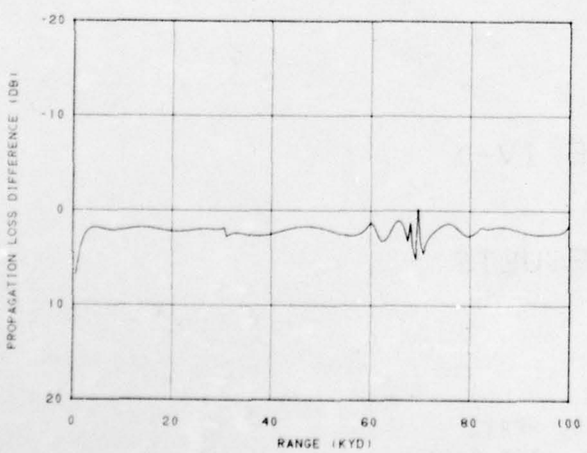

(III-6C) FFP ANALYTICAL FIT MINUS RAYMODE X (COHERENT) ANALYTICAL FIT

FIGURE III-6

RAYMODE X RESULTS
AND
COMPARISONS WITH FFP

CASE III:
FREQUENCY = 2000 HERTZ
SOURCE DEPTH = 50 FEET
RECEIVER DEPTH = 50 FEET

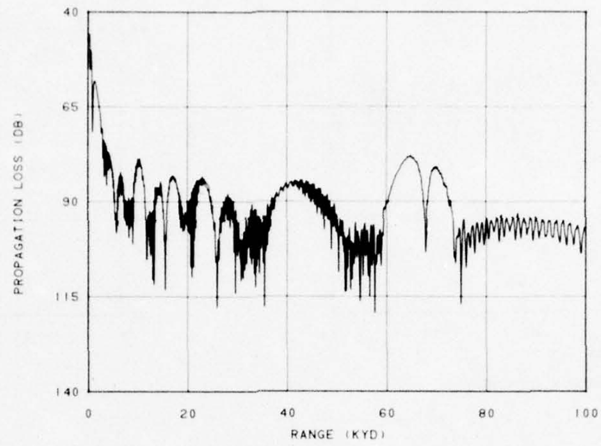

(IV-1A) FFP

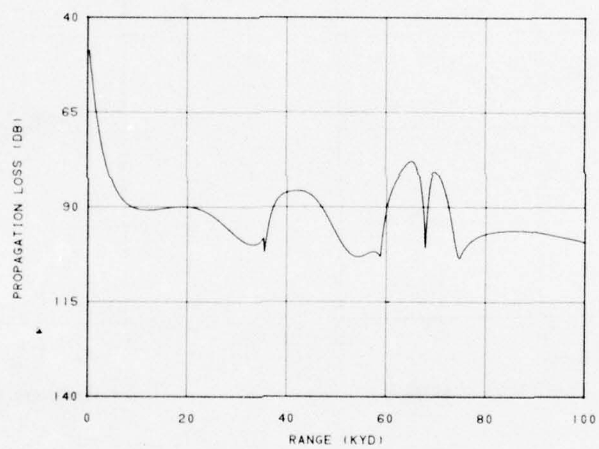

(IV-1B) ANALYTICAL FIT TO FFP

FIGURE IV-1

FFP RESULTS

CASE IV:
FREQUENCY = 50 HERTZ
SOURCE DEPTH = 500 FEET
RECEIVER DEPTH = 300 FEET

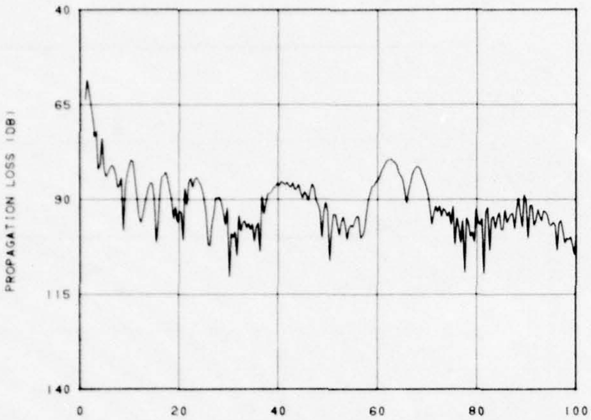

(IV-2A) CONGRATS V (COHERENT)

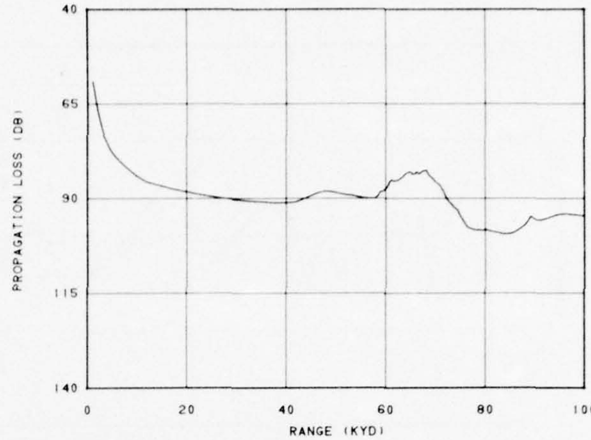

(IV-2D) CONGRATS V (INCOHERENT)

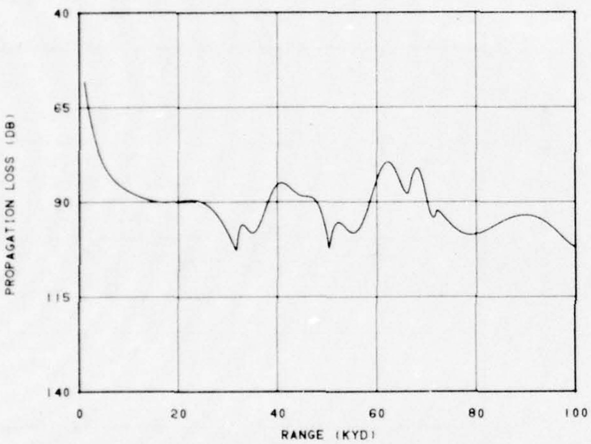

(IV-2B) ANALYTICAL FIT TO CONGRATS V (COHERENT)

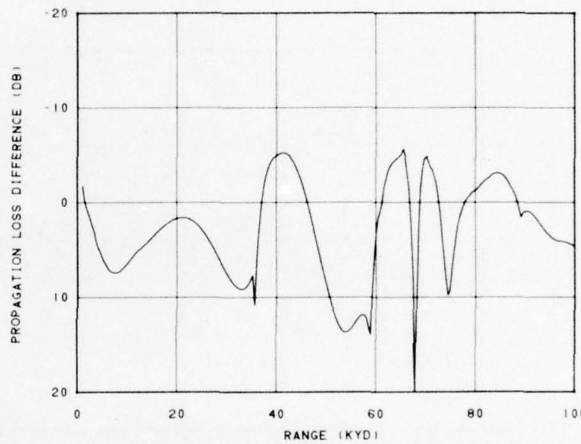

(IV-2E) FFP ANALYTICAL FIT MINUS CONGRATS V (INCOHERENT)

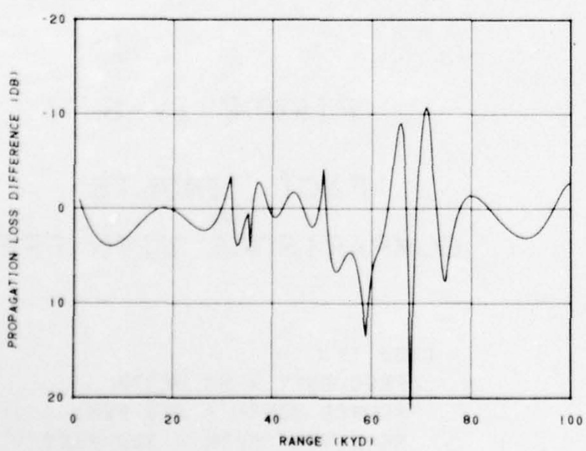

(IV-2C) FFP ANALYTICAL FIT MINUS CONGRATS V (COHERENT) ANALYTICAL FIT

FIGURE IV-2

CONGRATS V RESULTS
AND
COMPARISONS WITH FFP

CASE IV:
FREQUENCY = 50 HERTZ
SOURCE DEPTH = 500 FEET
RECEIVER DEPTH = 300 FEET

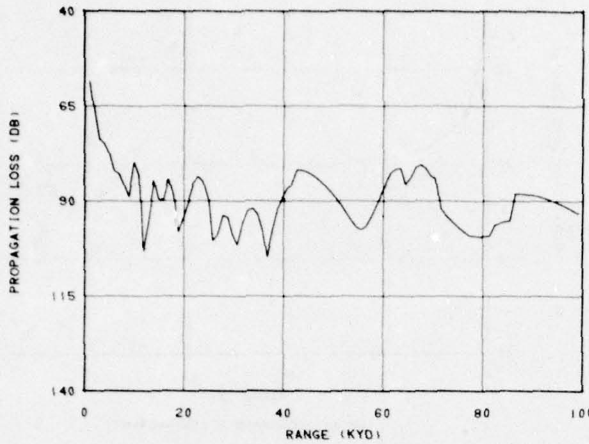

(IV-3A) FACT (COHERENT)

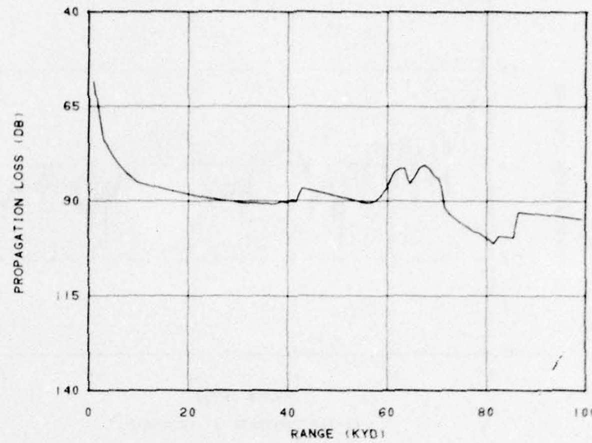

(IV-3D) FACT (INCOHERENT)

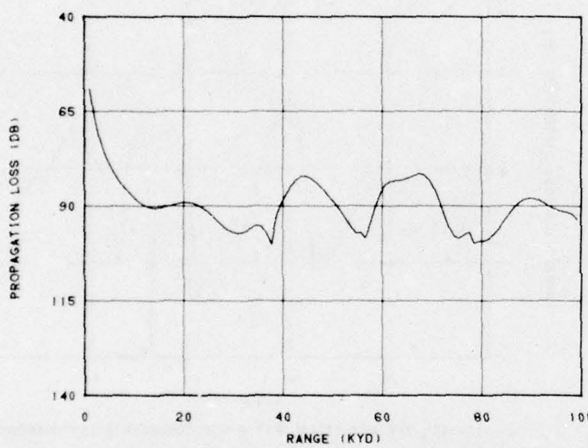

(IV-3B) ANALYTICAL FIT TO FACT (COHERENT)

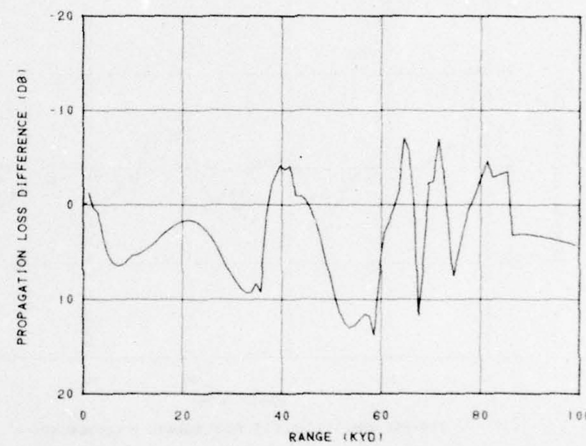

(IV-3E) FFP ANALYTICAL FIT MINUS FACT (INCOHERENT)

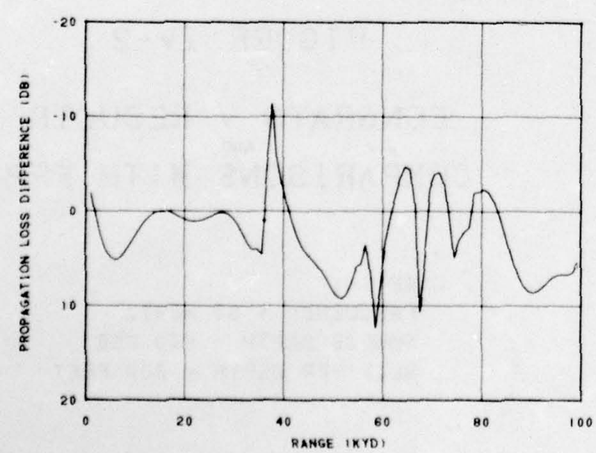

(IV-3C) FFP ANALYTICAL FIT MINUS FACT (COHERENT) ANALYTICAL FIT

FIGURE IV-3

FACT RESULTS
AND
COMPARISONS WITH FFP

CASE IV:
FREQUENCY = 50 HERTZ
SOURCE DEPTH = 500 FEET
RECEIVER DEPTH = 300 FEET

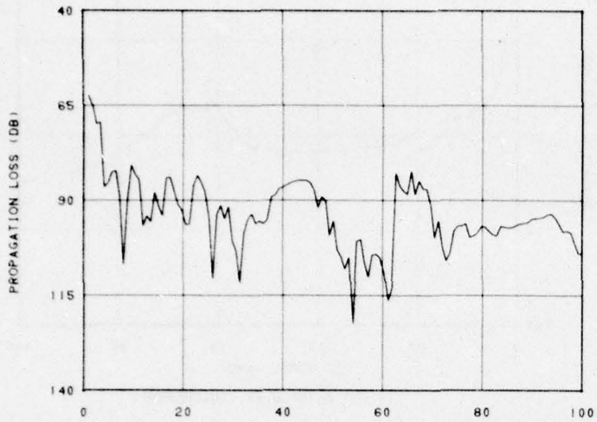

(IV-4A) NISSM II (COHERENT)

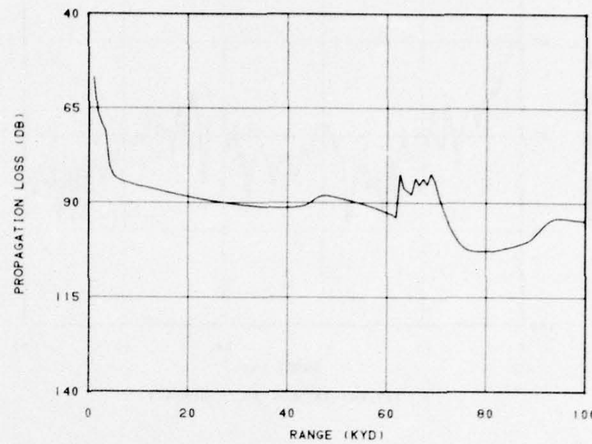

(IV-4D) NISSM II (INCOHERENT)

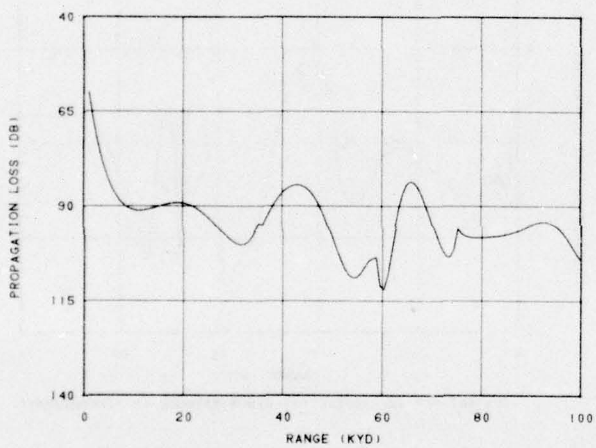

(IV-4B) ANALYTICAL FIT TO NISSM II (COHERENT)

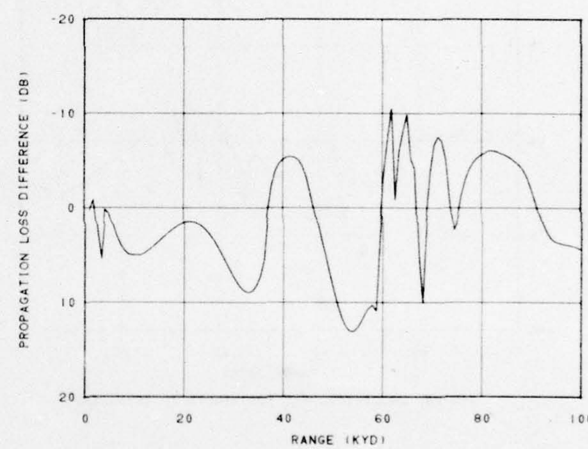

(IV-4E) FFP ANALYTICAL FIT MINUS NISSM II (INCOHERENT)

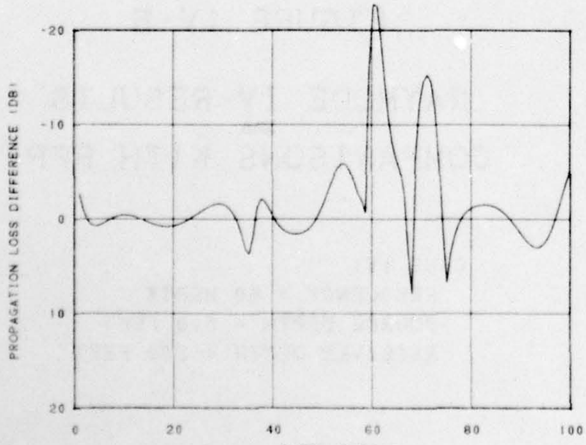

(IV-4C) FFP ANALYTICAL FIT MINUS NISSM II (COHERENT) ANALYTICAL FIT

FIGURE IV-4

NISSM II RESULTS AND COMPARISONS WITH FFP

CASE IV:
FREQUENCY = 50 HERTZ
SOURCE DEPTH = 500 FEET
RECEIVER DEPTH = 300 FEET

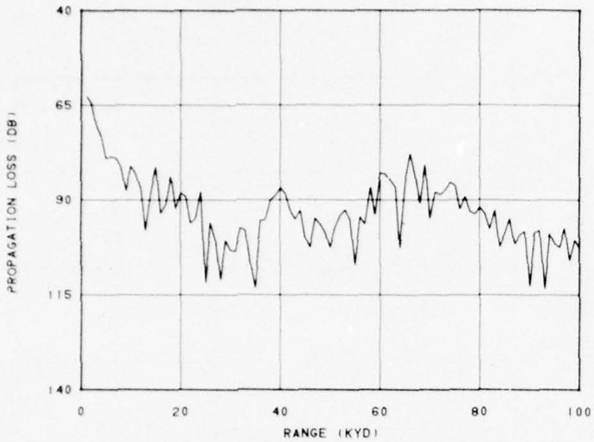

(IV-5A) RAYMODE IV (COHERENT)

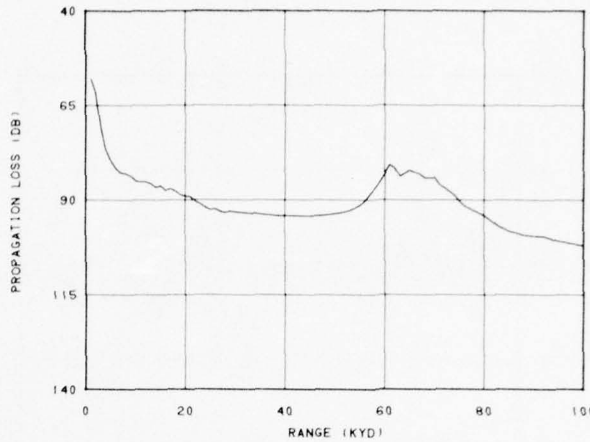

(IV-5D) RAYMODE IV (INCOHERENT)

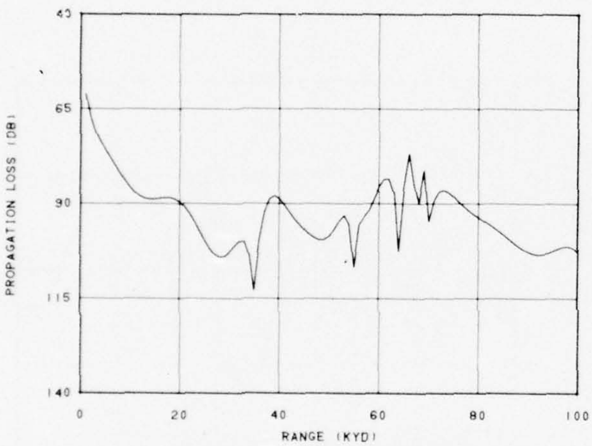

(IV-5B) ANALYTICAL FIT TO RAYMODE IV (COHERENT)

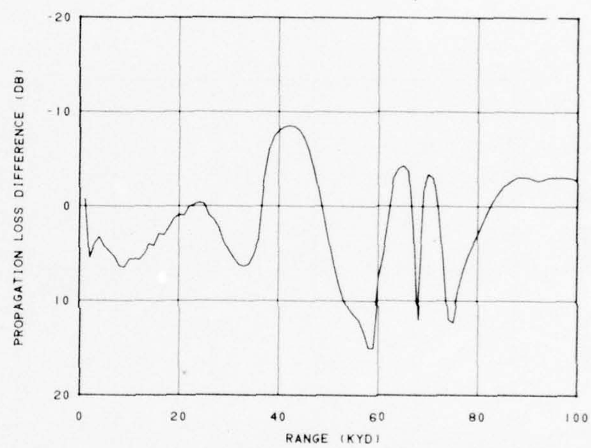

(IV-5E) FFP ANALYTICAL FIT MINUS RAYMODE IV (INCOHERENT)

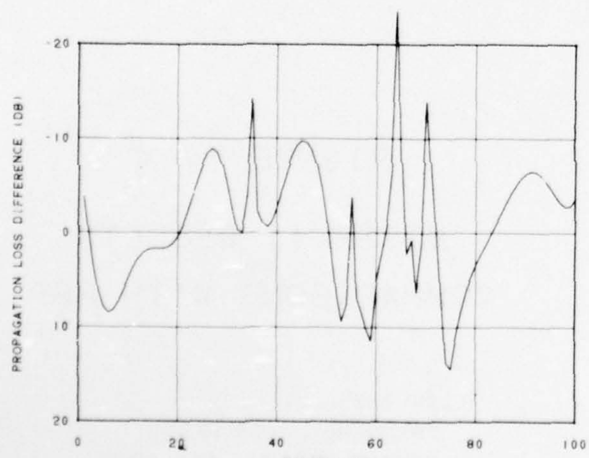

(IV-5C) FFP ANALYTICAL FIT MINUS RAYMODE IV (COHERENT) ANALYTICAL FIT

FIGURE IV-5

RAYMODE IV RESULTS
AND
COMPARISONS WITH FFP

CASE IV:
FREQUENCY = 50 HERTZ
SOURCE DEPTH = 500 FEET
RECEIVER DEPTH = 300 FEET

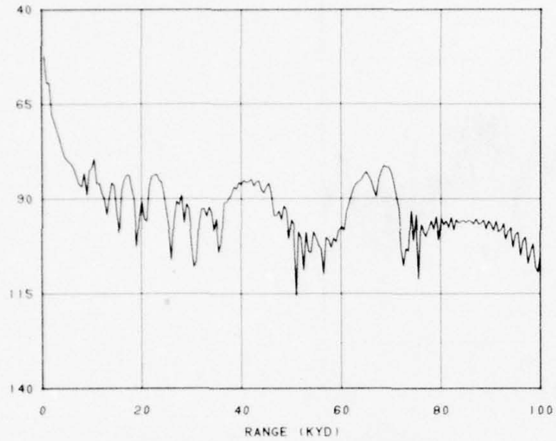

(IV-6A) RAYMODE X (COHERENT)

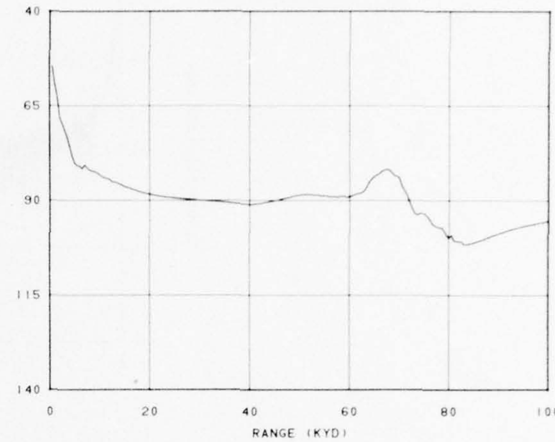

(IV-6D) RAYMODE X (INCOHERENT)

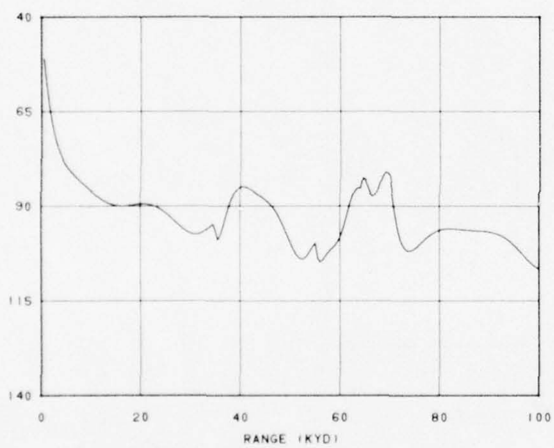

(IV-6B) ANALYTICAL FIT TO RAYMODE X (COHERENT)

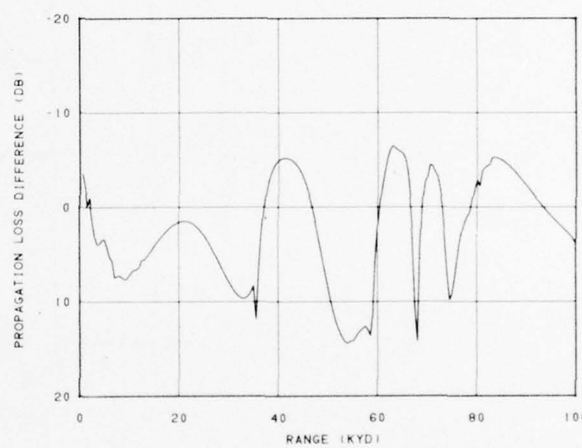

(IV-6E) FFP ANALYTICAL FIT MINUS RAYMODE X (INCOHERENT)

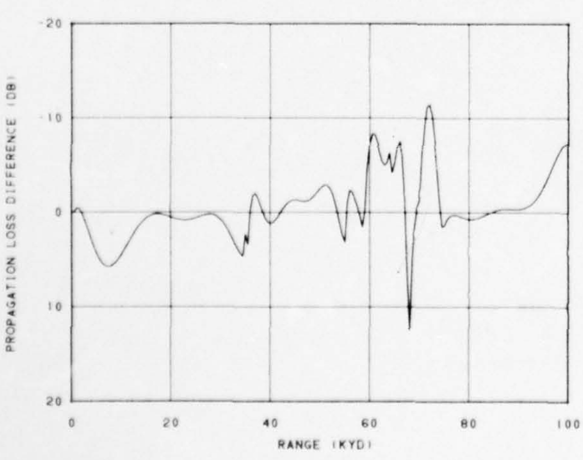

(IV-6C) FFP ANALYTICAL FIT MINUS RAYMODE X (COHERENT) ANALYTICAL FIT

FIGURE IV-6

RAYMODE X RESULTS
AND
COMPARISONS WITH FFP

CASE IV:
FREQUENCY = 50 HERTZ
SOURCE DEPTH = 500 FEET
RECEIVER DEPTH = 300 FEET

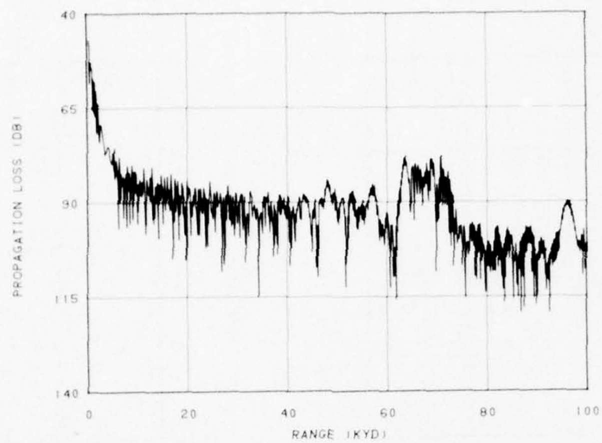

(V-1A) FFP

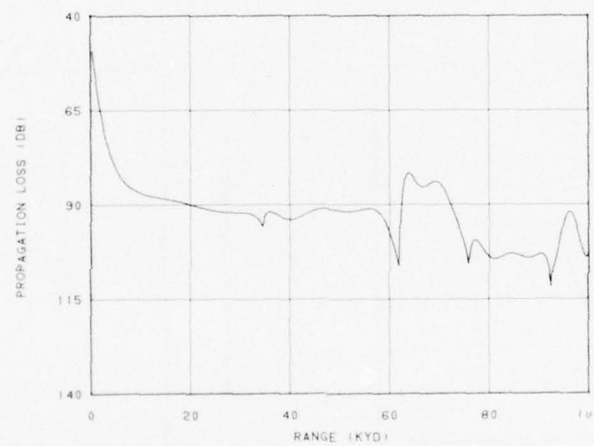

(V-1B) ANALYTICAL FIT TO FFP

FIGURE V-1

FFP RESULTS

CASE V:
FREQUENCY = 500 HERTZ
SOURCE DEPTH = 500 FEET
RECEIVER DEPTH = 300 FEET

AD-A038 160 NAVAL SEA SYSTEMS COMMAND WASHINGTON D C F/G 17/1
A METHODOLOGY FOR THE COMPARISON OF MODELS FOR SONAR SYSTEM APP--ETC(U)
DEC 76 R B LAUER, B SUSSMAN
UNCLASSIFIED NAVSEA-06H1/036-EVA/MOST- NL

2 OF 2
AD A038160

END
DATE
FILMED
5-77

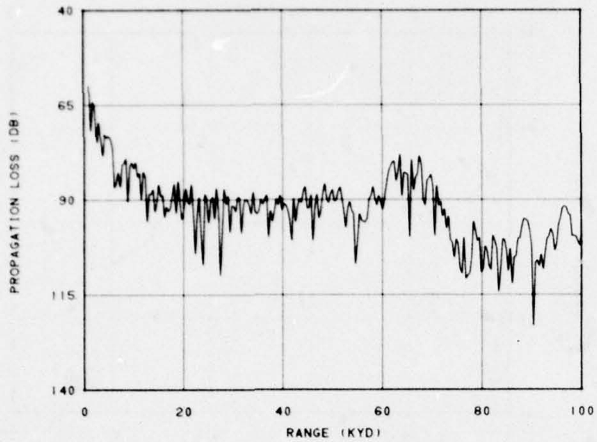

(V-2A) CONGRATS V (COHERENT)

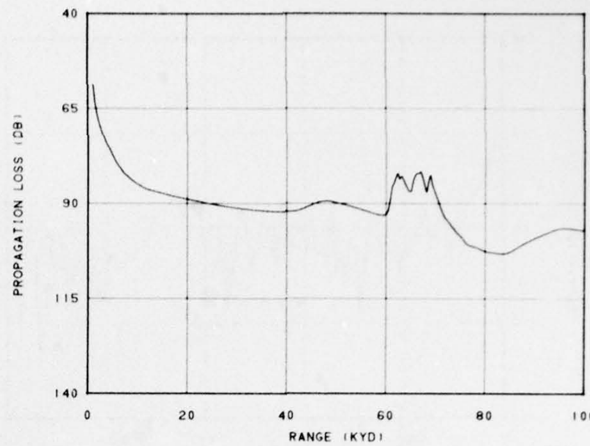

(V-2D) CONGRATS V (INCOHERENT)

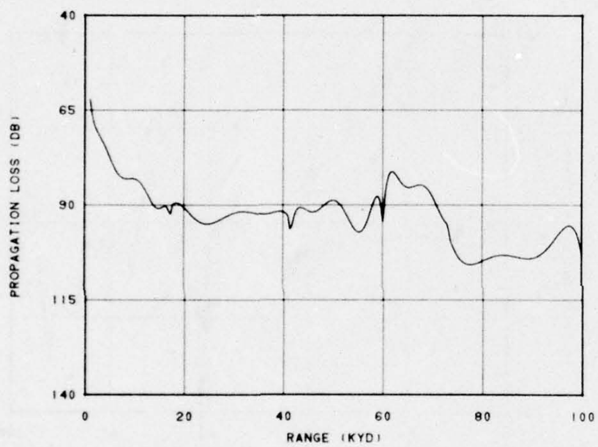

(V-2B) ANALYTICAL FIT TO CONGRATS V (COHERENT)

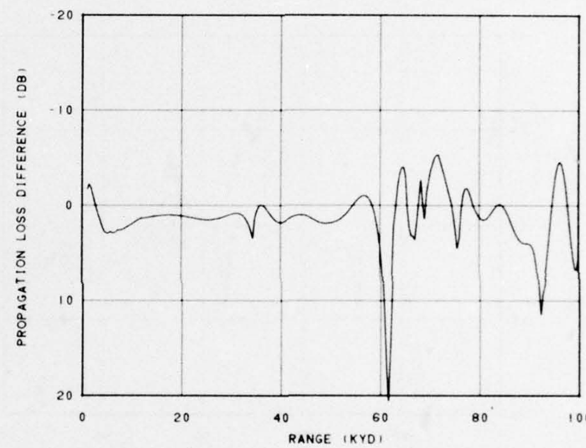

(V-2E) FFP ANALYTICAL FIT MINUS CONGRATS V (INCOHERENT)

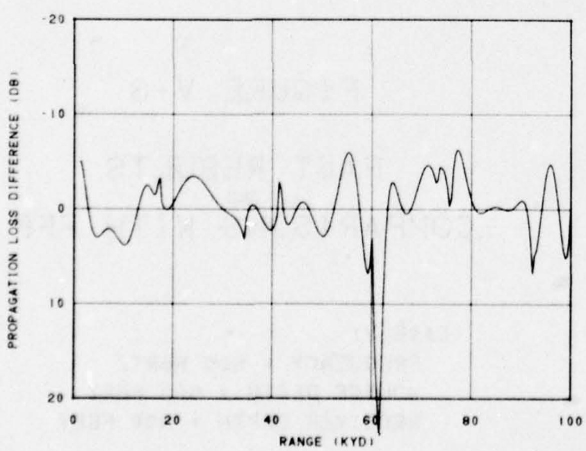

(V-2C) FFP ANALYTICAL FIT MINUS CONGRATS V (COHERENT) ANALYTICAL FIT

FIGURE V-2

CONGRATS V RESULTS
AND
COMPARISONS WITH FFP

CASE V:
FREQUENCY = 500 HERTZ
SOURCE DEPTH = 500 FEET
RECEIVER DEPTH = 300 FEET

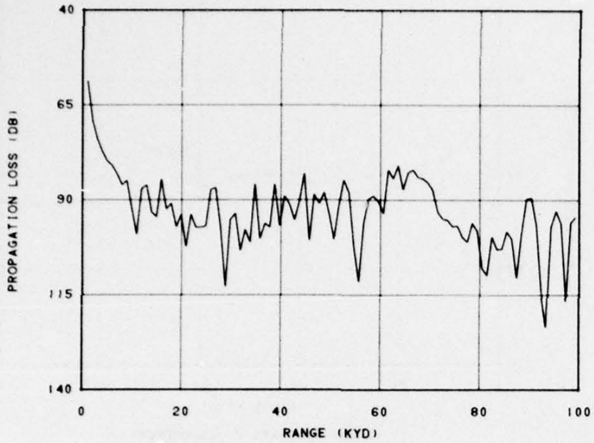

(V-3A) FACT (COHERENT)

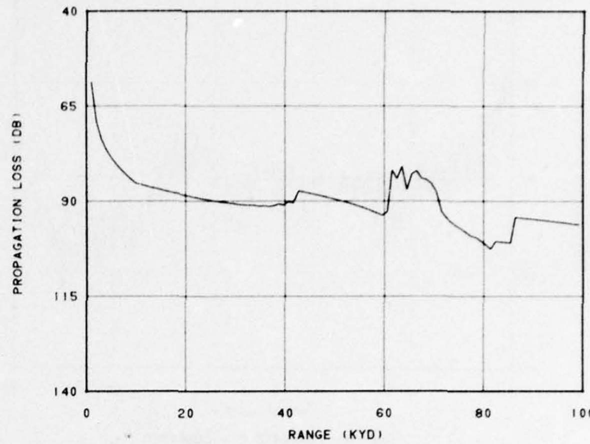

(V-3D) FACT (INCOHERENT)

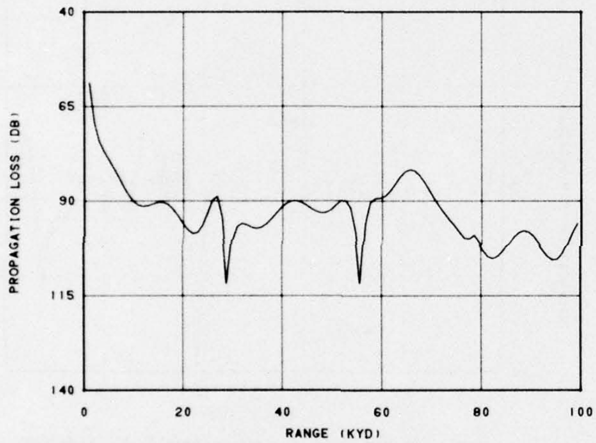

(V-3B) ANALYTICAL FIT TO FACT (COHERENT)

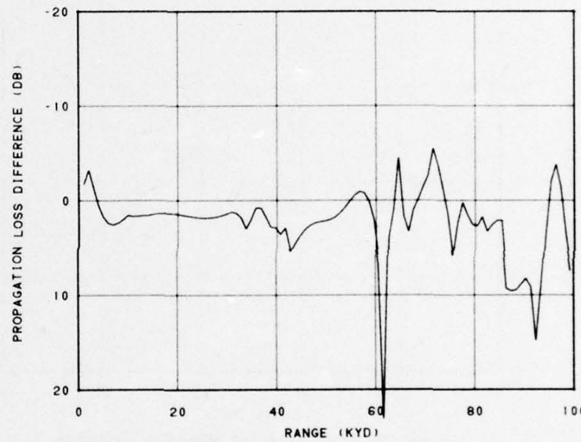

(V-3E) FFP ANALYTICAL FIT MINUS FACT (INCOHERENT)

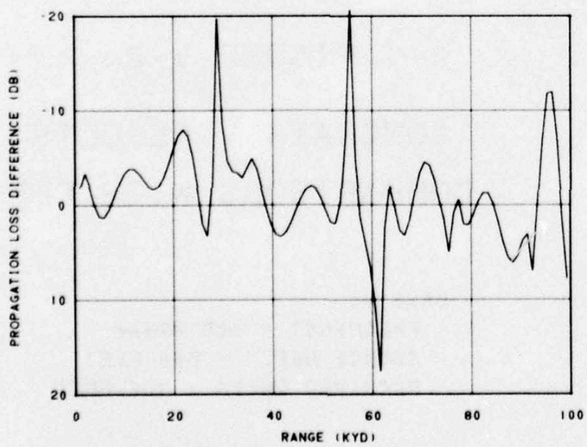

(V-3C) FFP ANALYTICAL FIT MINUS FACT (COHERENT) ANALYTICAL FIT

FIGURE V-3

FACT RESULTS
AND
COMPARISONS WITH FFP

CASE V:
FREQUENCY = 500 HERTZ
SOURCE DEPTH = 500 FEET
RECEIVER DEPTH = 300 FEET

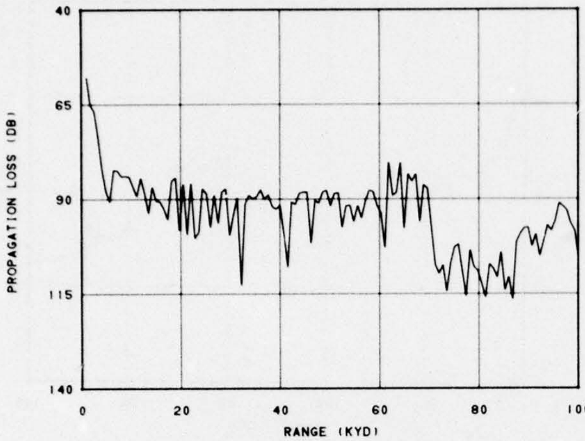

(V-4A) NISSM II (COHERENT)

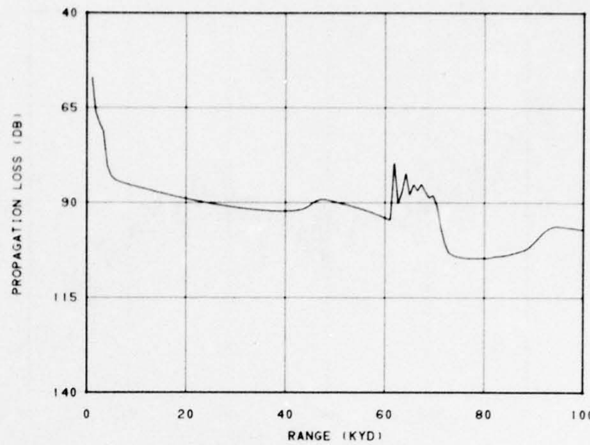

(V-4D) NISSM II (INCOHERENT)

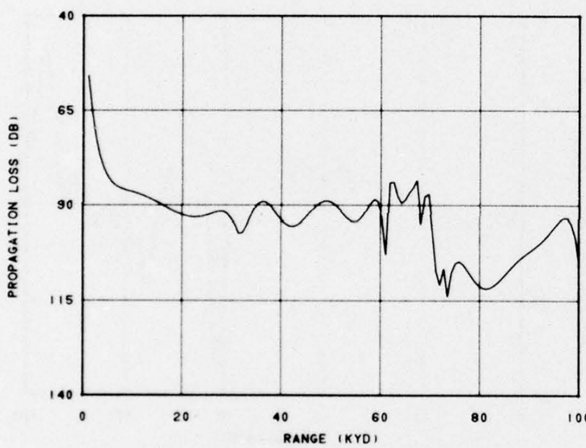

(V-4B) ANALYTICAL FIT TO NISSM II (COHERENT)

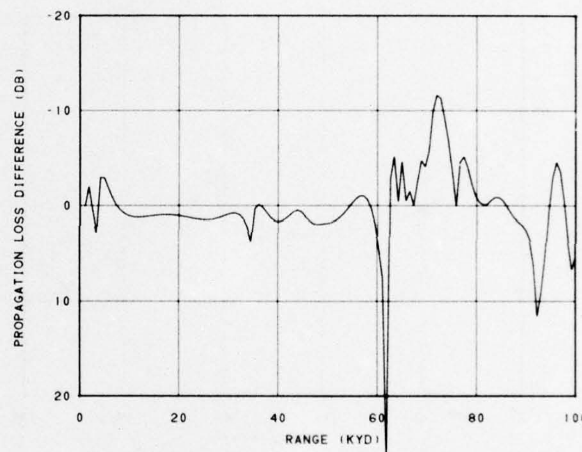

(V-4E) FFP ANALYTICAL FIT MINUS NISSM II (INCOHERENT)

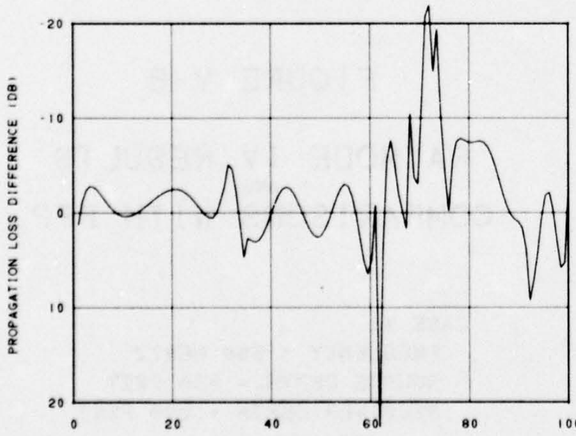

(V-4C) FFP ANALYTICAL FIT MINUS NISSM II (COHERENT) ANALYTICAL FIT

FIGURE V-4

NISSM II RESULTS
AND
COMPARISONS WITH FFP

CASE V:
FREQUENCY = 500 HERTZ
SOURCE DEPTH = 500 FEET
RECEIVER DEPTH = 300 FEET

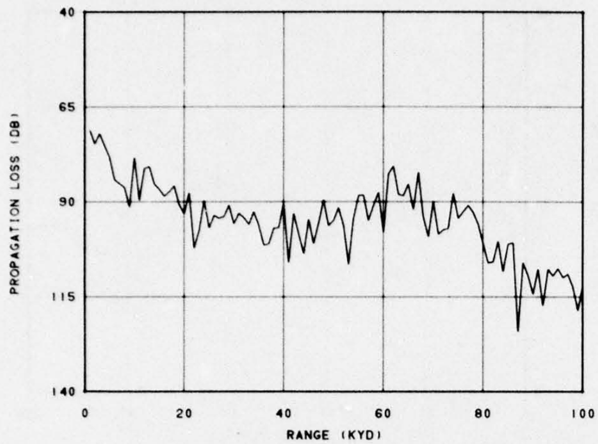

(V-5A) RAYMODE IV (COHERENT)

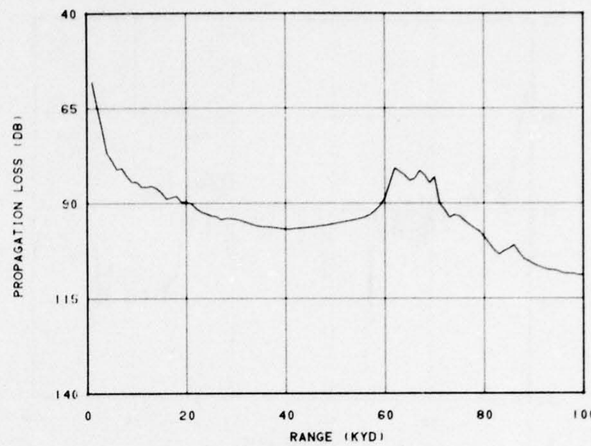

(V-5D) RAYMODE IV (INCOHERENT)

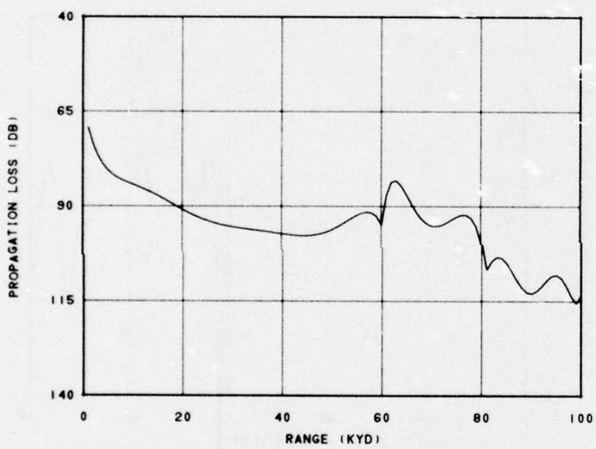

(V-5B) ANALYTICAL FIT TO RAYMODE IV (COHERENT)

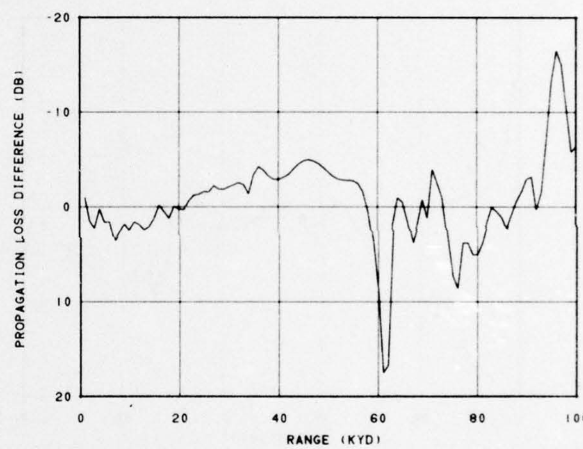

(V-5E) FFP ANALYTICAL FIT MINUS RAYMODE IV (INCOHERENT)

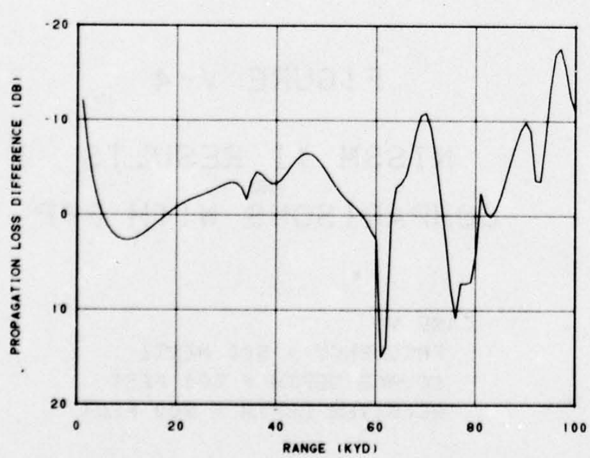

(V-5C) FFP ANALYTICAL FIT MINUS RAYMODE IV (COHERENT) ANALYTICAL FIT

FIGURE V-5

RAYMODE IV RESULTS
AND
COMPARISONS WITH FFP

CASE V:
FREQUENCY = 500 HERTZ
SOURCE DEPTH = 500 FEET
RECEIVER DEPTH = 300 FEET

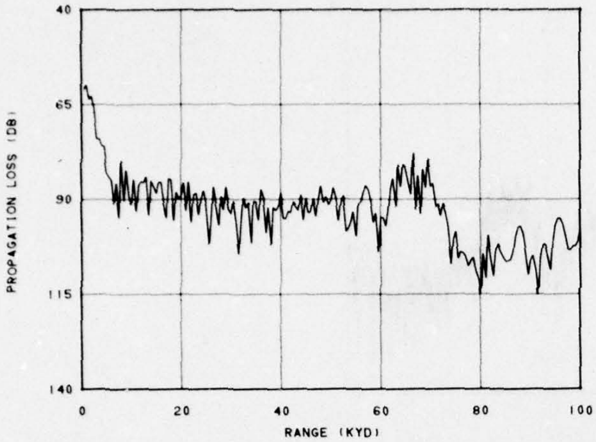

(V-6A) RAYMODE X (COHERENT)

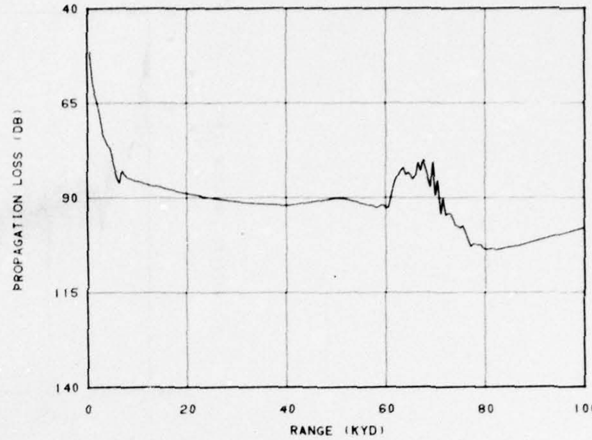

(V-6D) RAYMODE X (INCOHERENT)

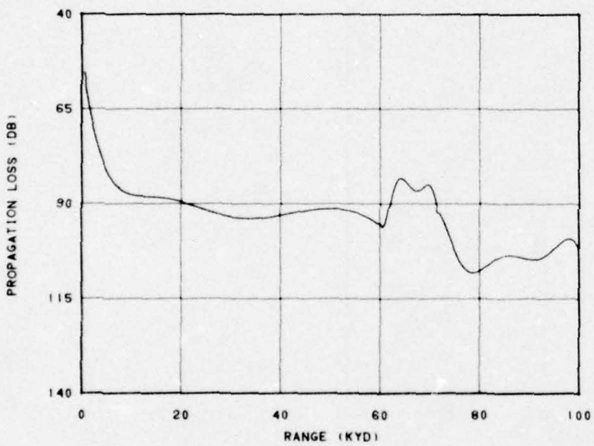

(V-6B) ANALYTICAL FIT TO RAYMODE X (COHERENT)

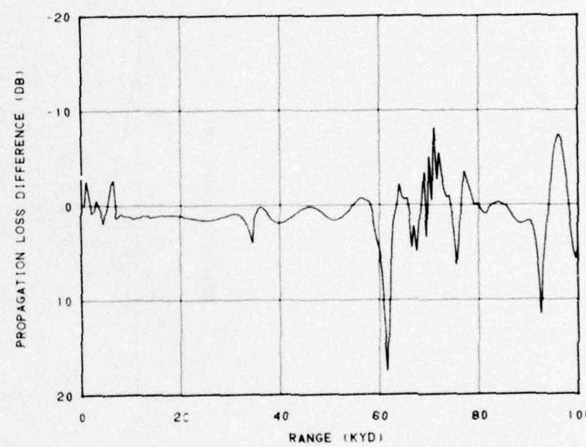

(V-6E) FFP ANALYTICAL FIT MINUS RAYMODE X (INCOHERENT)

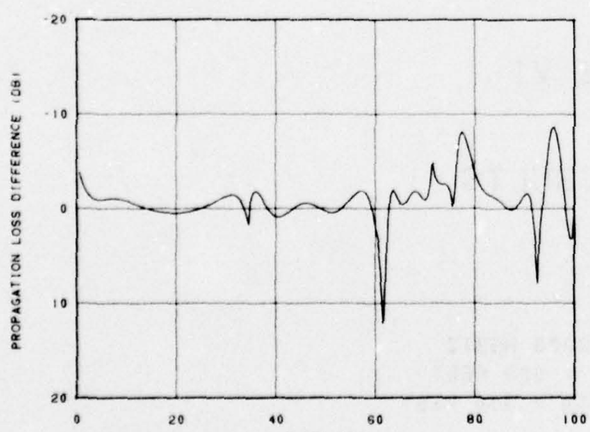

(V-6C) FFP ANALYTICAL FIT MINUS RAYMODE X (COHERENT) ANALYTICAL FIT

FIGURE V-6

RAYMODE X RESULTS
AND
COMPARISONS WITH FFP

CASE V:
FREQUENCY = 500 HERTZ
SOURCE DEPTH = 500 FEET
RECEIVER DEPTH = 300 FEET

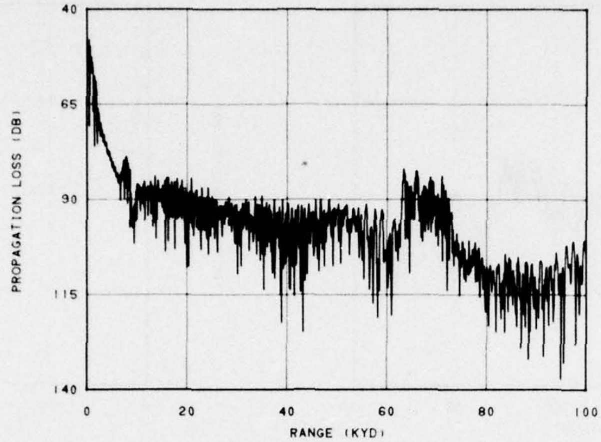

(VI-1A) FFP

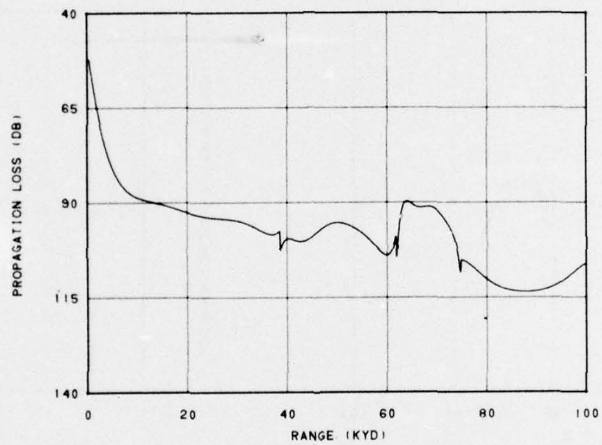

(VI-1B) ANALYTICAL FIT TO FFP

FIGURE VI-1

FFP RESULTS

CASE VI:
FREQUENCY = 2000 HERTZ
SOURCE DEPTH = 500 FEET
RECEIVER DEPTH = 300 FEET

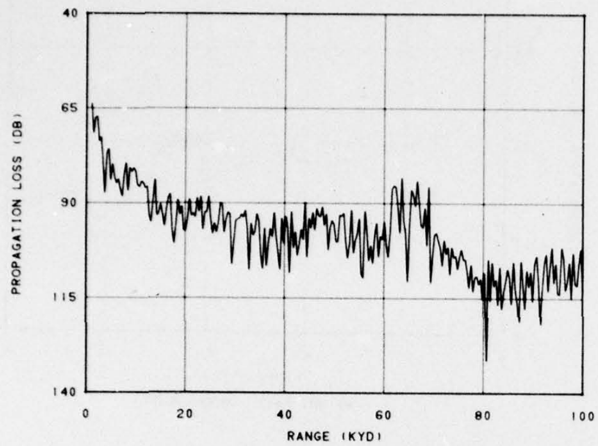

(VI-2A) CONGRATS V (COHERENT)

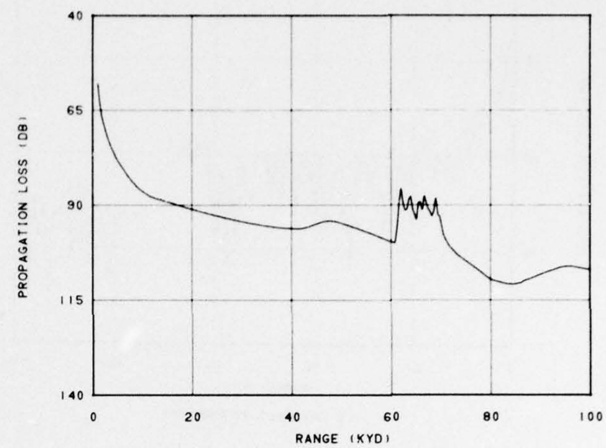

(VI-2D) CONGRATS V (INCOHERENT)

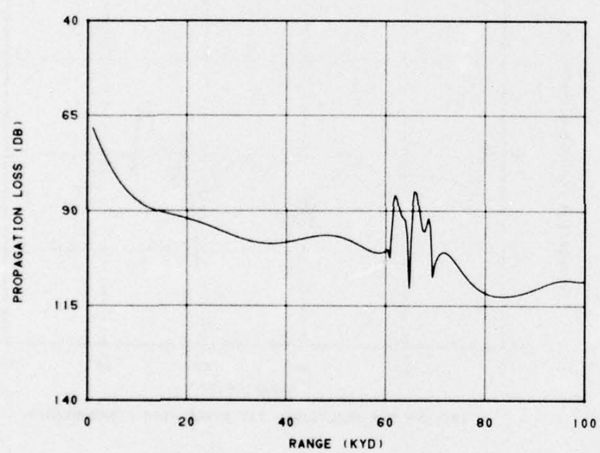

(VI-2B) ANALYTICAL FIT TO CONGRATS V (COHERENT)

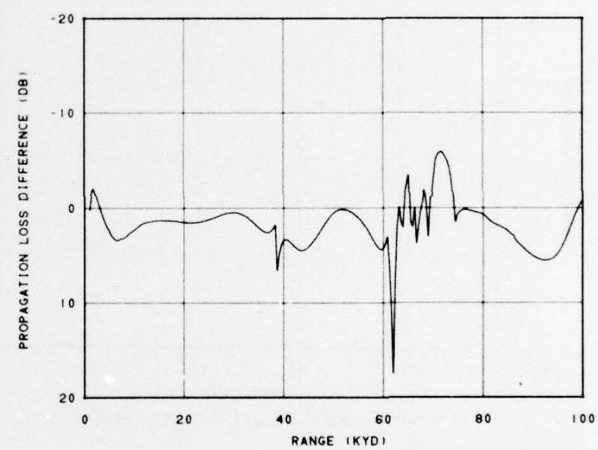

(VI-2E) FFP ANALYTICAL FIT MINUS CONGRATS V (INCOHERENT)

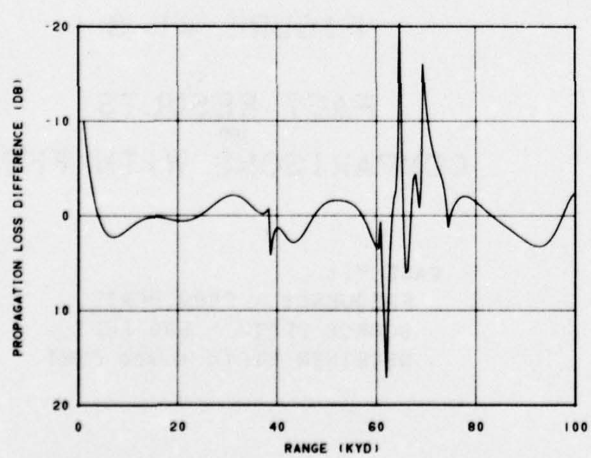

(VI-2C) FFP ANALYTICAL FIT MINUS CONGRATS V (COHERENT) ANALYTICAL FIT

FIGURE VI-2

CONGRATS V RESULTS
AND
COMPARISONS WITH FFP

CASE VI:
FREQUENCY = 2000 HERTZ
SOURCE DEPTH = 500 FEET
RECEIVER DEPTH = 300 FEET

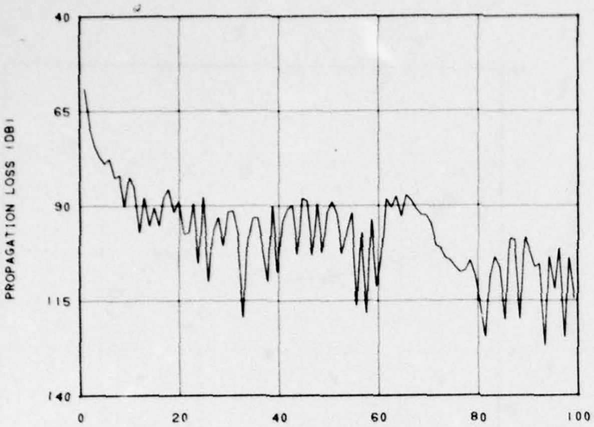

(VI-3A) FACT (COHERENT)

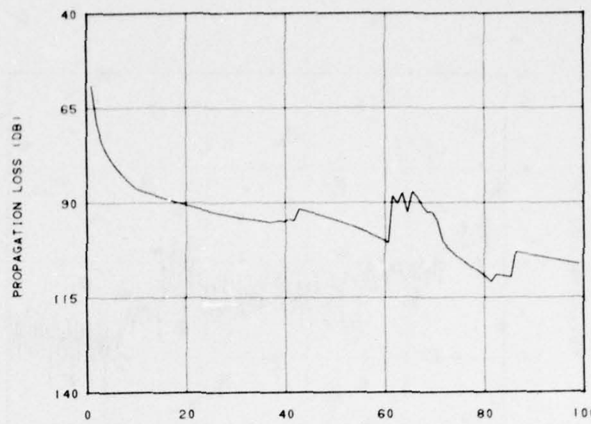

(VI-3D) FACT (INCOHERENT)

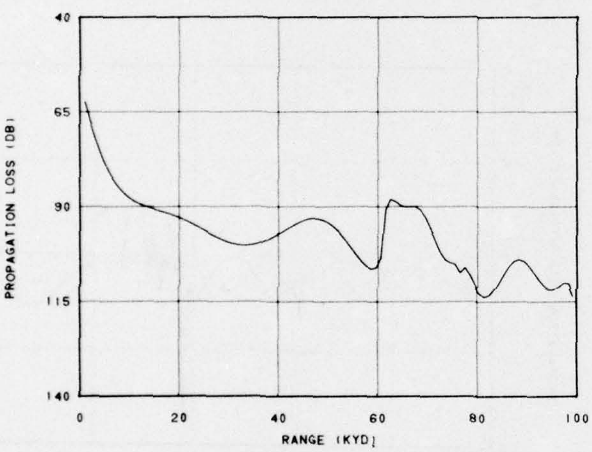

(VI-3B) ANALYTICAL FIT TO FACT (COHERENT)

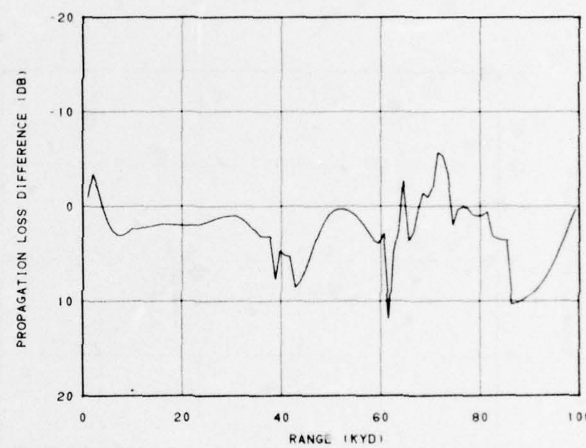

(VI-3E) FFP ANALYTICAL FIT MINUS FACT (INCOHERENT)

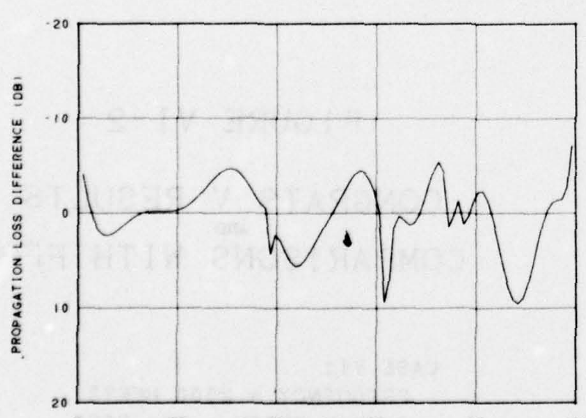

(VI-3C) FFP ANALYTICAL FIT MINUS FACT (COHERENT) ANALYTICAL FIT

FIGURE VI-3

FACT RESULTS
AND
COMPARISONS WITH FFP

CASE VI:
FREQUENCY = 2000 HERTZ
SOURCE DEPTH = 500 FEET
RECEIVER DEPTH = 300 FEET

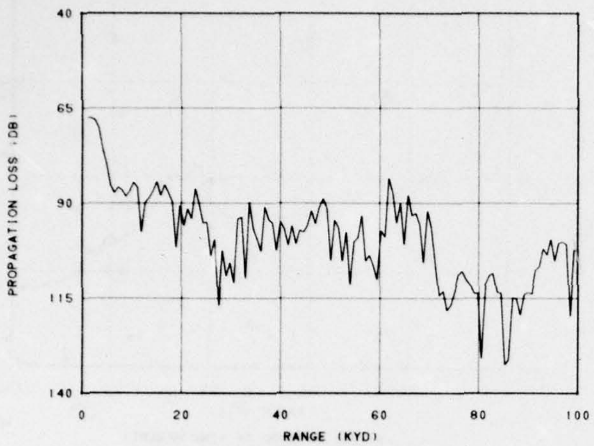

(VI-4A) NISSM II (COHERENT)

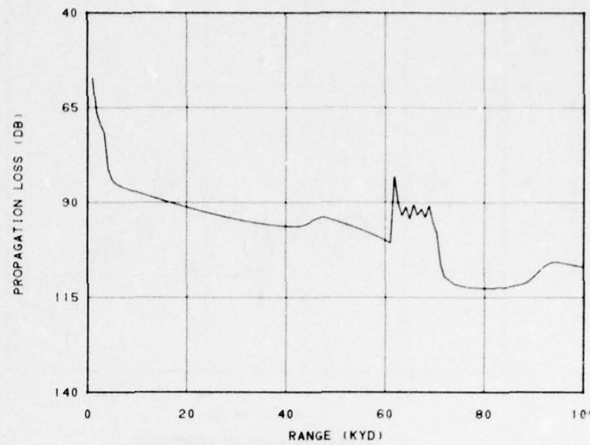

(VI-4D) NISSM II (INCOHERENT)

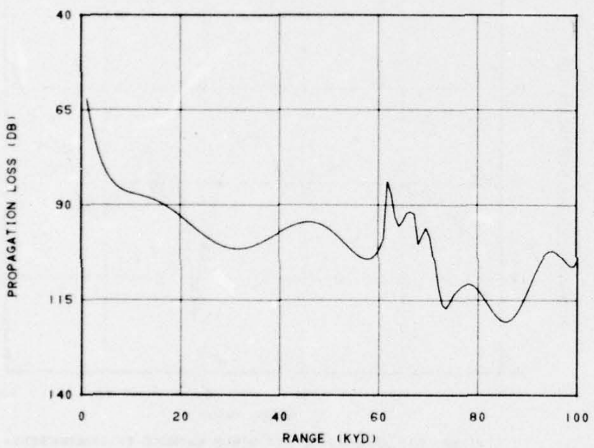

(VI-4B) ANALYTICAL FIT TO NISSM II (COHERENT)

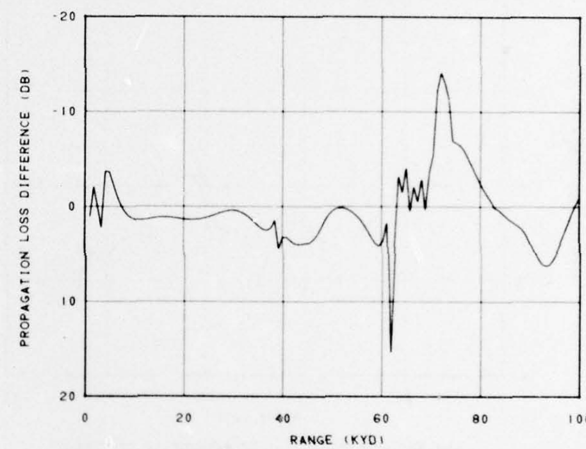

(VI-4E) FFP ANALYTICAL FIT MINUS NISSM II (INCOHERENT)

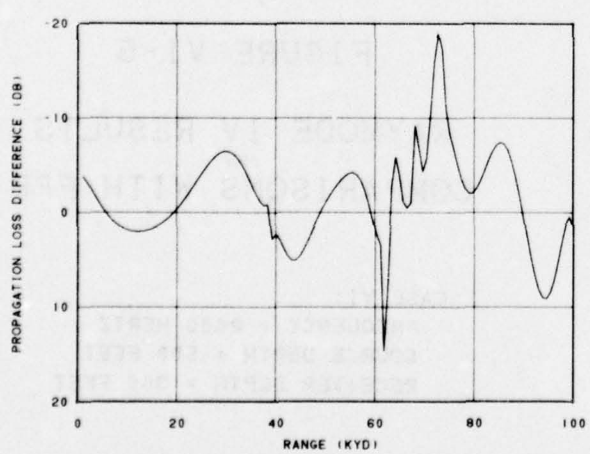

(VI-4C) FFP ANALYTICAL FIT MINUS NISSM II (COHERENT) ANALYTICAL FIT

FIGURE VI-4

NISSM II RESULTS AND COMPARISONS WITH FFP

CASE VI:
FREQUENCY = 2000 HERTZ
SOURCE DEPTH = 500 FEET
RECEIVER DEPTH = 300 FEET

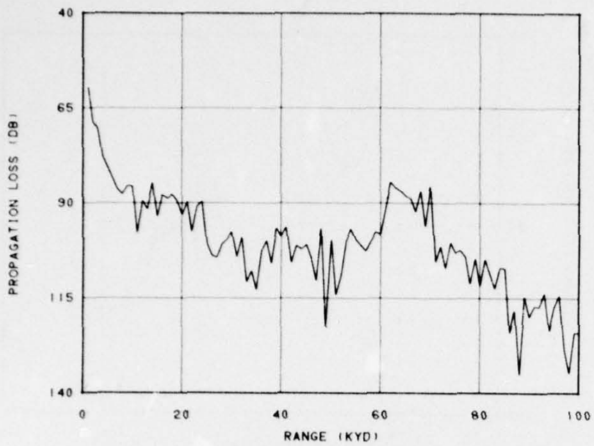

(VI-5A) RAYMODE IV (COHERENT)

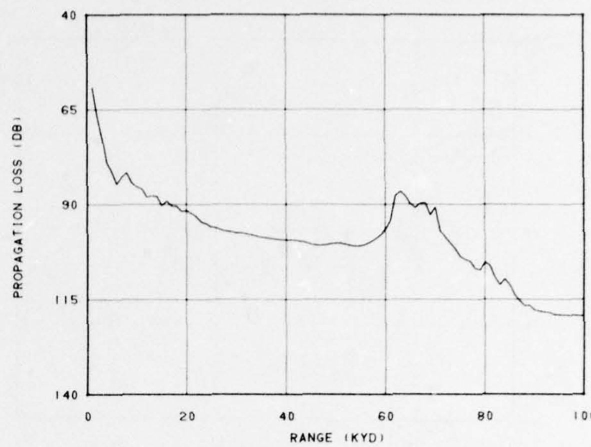

(VI-5D) RAYMODE IV (INCOHERENT)

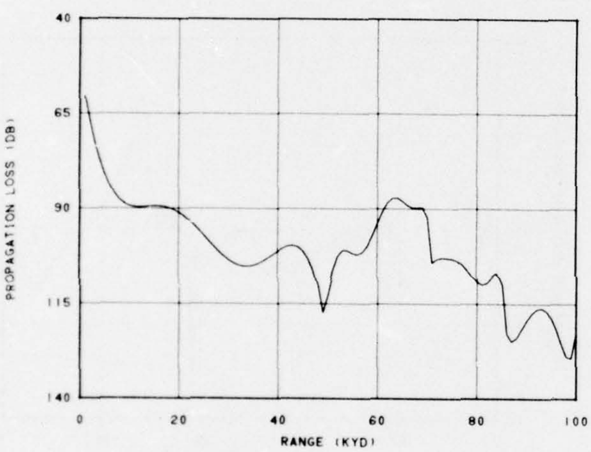

(VI-5B) ANALYTICAL FIT TO RAYMODE IV (COHERENT)

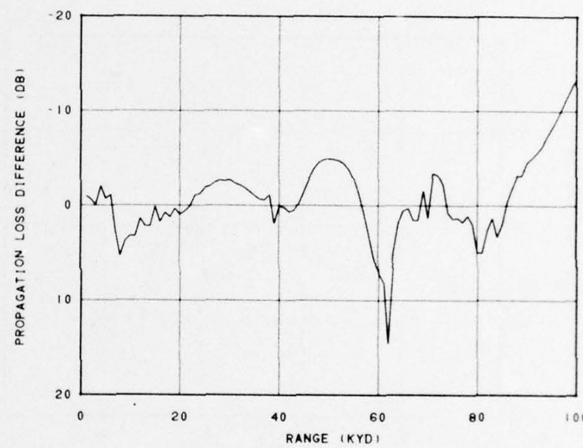

(VI-5E) FFP ANALYTICAL FIT MINUS RAYMODE IV (INCOHERENT)

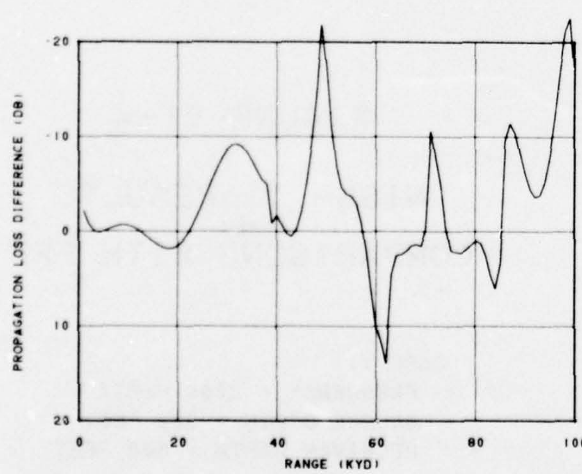

(VI-5C) FFP ANALYTICAL FIT MINUS RAYMODE IV (COHERENT) ANALYTICAL FIT

FIGURE VI-5

RAYMODE IV RESULTS
AND
COMPARISONS WITH FFP

CASE VI:
FREQUENCY = 2000 HERTZ
SOURCE DEPTH = 500 FEET
RECEIVER DEPTH = 300 FEET

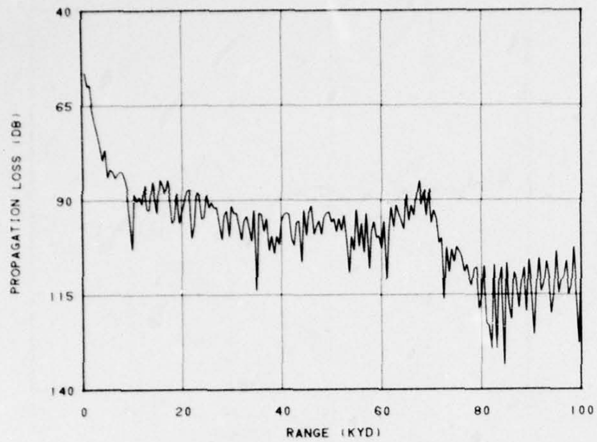

(VI-6A) RAYMODE X (COHERENT)

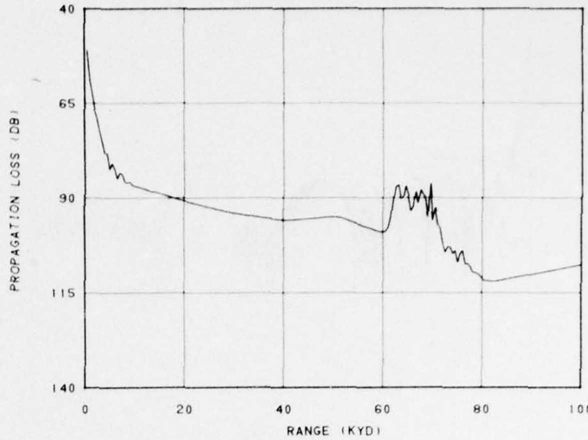

(VI-6D) RAYMODE X (INCOHERENT)

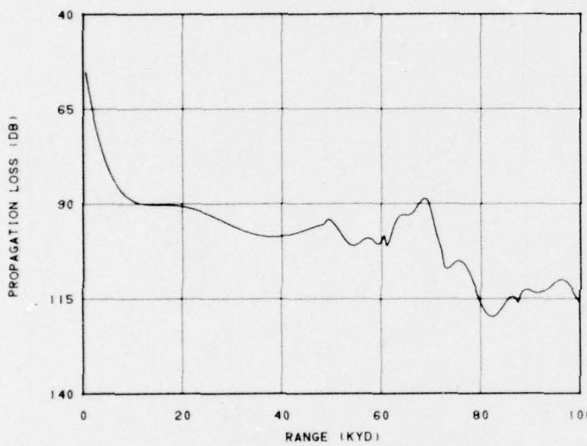

(VI-6B) ANALYTICAL FIT TO RAYMODE X (COHERENT)

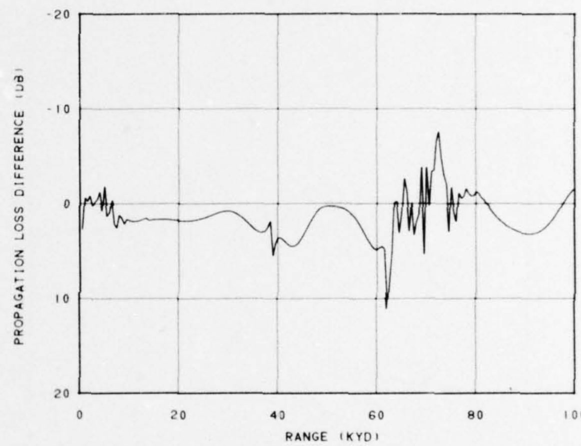

(VI-6E) FFP ANALYTICAL FIT MINUS RAYMODE X (INCOHERENT)

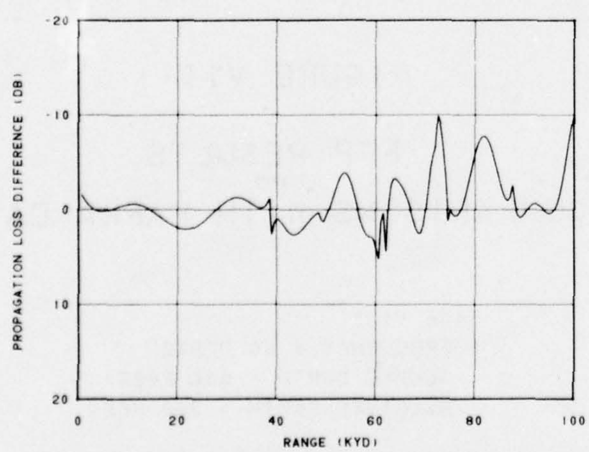

(VI-6C) FFP ANALYTICAL FIT MINUS RAYMODE X (COHERENT) ANALYTICAL FIT

FIGURE VI-6

RAYMODE X RESULTS
AND
COMPARISONS WITH FFP

CASE VI:
FREQUENCY = 2000 HERTZ
SOURCE DEPTH = 500 FEET
RECEIVER DEPTH = 300 FEET

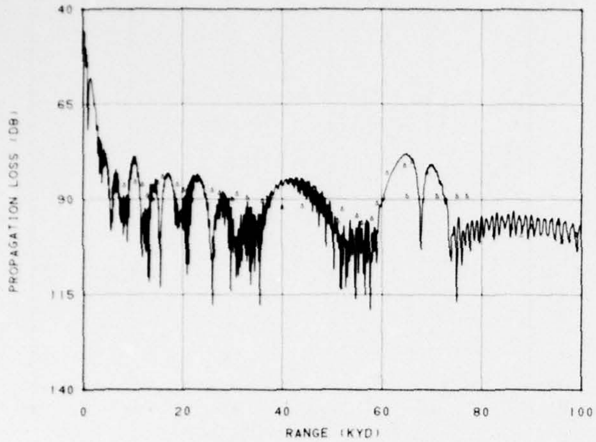

(VII-1A) Δ PARKA EXPERIMENTAL DATA; — FFP MODEL

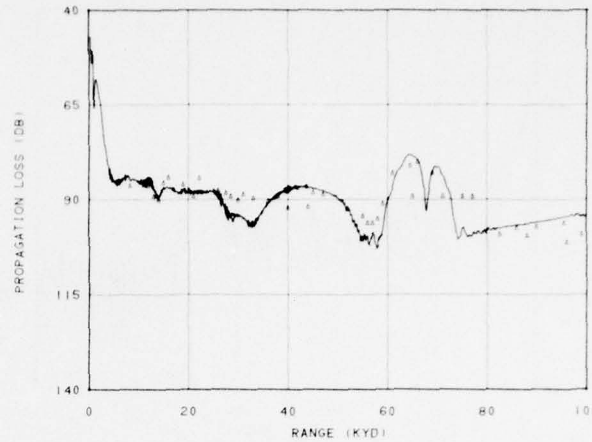

(VII-1D) Δ PARKA EXPERIMENTAL DATA; — FFP MODEL (1/3 OCTAVE)

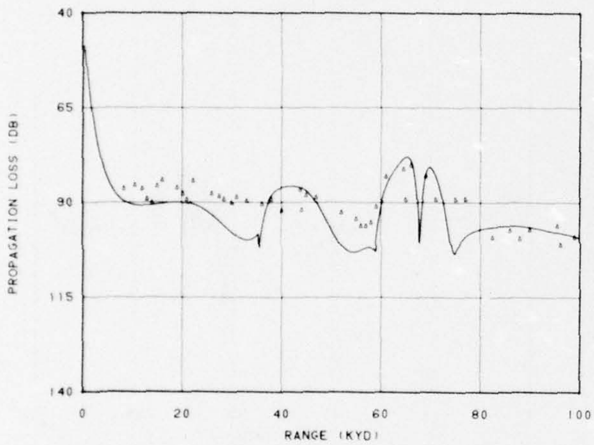

(VII-1B) Δ PARKA DATA; — ANALYTICAL FIT TO FFP

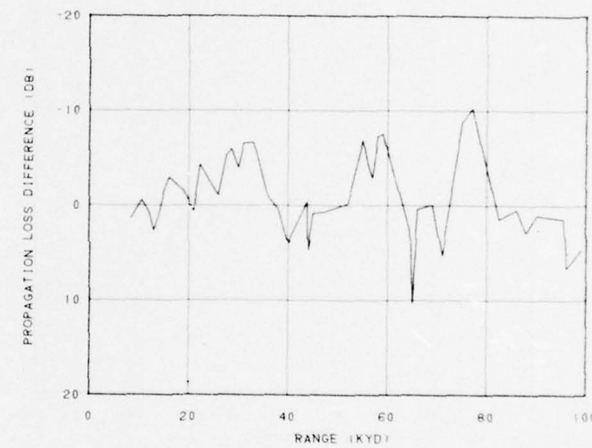

(VII-1E) PARKA DATA MINUS FFP (1/3 OCTAVE)

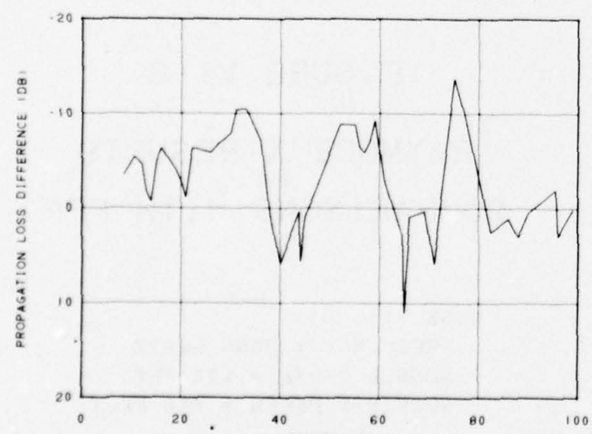

(VII-1C) PARKA DATA MINUS FFP ANALYTICAL FIT

FIGURE VII-1

FFP RESULTS
AND
COMPARISONS WITH PARKA DATA

CASE VII:
FREQUENCY = 50 HERTZ
SOURCE DEPTH = 500 FEET
RECEIVER DEPTH = 300 FEET

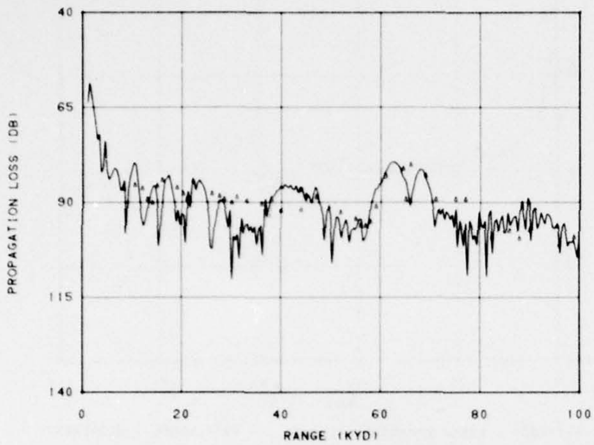

(VII-2A) Δ PARKA EXPERIMENTAL DATA; — CONGRATS V MODEL (COHERENT)

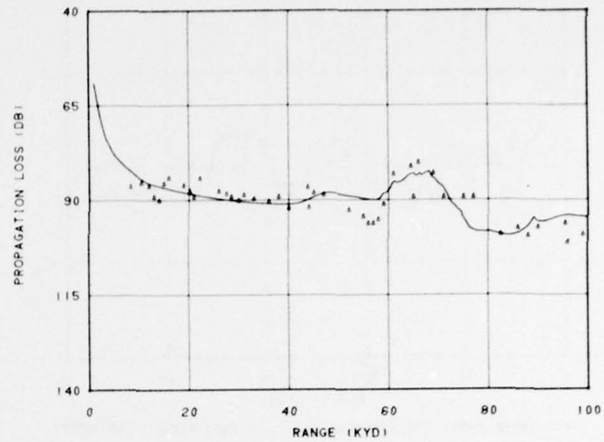

(VII-2D) Δ PARKA EXPERIMENTAL DATA; — CONGRATS V MODEL (INCOHERENT)

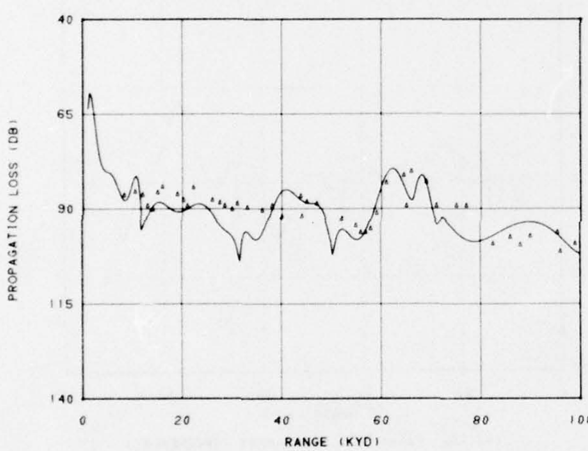

(VII-2B) Δ PARKA DATA; — ANALYTICAL FIT TO CONGRATS V (COHERENT)

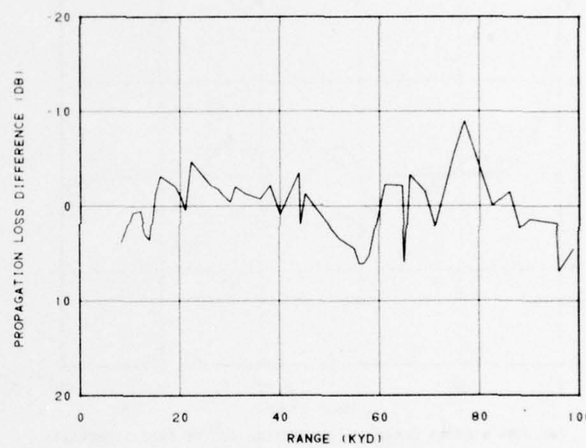

(VII-2E) PARKA DATA MINUS CONGRATS V (INCOHERENT)

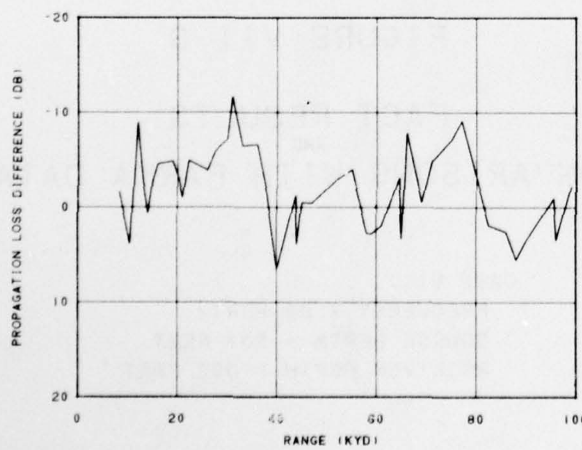

(VII-2C) PARKA DATA MINUS CONGRATS V (COHERENT) ANALYTICAL FIT

FIGURE VII-2

CONGRATS V RESULTS
AND
COMPARISONS WITH PARKA DATA

CASE VII:
FREQUENCY = 50 HERTZ
SOURCE DEPTH = 500 FEET
RECEIVER DEPTH = 300 FEET

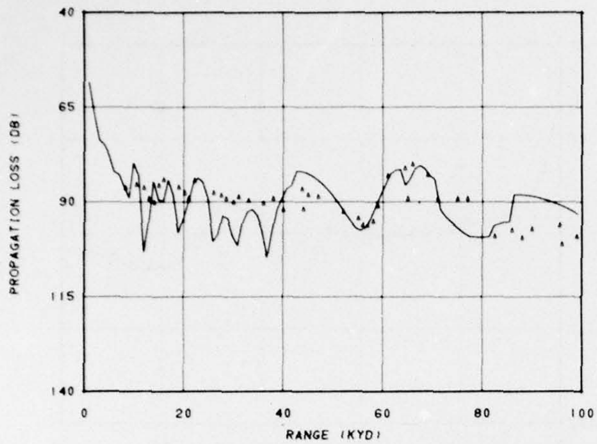

(VII-3A) ▲ PARKA EXPERIMENTAL DATA; — FACT MODEL (COHERENT)

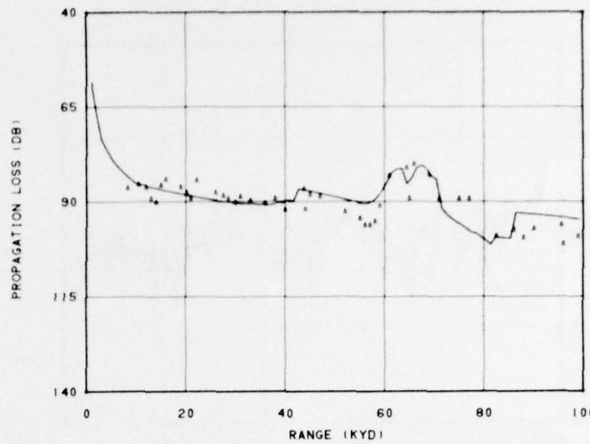

(VII-3D) ▲ PARKA EXPERIMENTAL DATA; — FACT MODEL (INCOHERENT)

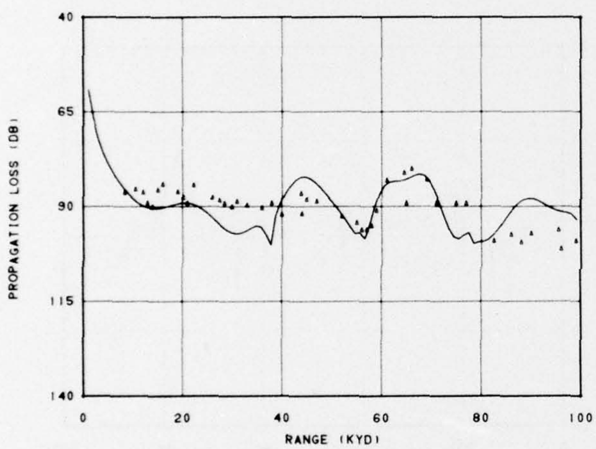

(VII-3B) ▲ PARKA DATA; — ANALYTICAL FIT TO FACT (COHERENT)

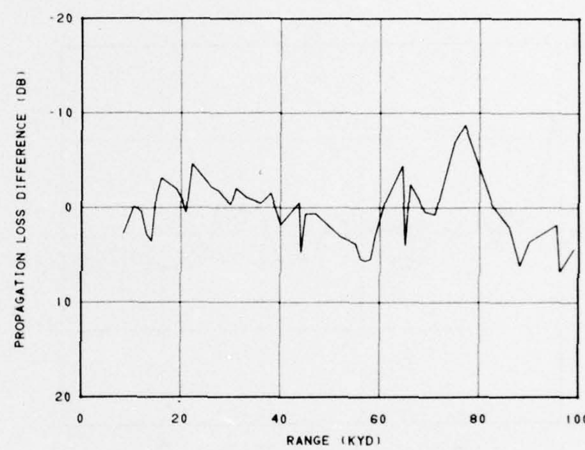

(VII-3E) PARKA DATA MINUS FACT (INCOHERENT)

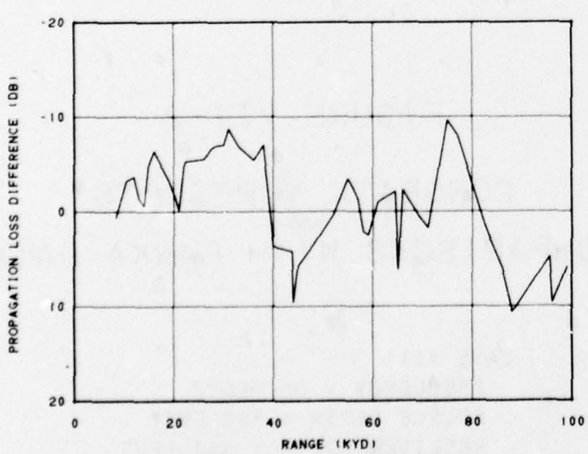

(VII-3C) PARKA DATA MINUS FACT (COHERENT) ANALYTICAL FIT

FIGURE VII-3

FACT RESULTS AND COMPARISONS WITH PARKA DATA

CASE VII:
FREQUENCY = 50 HERTZ
SOURCE DEPTH = 500 FEET
RECEIVER DEPTH = 300 FEET

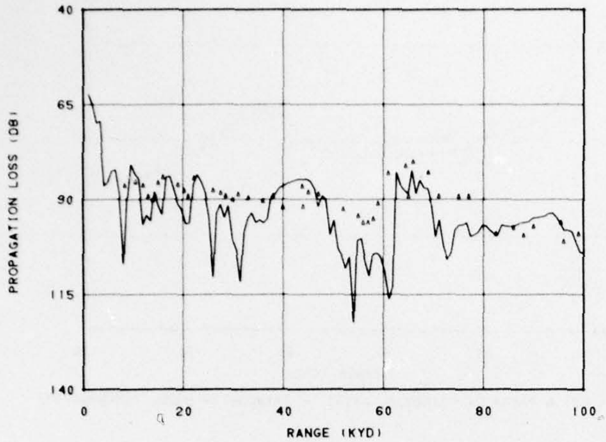

(VII-4A) Δ PARKA EXPERIMENTAL DATA; — NISSM II MODEL (COHERENT)

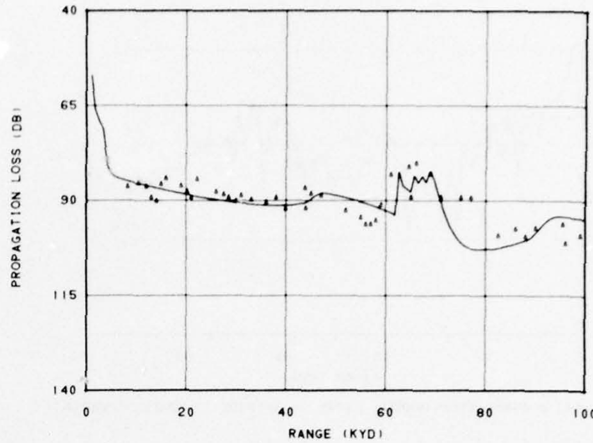

(VII-4D) Δ PARKA EXPERIMENTAL DATA; — NISSM II MODEL (INCOHERENT)

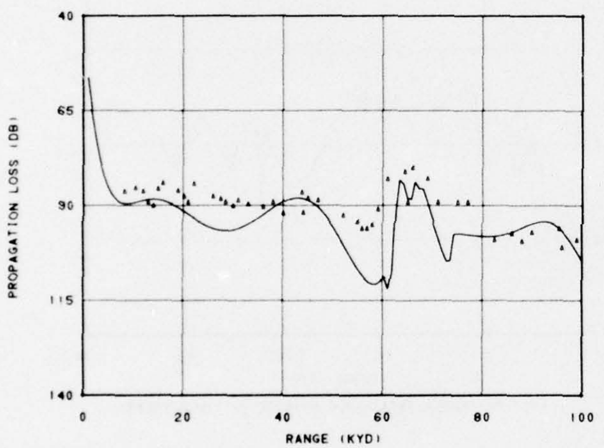

(VII-4B) Δ PARKA DATA; — ANALYTICAL FIT TO NISSM II (COHERENT)

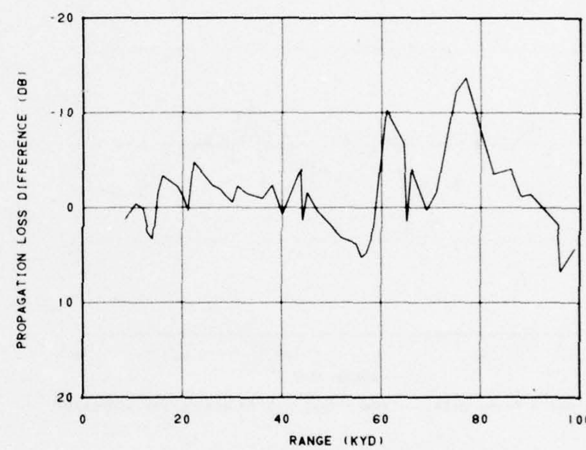

(VII-4E) PARKA DATA MINUS NISSM II (INCOHERENT)

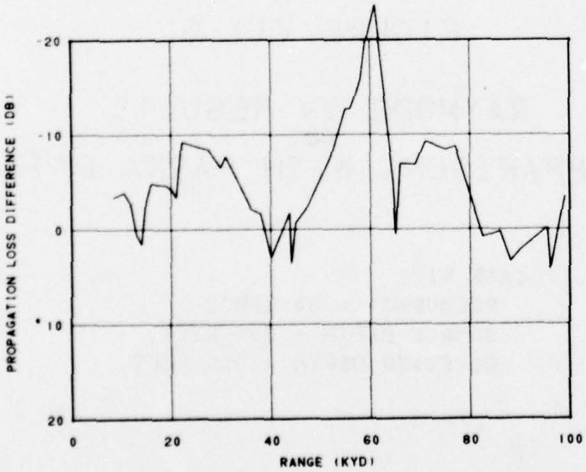

(VII-4C) PARKA DATA MINUS NISSM II (COHERENT) ANALYTICAL FIT

FIGURE VII-4

NISSM II RESULTS
AND
COMPARISONS WITH PARKA DATA

CASE VII:
FREQUENCY = 50 HERTZ
SOURCE DEPTH = 500 FEET
RECEIVER DEPTH = 300 FEET

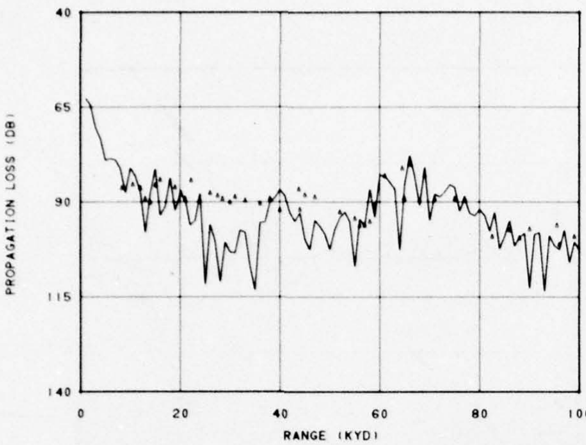

(VII-5A) ▲ PARKA EXPERIMENTAL DATA; — RAYMODE IV MODEL (COHERENT)

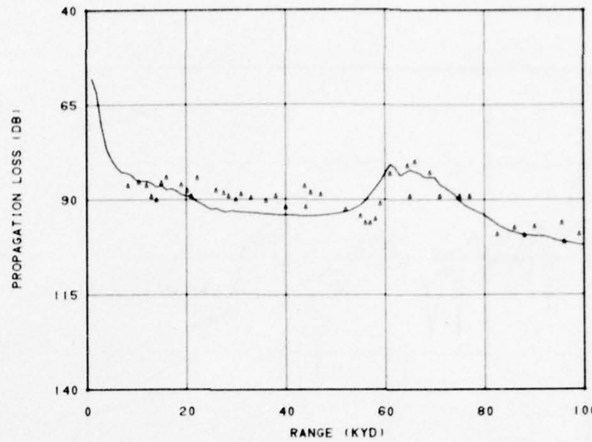

(VII-5D) ▲ PARKA EXPERIMENTAL DATA; — RAYMODE IV MODEL (INCOHERENT)

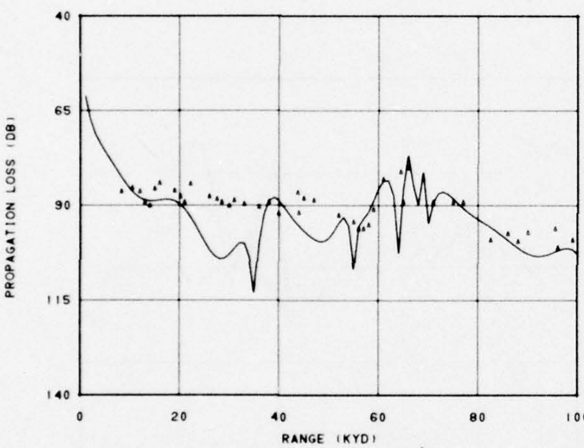

(VII-5B) ▲ PARKA DATA; — ANALYTICAL FIT TO RAYMODE IV (COHERENT)

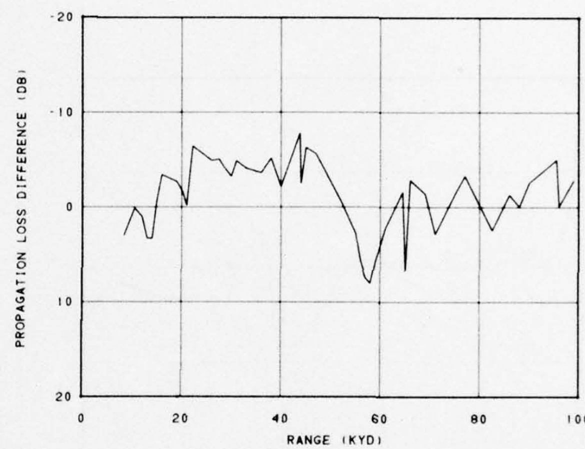

(VII-5E) PARKA DATA MINUS RAYMODE IV (INCOHERENT)

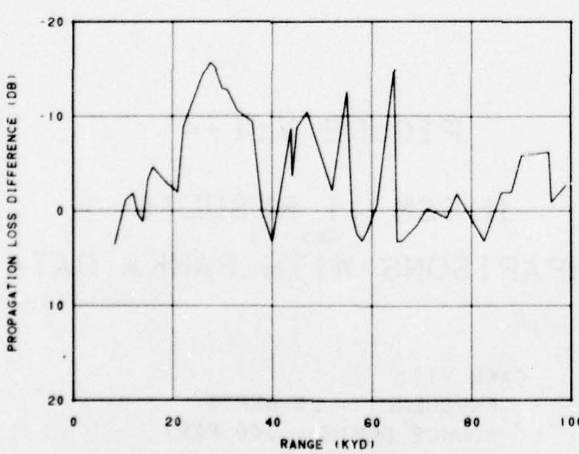

(VII-5C) PARKA DATA MINUS RAYMODE IV (COHERENT) ANALYTICAL FIT

FIGURE VII-5

RAYMODE IV RESULTS AND COMPARISONS WITH PARKA DATA

CASE VII:
FREQUENCY = 50 HERTZ
SOURCE DEPTH = 500 FEET
RECEIVER DEPTH = 300 FEET

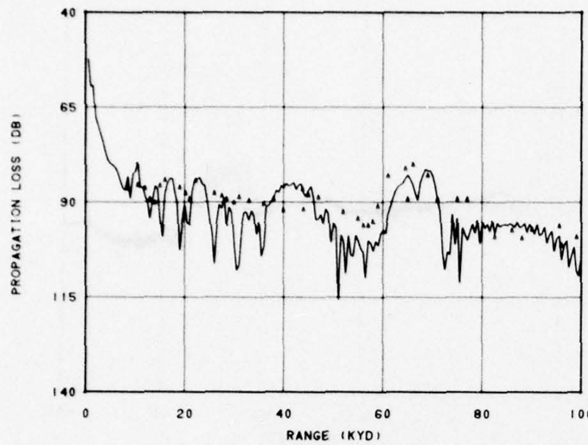

(VII-6A) ▲ PARKA EXPERIMENTAL DATA; — RAYMODE X MODEL (COHERENT)

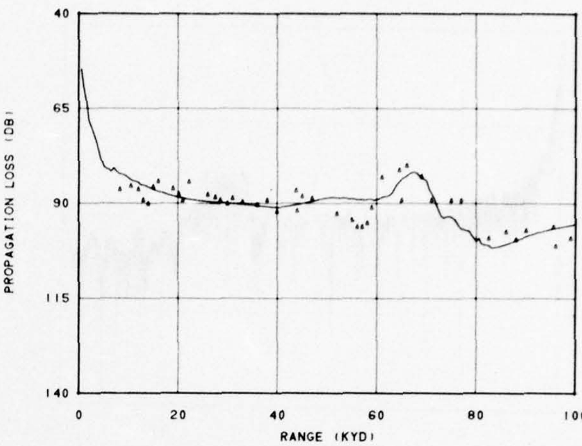

(VII-6D) ▲ PARKA EXPERIMENTAL DATA; — RAYMODE X MODEL (INCOHERENT)

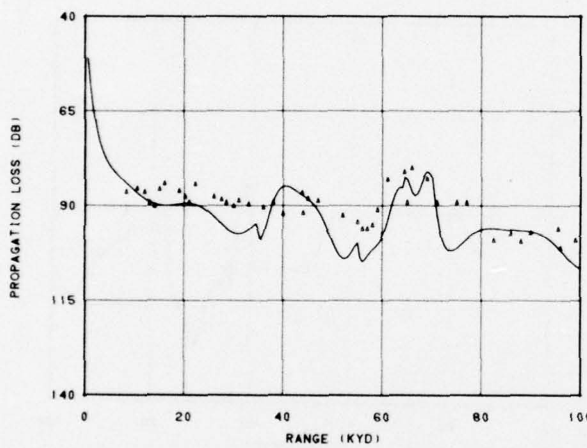

(VII-6B) ▲ PARKA DATA; — ANALYTICAL FIT TO RAYMODE X (COHERENT)

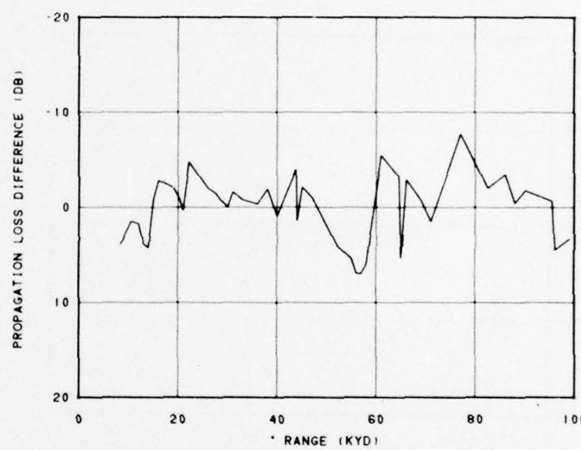

(VII-6E) PARKA DATA MINUS RAYMODE X (INCOHERENT)

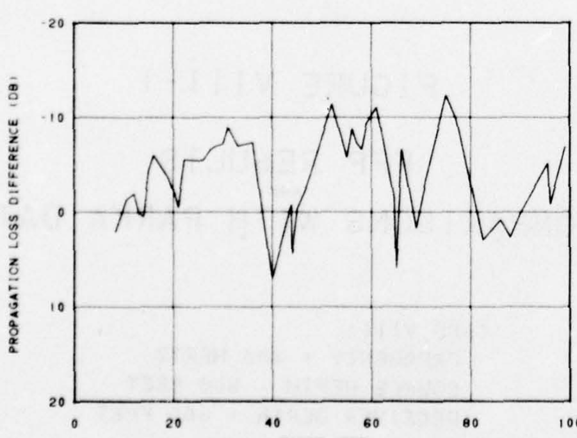

(VII-6C) PARKA DATA MINUS RAYMODE X (COHERENT) ANALYTICAL FIT

FIGURE VII-6

RAYMODE X RESULTS
AND
COMPARISONS WITH PARKA DATA

CASE VII:
FREQUENCY = 50 HERTZ
SOURCE DEPTH = 500 FEET
RECEIVER DEPTH = 300 FEET

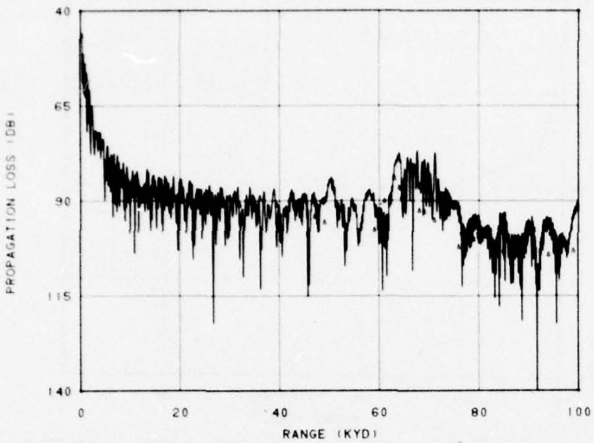

(VIII-1A) ▲ PARKA EXPERIMENTAL DATA; — FFP MODEL

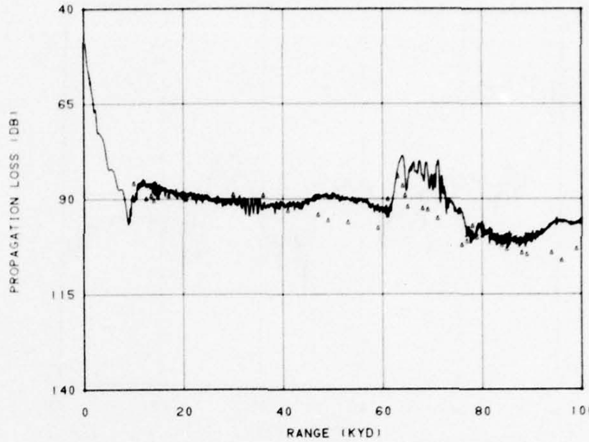

(VIII-1D) ▲ PARKA EXPERIMENTAL DATA; — FFP MODEL (1/3 OCTAVE)

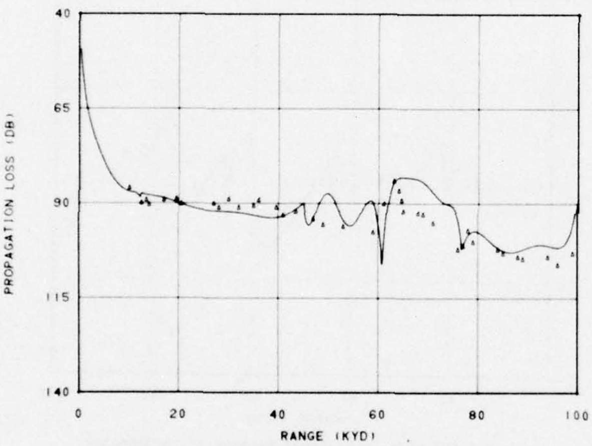

(VIII-1B) ▲ PARKA DATA; — ANALYTICAL FIT TO FFP

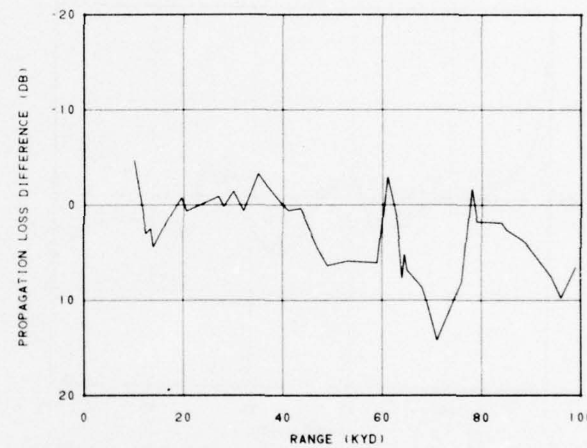

(VIII-1E) PARKA DATA MINUS FFP (1/3 OCTAVE)

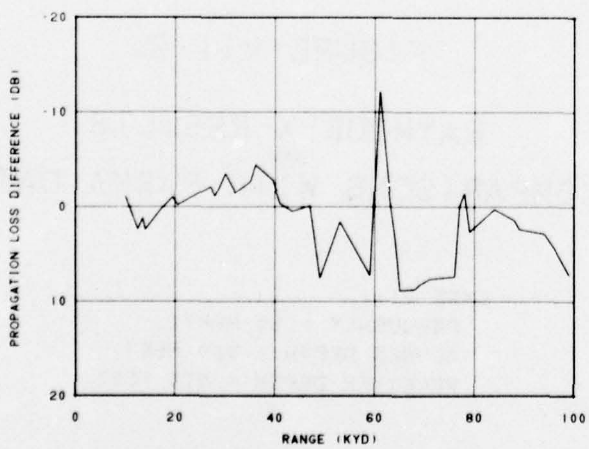

(VIII-1C) PARKA DATA MINUS FFP ANALYTICAL FIT

FIGURE VIII-1

FFP RESULTS
AND
COMPARISONS WITH PARKA DATA

CASE VIII:
FREQUENCY = 400 HERTZ
SOURCE DEPTH = 500 FEET
RECEIVER DEPTH = 300 FEET

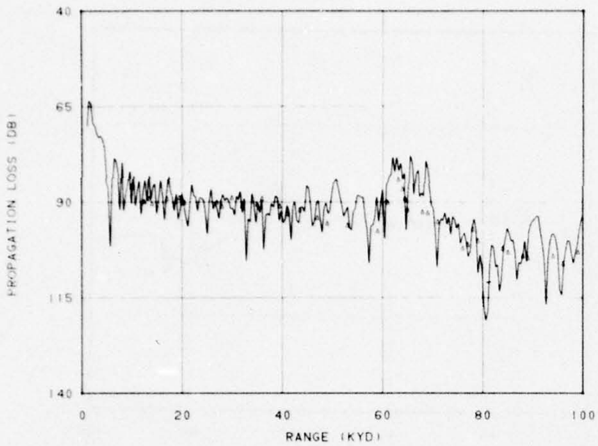

(VIII-2A) Δ PARKA EXPERIMENTAL DATA; — CONGRATS V MODEL (COHERENT)

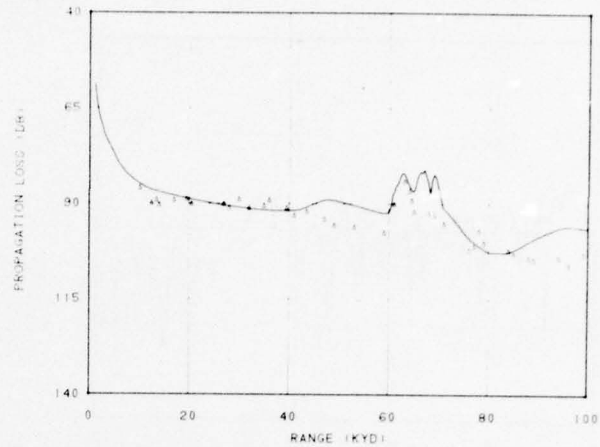

(VIII-2D) Δ PARKA EXPERIMENTAL DATA; — CONGRATS V MODEL (INCOHERENT)

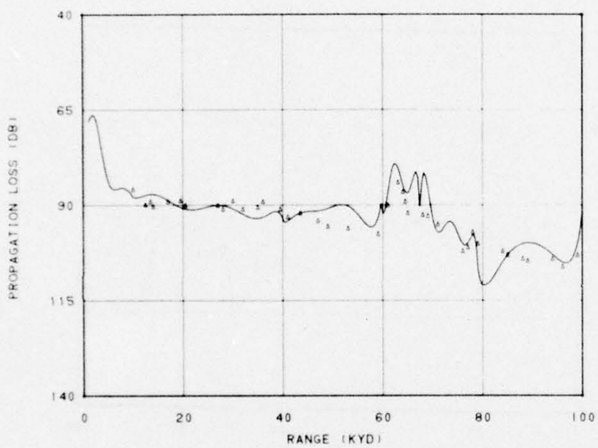

(VIII-2B) Δ PARKA DATA; — ANALYTICAL FIT TO CONGRATS V (COHERENT)

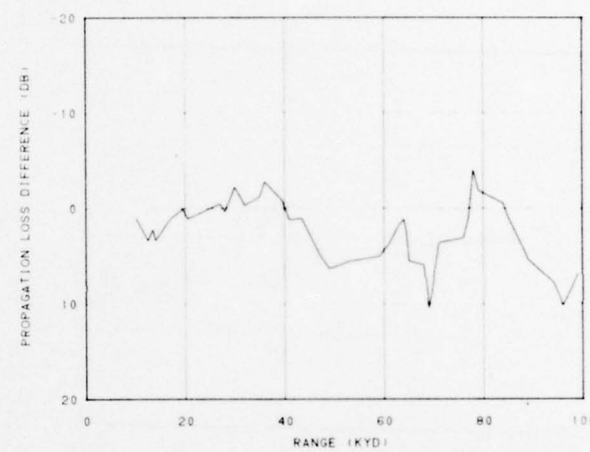

(VIII-2E) PARKA DATA MINUS CONGRATS V (INCOHERENT)

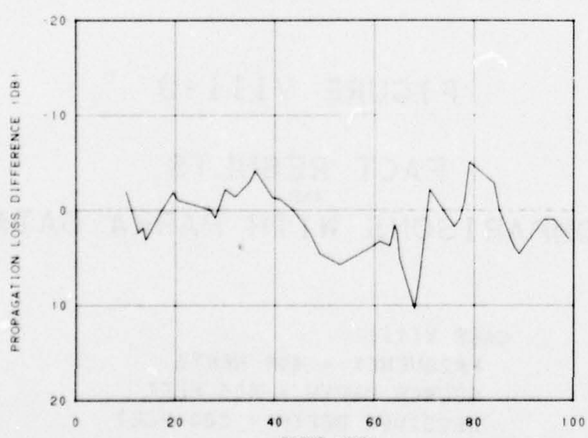

(VIII-2C) PARKA DATA MINUS CONGRATS V (COHERENT) ANALYTICAL FIT

FIGURE VIII-2

CONGRATS V RESULTS
AND
COMPARISONS WITH PARKA DATA

CASE VIII:
FREQUENCY = 400 HERTZ
SOURCE DEPTH = 500 FEET
RECEIVER DEPTH = 300 FEET

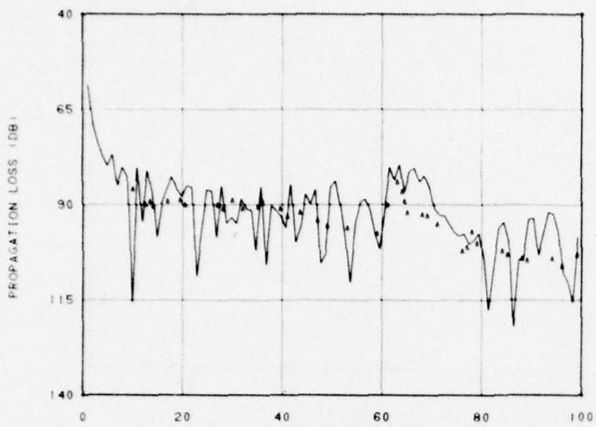

(VIII-3A) ▲ PARKA EXPERIMENTAL DATA; — FACT MODEL (COHERENT)

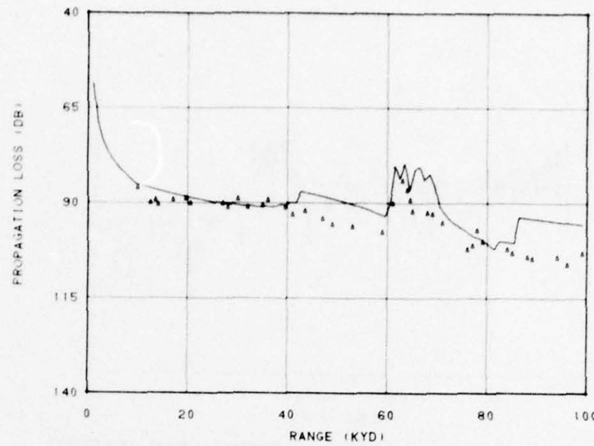

(VIII-3D) ▲ PARKA EXPERIMENTAL DATA; — FACT MODEL (INCOHERENT)

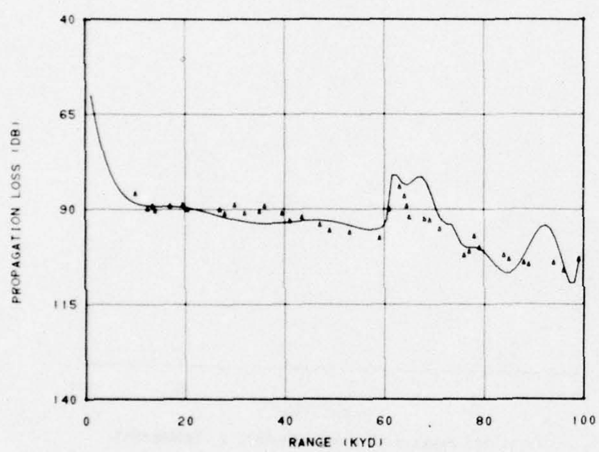

(VIII-3B) ▲ PARKA DATA; — ANALYTICAL FIT TO FACT (COHERENT)

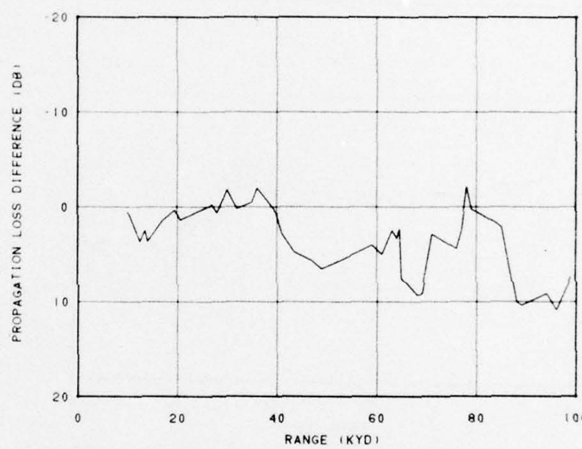

(VIII-3E) PARKA DATA MINUS FACT (INCOHERENT)

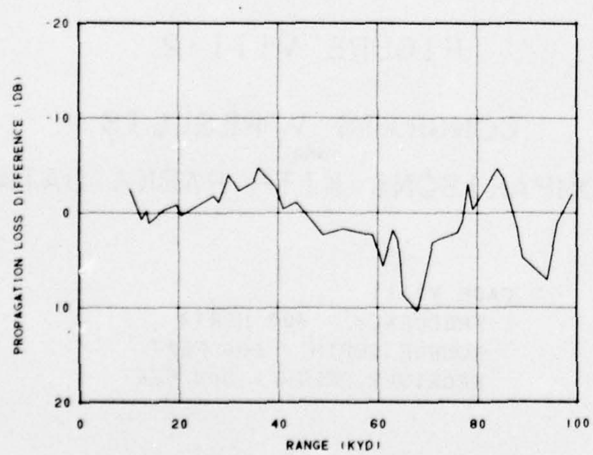

(VIII-3C) PARKA DATA MINUS FACT (COHERENT) ANALYTICAL FIT

FIGURE VIII-3

FACT RESULTS
AND
COMPARISONS WITH PARKA DATA

CASE VIII:
FREQUENCY = 400 HERTZ
SOURCE DEPTH = 500 FEET
RECEIVER DEPTH = 300 FEET

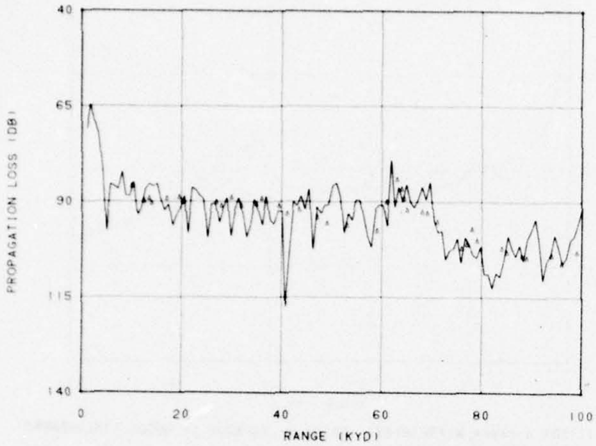

(VIII-4A) Δ PARKA EXPERIMENTAL DATA; — NISSM II MODEL (COHERENT)

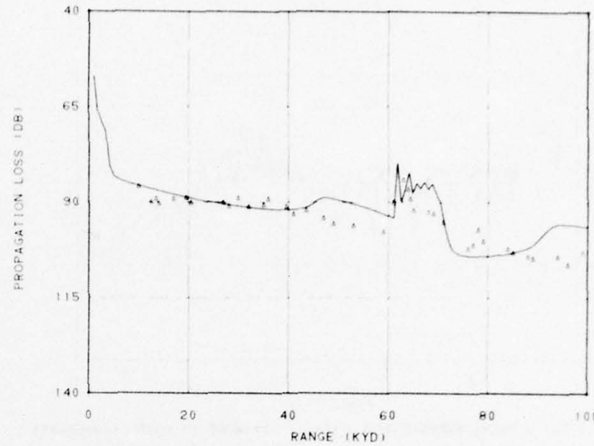

(VIII-4D) Δ PARKA EXPERIMENTAL DATA; — NISSM II MODEL (INCOHERENT)

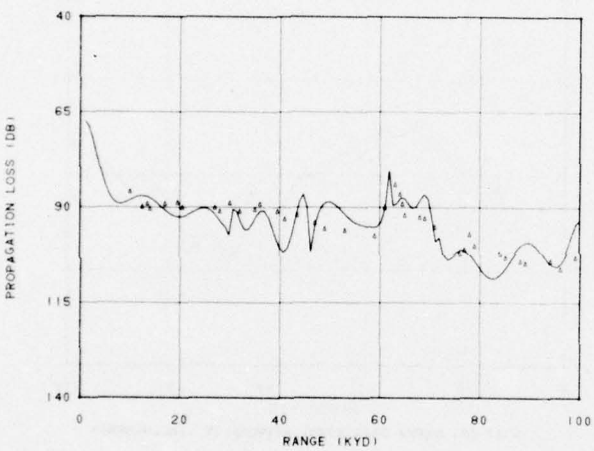

(VIII-4B) Δ PARKA DATA; — ANALYTICAL FIT TO NISSM II (COHERENT)

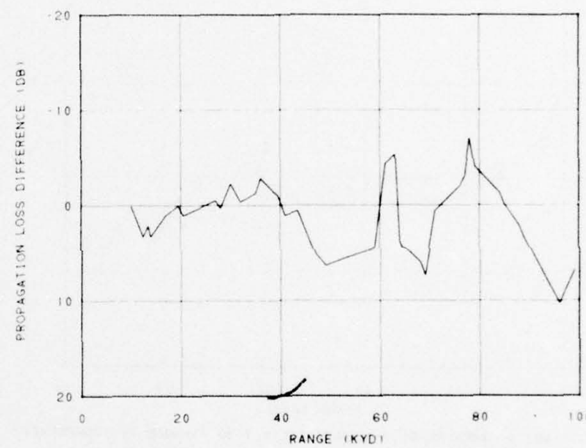

(VIII-4E) PARKA DATA MINUS NISSM II (INCOHERENT)

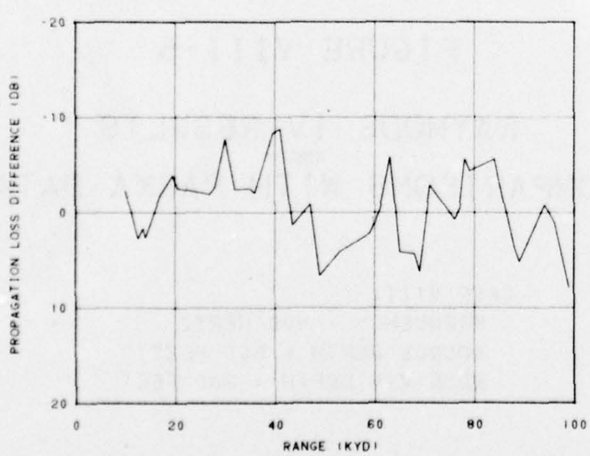

(VIII-4C) PARKA DATA MINUS NISSM II (COHERENT) ANALYTICAL FIT

FIGURE VIII-4

NISSM II RESULTS
AND
COMPARISONS WITH PARKA DATA

CASE VIII:
FREQUENCY = 400 HERTZ
SOURCE DEPTH = 500 FEET
RECEIVER DEPTH = 300 FEET

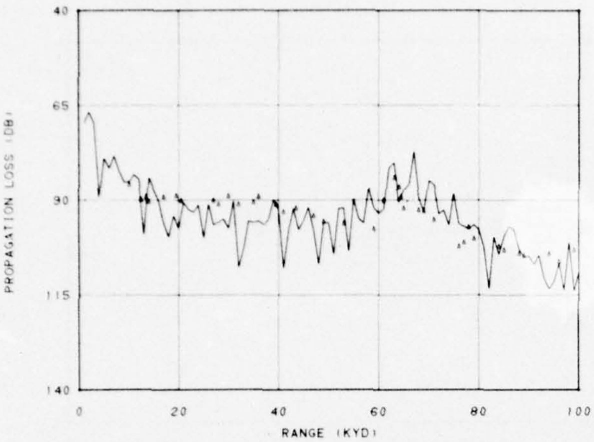

(VIII-5A) ▵ PARKA EXPERIMENTAL DATA; — RAYMODE IV MODEL (COHERENT)

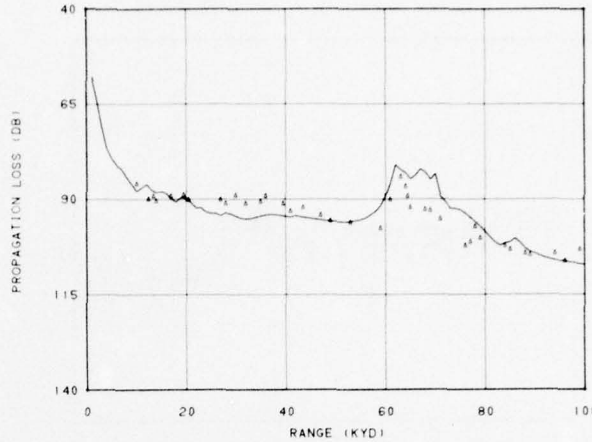

(VIII-5D) ▵ PARKA EXPERIMENTAL DATA; — RAYMODE IV MODEL (INCOHERENT)

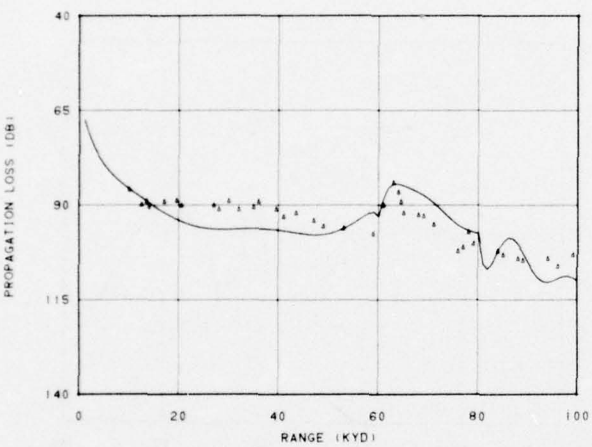

(VIII-5B) ▵ PARKA DATA; — ANALYTICAL FIT TO RAYMODE IV (COHERENT)

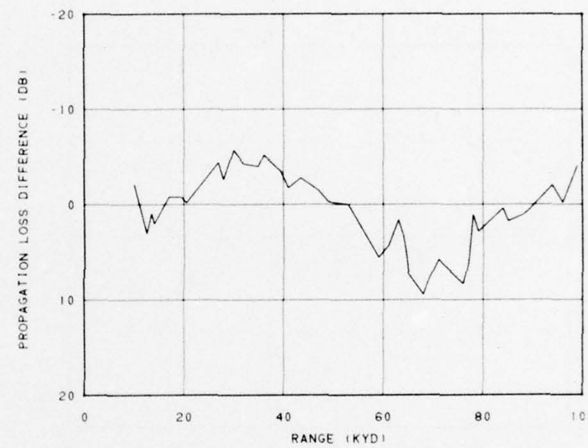

(VIII-5E) PARKA DATA MINUS RAYMODE IV (INCOHERENT)

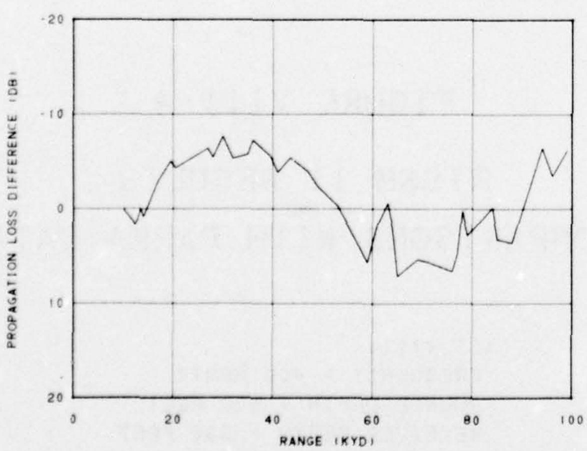

(VIII-5C) PARKA DATA MINUS RAYMODE IV (COHERENT) ANALYTICAL FIT

FIGURE VIII-5

RAYMODE IV RESULTS
AND
COMPARISONS WITH PARKA DATA

CASE VIII:
FREQUENCY = 400 HERTZ
SOURCE DEPTH = 500 FEET
RECEIVER DEPTH = 300 FEET

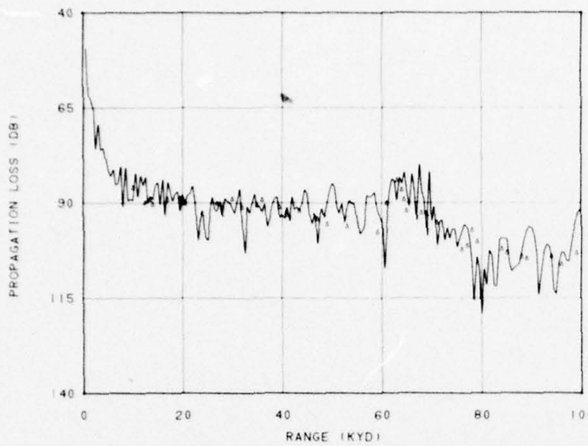

(VIII-6A) Δ PARKA EXPERIMENTAL DATA; — RAYMODE X MODEL (COHERENT)

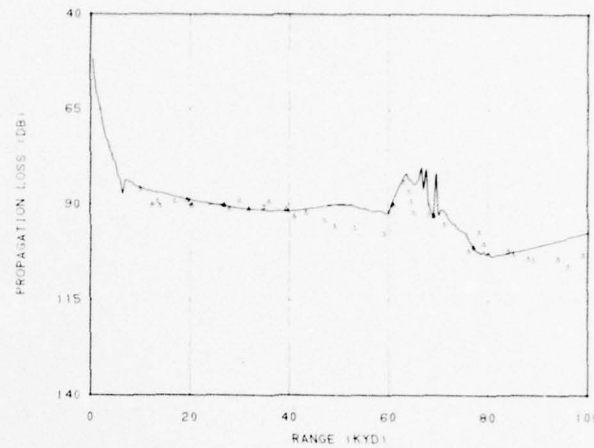

(VIII-6D) Δ PARKA EXPERIMENTAL DATA; — RAYMODE X MODEL (INCOHERENT)

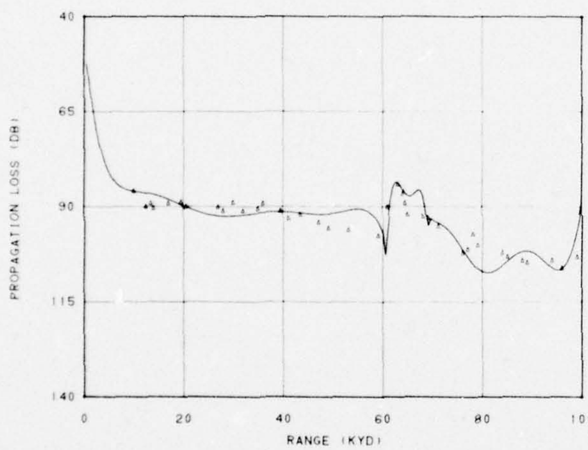

(VIII-6B) Δ PARKA DATA; — ANALYTICAL FIT TO RAYMODE X (COHERENT)

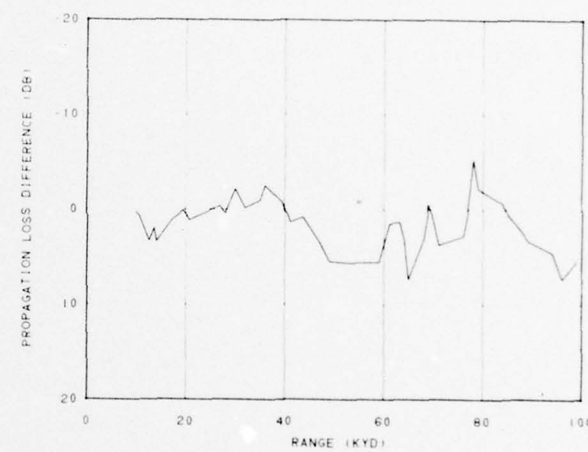

(VIII-6E) PARKA DATA MINUS RAYMODE X (INCOHERENT)

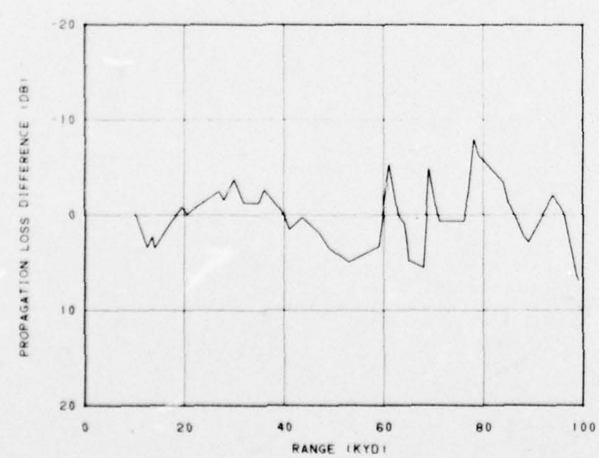

(VIII-6C) PARKA DATA MINUS RAYMODE X (COHERENT) ANALYTICAL FIT

FIGURE VIII-6

RAYMODE X RESULTS
AND
COMPARISONS WITH PARKA DATA

CASE VIII:
FREQUENCY = 400 HERTZ
SOURCE DEPTH = 500 FEET
RECEIVER DEPTH = 300 FEET

APPENDIX C

TABLES FOR USE IN QUANTITATIVE MODEL COMPARISON, ARRANGED BY CASE

Table C-1

MEANS AND STANDARD DEVIATIONS OF DIFFERENCES BETWEEN THE FFP* AND PROPAGATION LOSS MODELS: CASE 1

RANGE INTERVAL (KILOYARDS)	0-20		20-40		40-60		60-80		80-100		0-100	
	μ	σ	μ	σ	μ	σ	μ	σ	μ	σ	μ	σ
CONGRATS V COHERENT *	3.3	6.3	0.2	0.8	0.5	1.3	1.0	4.2	1.3	1.2	1.2	3.6
CONGRATS V INCOHERENT	8.0	11.2	-2.6	1.6	3.6	1.4	8.5	5.8	3.7	1.0	4.2	6.9
FACT COHERENT*	2.9	3.7	-0.4	0.6	0.0	1.1	-0.4	5.0	1.6	2.3	0.7	3.2
FACT INCOHERENT	2.8	8.4	-3.1	2.0	3.6	1.2	5.7	8.7	4.5	2.6	2.7	6.3
NISSM II COHERENT*	6.5	8.1	0.0	0.7	-0.5	1.1	-1.0	7.1	0.4	1.8	1.0	5.6
NISSM II INCOHERENT	7.3	12.6	-3.3	1.7	2.9	1.3	3.8	6.7	2.3	1.9	2.6	7.2
RAYMODE IV COHERENT*	6.3	10.8	-5.5	5.3	-6.6	3.5	6.5	3.9	-5.5	3.7	-0.9	8.5
RAYMODE IV INCOHERENT	13.9	10.7	4.8	1.4	7.6	1.6	15.5	4.1	11.7	3.6	10.7	6.7
RAYMODE X COHERENT*	4.5	7.5	0.1	0.4	-0.5	0.9	-1.1	4.7	-0.6	1.1	0.5	4.5
RAYMODE X INCOHERENT	3.5	8.9	-3.1	1.9	3.0	1.6	9.3	6.0	1.2	0.6	2.8	6.3

*AS SMOOTHED BY POLYNOMIAL FITS

TABLE C-2

MEANS AND STANDARD DEVIATIONS OF DIFFERENCES BETWEEN THE FFP* AND PROPAGATION LOSS MODELS: CASE 2

RANGE INTERVAL (KILOYARDS)	0-20		20-40		40-60		60-80		80-100		0-100	
	μ	σ	μ	σ	μ	σ	μ	σ	μ	σ	μ	σ
CONGRATS V COHERENT*	-3.4	2.5	-0.7	0.5	-1.1	0.7	-2.7	6.7	-9.9	5.0	-3.6	5.2
CONGRATS V INCOHERENT	1.0	1.3	2.8	0.8	5.5	0.8	2.4	5.9	2.0	2.5	2.7	3.3
FACT COHERENT*	1.0	1.9	-0.5	0.6	-0.9	0.9	-4.9	10.1	-11.0	3.4	-3.3	6.5
FACT INCOHERENT	1.0	1.8	-0.4	0.6	0.3	0.6	-5.9	9.0	-7.6	2.3	-2.5	5.5
NISSM II COHERENT*	-7.5	2.6	-7.7	1.6	-7.3	1.4	-7.1	9.8	-12.9	4.6	-8.5	5.5
NISSM II INCOHERENT	-6.5	3.2	-6.8	0.8	-2.5	1.4	-7.8	9.2	-9.9	2.5	-6.7	5.1
RAYMODE IV COHERENT*	2.5	3.3	0.3	1.6	4.9	3.7	4.2	6.6	-2.2	3.9	2.0	4.8
RAYMODE IV INCOHERENT	4.4	1.2	5.2	0.7	6.0	0.4	2.7	5.1	-3.0	3.3	3.1	4.2
RAYMODE X COHERENT*	1.1	2.7	4.4	0.8	7.1	0.6	4.5	5.5	4.5	2.4	4.3	3.5
RAYMODE X INCOHERENT	-0.6	1.6	2.4	0.9	5.5	0.8	2.9	5.5	2.4	2.4	2.5	3.4

*AS SMOOTHED BY POLYNOMIAL FITS

TABLE C-3

MEANS AND STANDARD DEVIATIONS OF DIFFERENCES BETWEEN THE FFP* AND PROPAGATION LOSS MODELS: CASE 3

RANGE INTERVAL (KILOYARDS)	0-20		20-40		40-60		60-80		80-100		0-100	
	μ	σ	μ	σ	μ	σ	μ	σ	μ	σ	μ	σ
CONGRATS V COHERENT*	-1.0	1.7	-0.7	0.6	0.1	0.3	-0.2	1.6	-0.1	0.3	-0.4	1.1
CONGRATS V INCOHERENT	-2.7	1.0	-3.6	0.2	-3.6	0.1	-3.0	1.8	-3.6	0.3	-3.3	1.0
FACT COHERENT*	-3.4	0.3	-3.9	0.3	-4.4	0.2	-4.1	1.9	-5.2	0.3	-4.2	1.1
FACT INCOHERENT	-3.5	0.5	-3.8	0.2	-4.3	0.2	-4.3	1.7	-5.2	0.2	-4.2	1.0
NISSM II COHERENT*	-12.7	3.7	-14.8	0.5	-12.7	0.6	-15.0	5.0	-15.1	2.0	-14.1	3.1
NISSM II INCOHERENT	-12.8	3.0	-15.0	0.2	-13.6	0.7	-14.2	4.4	-15.5	1.2	-14.2	2.6
RAYMODE IV COHERENT*	-1.7	1.5	-6.6	0.7	-9.4	3.1	-9.6	7.9	-29.6	6.0	-11.4	10.6
RAYMODE IV INCOHERENT	-0.9	1.3	-4.0	1.0	-8.3	1.4	-9.2	4.2	-23.7	3.7	-9.2	8.3
RAYMODE X COHERENT*	2.3	1.0	2.3	0.3	2.1	0.3	2.3	1.0	2.1	0.3	2.2	0.7
RAYMODE X INCOHERENT	-0.7	1.9	-0.8	1.2	-0.9	1.2	-0.5	1.4	-0.8	1.2	-0.7	1.4

*AS SMOOTHED BY POLYNOMIAL FITS

Table C-4

MEANS AND STANDARD DEVIATIONS OF DIFFERENCES BETWEEN THE FFP* AND PROPAGATION LOSS MODELS: CASE 4

RANGE INTERVAL (KILOYARDS)	0-20		20-40		40-60		60-80		80-100		0-100	
	μ	σ	μ	σ	μ	σ	μ	σ	μ	σ	μ	σ
CONGRATS V COHERENT *	1.9	1.5	0.7	1.8	2.9	4.0	0.0	6.3	0.8	1.8	1.3	3.7
CONGRATS V INCOHERENT	4.3	2.3	4.0	4.2	5.6	7.3	0.4	5.1	0.7	2.8	3.0	5.1
FACT COHERENT*	1.8	2.1	0.1	3.8	6.0	3.0	0.1	4.0	5.0	3.6	2.6	4.1
FACT INCOHERENT	3.7	2.2	4.2	4.2	6.2	6.2	0.5	4.8	1.4	3.3	3.2	4.8
NISSM II COHERENT*	0.1	0.7	-0.3	1.5	-1.9	3.9	-6.5	8.7	-0.1	2.2	-1.8	5.1
NISSM II INCOHERENT	3.0	1.8	3.6	4.3	5.1	7.0	-3.5	4.7	-1.0	4.3	1.4	5.6
RAYMODE IV COHERENT*	3.4	3.2	-4.4	3.7	-0.3	7.8	1.2	9.2	-3.4	2.6	-0.7	6.5
RAYMODE IV INCOHERENT	4.0	1.9	1.1	4.4	3.1	8.8	2.8	5.7	-2.3	1.3	1.7	5.6
RAYMODE X COHERENT*	2.3	2.1	1.0	1.5	-1.1	1.8	-2.8	5.1	-1.7	2.5	-0.5	3.4
RAYMODE X INCOHERENT	4.0	2.7	4.2	4.5	5.6	7.6	-0.1	5.3	-1.5	2.9	2.4	5.6

*AS SMOOTHED BY POLYNOMIAL FITS

Table C-5

MEANS AND STANDARD DEVIATIONS OF DIFFERENCES BETWEEN THE FFP* AND PROPAGATION LOSS MODELS: CASE 5

RANGE INTERVAL (KILOYARDS)	0-20		20-40		40-60		60-80		80-100		0-100	
	μ	σ	μ	σ	μ	σ	μ	σ	μ	σ	μ	σ
CONGRATS V COHERENT *	0.5	2.5	-0.6	1.9	0.1	3.1	-0.3	6.7	0.3	2.4	0.0	3.7
CONGRATS V INCOHERENT	1.4	1.2	1.2	0.6	1.0	1.0	0.9	5.5	2.4	3.5	1.4	3.1
FACT COHERENT*	-2.1	1.9	-4.0	5.0	-0.6	5.6	1.6	5.2	0.3	5.7	-1.0	5.2
FACT INCOHERENT	1.1	1.5	1.8	0.6	1.9	1.7	1.8	6.0	5.0	4.8	2.3	3.8
NISSM II COHERENT*	-1.0	1.2	-0.3	2.5	0.1	2.6	-5.6	9.0	-0.7	4.9	-1.5	5.3
NISSM II INCOHERENT	0.4	1.4	1.2	0.7	0.9	1.0	-2.4	7.4	1.8	3.8	0.4	4.1
RAYMODE IV COHERENT*	-0.3	3.8	-2.8	0.9	-3.1	2.8	0.6	8.1	-7.6	5.6	-2.6	5.6
RAYMODE IV INCOHERENT	1.4	1.1	-2.2	1.1	-2.4	3.3	3.6	5.6	-3.7	6.0	-0.6	4.8
RAYMODE X COHERENT*	-0.6	0.9	-0.4	0.8	-0.2	0.9	-1.7	3.9	-1.3	3.3	-0.8	2.4
RAYMODE X INCOHERENT	0.7	1.1	1.4	0.6	0.9	1.1	1.0	4.9	0.8	3.8	0.9	2.9

*AS SMOOTHED BY POLYNOMIAL FITS

Table C-6

MEANS AND STANDARD DEVIATIONS OF DIFFERENCES BETWEEN THE FFP* AND PROPAGATION LOSS MODELS: CASE 6

RANGE INTERVAL (KILOYARDS)	0-20		20-40		40-60		60-80		80-100		0-100	
	μ	σ	μ	σ	μ	σ	μ	σ	μ	σ	μ	σ
CONGRATS V COHERENT *	0.0	2.5	-0.5	1.3	0.4	1.6	-1.8	6.3	1.1	1.7	-0.2	3.4
CONGRATS V INCOHERENT	1.6	1.2	1.6	1.2	2.4	1.6	0.3	4.2	3.2	1.8	1.8	2.5
FACT COHERENT*	0.4	1.5	-2.0	2.3	0.7	3.6	0.2	3.4	2.1	4.8	0.3	3.6
FACT INCOHERENT	1.5	1.7	2.3	1.6	3.2	2.6	0.6	3.9	5.5	3.5	2.6	3.2
NISSM II COHERENT*	0.4	1.7	-3.3	2.6	0.1	3.3	-4.5	7.2	0.3	5.8	-1.4	5.0
NISSM II INCOHERENT	0.4	1.6	1.4	1.0	2.3	1.5	-3.4	6.1	2.3	2.5	0.6	3.8
RAYMODE IV COHERENT*	0.2	1.1	-5.0	3.4	-4.3	7.6	1.5	5.4	-7.1	8.3	-2.9	6.5
RAYMODE IV INCOHERENT	1.2	1.9	-1.2	1.2	-1.3	3.5	1.9	4.0	-4.4	5.5	-0.8	4.2
RAYMODE X COHERENT*	0.1	0.8	0.3	1.2	0.6	2.2	-1.6	3.4	-2.8	3.3	-0.7	2.7
RAYMODE X INCOHERENT	1.2	1.1	1.9	1.0	2.3	1.7	0.3	3.8	1.5	1.5	1.4	2.2

*AS SMOOTHED BY POLYNOMIAL FITS

Table C-7

MEANS AND STANDARD DEVIATIONS OF DIFFERENCES BETWEEN PARKA DATA AND MODEL RESULTS: CASE 7

RANGE INTERVAL (KYD)	0-20		20-40		40-60		60-80		80-100		0-100	
MEAN AND STANDARD DEVIATION (dB)	μ	σ	μ	σ	μ	σ	μ	σ	μ	σ	μ	σ
CONGRATS V COHERENT*	-2.7	3.8	-4.3	4.5	-0.1	2.6	-3.4	4.6	2.0	2.7	-1.9	4.3
CONGRATS V INCOHERENT	0.7	2.7	-1.3	1.4	2.5	3.2	-2.0	4.5	2.2	2.8	0.3	3.4
FACT COHERENT*	-2.8	2.3	-4.8	3.6	2.2	4.0	-1.8	5.1	6.8	3.2	-0.6	5.4
FACT INCOHERENT	0.4	2.5	-1.1	1.6	3.2	2.2	-2.2	4.2	3.5	2.5	0.6	3.4
FFP CW*	-3.9	1.9	-4.9	4.8	-4.1	5.1	-0.7	8.1	1.2	1.8	-2.9	5.3
FFP 1/3 - OCTAVE	-0.1	1.8	-2.5	3.4	-2.3	4.1	-0.5	6.9	0.8	1.5	-1.2	4.1
NISSM II COHERENT*	-2.5	2.3	-5.2	3.6	-8.3	7.7	-8.5	6.8	1.0	2.6	-5.0	6.0
NISSM II INCOHERENT	0.0	2.3	-1.5	1.4	1.5	3.1	-5.8	5.8	0.4	4.1	-1.0	4.1
RAYMODE IV COHERENT*	-1.1	2.7	-8.4	6.5	-3.8	5.9	-1.1	5.9	-2.3	3.2	-3.8	5.9
RAYMODE IV INCOHERENT	0.5	2.7	-3.8	1.8	0.7	6.0	0.2	3.4	-1.3	2.4	-0.9	3.9
RAYMODE X COHERENT*	-1.8	2.7	-4.2	4.6	-4.9	4.9	-4.7	6.5	-0.9	3.8	-3.5	4.7
RAYMODE X INCOHERENT	1.2	2.8	-1.1	1.5	2.6	3.9	-2.2	4.2	-0.1	2.9	0.1	3.4

*AS SMOOTHED BY POLYNOMIAL FITS

Table C-8

MEANS AND STANDARD DEVIATIONS OF DIFFERENCES BETWEEN PARKA DATA AND MODEL RESULTS: CASE 8

RANGE INTERVAL (KYD)	0-20		20-40		40-60		60-80		80-100		0-100	
MEAN AND STANDARD DEVIATION (dB)	μ	σ	μ	σ	μ	σ	μ	σ	μ	σ	μ	σ
CONGRATS V COHERENT*	0.6	2.2	-1.5	1.6	2.6	2.7	2.3	4.1	1.5	2.6	1.2	3.2
CONGRATS V INCOHERENT	1.8	1.4	-0.8	1.3	4.0	2.3	2.7	3.7	4.9	3.8	2.5	3.4
FACT COHERENT*	-0.3	1.3	-2.4	1.6	1.0	1.5	3.8	3.9	0.6	4.4	0.9	3.7
FACT INCOHERENT	2.0	1.5	-0.2	1.1	4.9	1.3	3.9	3.4	7.4	3.9	3.6	3.6
FFP CW*	0.7	1.6	-2.3	1.3	2.7	3.7	3.2	6.1	2.7	2.4	1.5	4.3
FFP 1/3 - OCTAVE	1.0	3.3	-0.8	1.4	4.0	2.8	5.3	5.0	5.2	2.9	3.1	4.2
NISSM II COHERENT*	-0.1	2.9	-3.7	2.6	0.8	5.3	-0.3	3.9	1.2	4.7	-0.5	4.1
NISSM II INCOHERENT	1.7	1.5	-0.8	1.3	3.9	2.4	0.1	5.0	4.2	4.4	1.5	3.9
RAYMODE IV COHERENT*	-0.9	2.6	-6.0	1.1	-1.7	4.0	3.8	2.5	-1.1	4.3	-0.6	4.5
RAYMODE IV INCOHERENT	0.4	2.0	-3.7	1.7	-0.1	2.9	5.3	2.7	-0.3	2.0	0.9	4.0
RAYMODE X COHERENT*	1.5	1.8	-1.7	1.2	2.6	1.7	-0.9	4.4	0.7	3.6	0.1	3.3
RAYMODE X INCOHERENT	1.7	1.5	-0.7	1.2	3.7	2.2	1.7	3.4	3.3	2.8	1.8	2.8

* AS SMOOTHED BY POLYNOMIAL FITS

Table C-9

MEANS AND STANDARD DEVIATIONS OF DIFFERENCES BETWEEN THE FFP* AND PROPAGATION LOSS MODELS: CASES 1-3

RANGE INTERVAL (KILOYARDS)	0-20		20-40		40-60		60-80		80-100		0-100	
	μ	σ	μ	σ	μ	σ	μ	σ	μ	σ	μ	σ
CONGRATS V COHERENT *	-0.4	4.9	-0.4	0.8	-0.1	1.1	-0.6	4.9	-2.9	5.8	-0.9	4.2
CONGRATS V INCOHERENT	2.1	7.9	-1.1	3.0	1.8	4.0	2.6	6.8	0.7	3.5	1.2	5.5
FACT COHERENT*	0.2	3.6	-1.6	1.7	-1.8	2.1	-3.1	6.8	-4.8	5.7	-2.2	4.7
FACT INCOHERENT	0.1	5.6	-2.4	1.9	-0.1	3.4	-1.5	8.8	-2.7	5.6	-1.3	5.7
NISSM II COHERENT*	-4.5	9.7	-7.5	6.2	-6.8	5.1	-7.7	9.4	-9.2	7.5	-7.2	7.9
NISSM II INCOHERENT	-4.0	11.4	-8.4	5.0	-4.4	7.0	-6.0	10.3	-7.7	7.7	-6.1	8.7
RAYMODE IV COHERENT*	2.4	7.3	-3.9	4.4	-3.7	7.1	0.4	9.5	-12.4	13.1	-3.5	10.1
RAYMODE IV INCOHERENT	5.8	8.7	2.0	4.4	1.8	7.3	3.0	11.1	-5.0	15.1	1.5	10.5
RAYMODE X COHERENT*	2.6	4.8	2.3	1.8	2.9	3.2	1.9	4.8	2.0	2.6	2.3	3.7
RAYMODE X INCOHERENT	0.7	5.6	-0.5	2.7	2.5	2.9	3.9	6.3	1.0	2.1	1.5	4.5

*AS SMOOTHED BY POLYNOMIAL FITS

Table C-10

MEANS AND STANDARD DEVIATIONS OF DIFFERENCES BETWEEN THE FFP* AND PROPAGATION LOSS MODELS: CASES 4-6

RANGE INTERVAL (KILOYARDS)	0-20		20-40		40-60		60-80		80-100		0-100	
	μ	σ	μ	σ	μ	σ	μ	σ	μ	σ	μ	σ
CONGRATS V COHERENT *	0.8	2.4	-0.1	1.8	1.1	3.3	-0.7	6.4	0.7	2.0	0.4	3.7
CONGRATS V INCOHERENT	2.4	2.1	2.3	2.8	3.0	4.7	0.5	4.9	2.1	3.0	2.1	3.8
FACT COHERENT*	0.0	2.4	-2.0	4.1	2.0	5.1	0.6	4.2	2.5	5.1	0.6	4.6
FACT INCOHERENT	2.1	2.1	2.8	2.8	3.8	4.4	1.0	4.9	4.0	4.3	2.7	4.0
NISSM II COHERENT*	-0.2	1.4	-1.3	2.6	-0.6	3.4	-5.5	8.3	-0.2	4.5	-1.6	5.1
NISSM II INCOHERENT	1.3	2.0	2.1	2.8	2.8	4.5	-3.1	6.1	1.0	3.8	0.8	4.6
RAYMODE IV COHERENT*	1.1	3.3	-4.0	3.1	-2.5	6.6	1.1	7.6	-6.0	6.1	-2.1	6.3
RAYMODE IV INCOHERENT	2.2	2.1	-0.8	3.0	-0.2	6.2	2.8	5.1	-3.4	4.8	0.1	5.0
RAYMODE X COHERENT*	0.6	1.9	0.3	1.3	-0.2	1.8	-2.0	4.2	-1.9	3.1	-0.7	2.9
RAYMODE X INCOHERENT	2.0	2.3	2.5	2.9	2.9	4.9	0.4	4.7	0.3	3.1	1.6	3.9

*AS SMOOTHED BY POLYNOMIAL FITS

Table C-11

MEANS AND STANDARD DEVIATIONS OF DIFFERENCES BETWEEN THE FFP* AND PROPAGATION LOSS MODELS: CASES 1-6

RANGE INTERVAL (KILOYARDS)	0-20		20-40		40-60		60-80		80-100		0-100	
	μ	σ	μ	σ	μ	σ	μ	σ	μ	σ	μ	σ
CONGRATS V COHERENT *	0.2	3.9	-0.3	1.4	0.5	2.5	-0.6	5.7	-1.1	4.7	-0.3	4.0
CONGRATS V INCOHERENT	2.3	5.8	0.6	3.4	2.4	4.4	1.6	6.0	1.4	3.3	1.6	4.7
FACT COHERENT*	0.1	3.0	-1.8	3.2	0.1	4.3	-1.3	5.9	-1.2	6.5	-0.8	4.9
FACT INCOHERENT	1.1	4.3	0.2	3.5	1.8	4.3	-0.3	7.2	0.6	6.0	0.7	5.3
NISSM II COHERENT*	-2.4	7.3	-4.4	5.7	-3.7	5.4	-6.6	8.9	-4.7	7.7	-4.4	7.2
NISSM II INCOHERENT	-1.4	8.6	-3.1	6.6	-0.8	6.9	-4.6	8.5	-3.3	7.5	-2.7	7.8
RAYMODE IV COHERENT*	1.7	5.7	-4.0	3.8	-3.1	6.9	0.7	8.6	-9.2	10.7	-2.8	8.4
RAYMODE IV INCOHERENT	4.0	6.6	0.6	4.0	0.8	6.8	2.9	8.6	-4.2	11.2	0.8	8.3
RAYMODE X COHERENT*	1.6	3.8	1.3	1.9	1.3	3.0	-0.1	4.9	0.1	3.5	0.8	3.6
RAYMODE X INCOHERENT	1.4	4.4	1.0	3.2	2.7	4.0	2.1	5.8	0.6	2.7	1.6	4.2

*AS SMOOTHED BY POLYNOMIAL FITS

Table C-12

MEANS AND STANDARD DEVIATIONS OF DIFFERENCES BETWEEN PARKA DATA AND MODEL RESULTS: CASES 7-8

RANGE INTERVAL (KYD)	0-20		20-40		40-60		60-80		80-100		0-100	
MEAN AND STANDARD DEVIATION (dB)	μ	σ	μ	σ	μ	σ	μ	σ	μ	σ	μ	σ
CONGRATS V COHERENT*	-1.3	3.5	-3.2	3.8	0.9	2.9	0.0	5.1	1.7	2.5	-0.5	4.1
CONGRATS V INCOHERENT	1.2	2.2	-1.1	1.4	3.1	2.9	0.9	4.6	3 6	3.5	1.3	3.5
FACT COHERENT*	-1.8	2.3	-3.8	3.1	1.7	3.3	1.5	5.2	3.7	4.9	0.1	4.7
FACT INCOHERENT	1.1	2.2	-0.8	1.5	3.8	2.1	1.5	4.8	5.4	3.7	2.0	3.8
FFP CW*	-1.9	2.9	-3.9	4.0	-1.5	5.6	1.6	7.1	2.0	2.2	-0.8	5.3
FFP 1/3 - OCTAVE	0.4	2.5	-1.8	2.9	0.0	4.8	2.9	6.4	3.0	3.1	0.8	4.6
NISSM II COHERENT*	-1.5	2.8	-4.6	3.3	-4.9	8.1	-3.6	6.6	1.1	3.7	-2.9	5.7
NISSM II INCOHERENT	0.7	2.1	-1.2	1.4	2.4	3.0	-2.3	5.9	2.3	4.5	0.1	4.2
RAYMODE IV COHERENT*	-1.0	2.5	-7.4	5.1	-3.0	5.2	1.8	4.7	-1.7	3.7	-2.3	5.5
RAYMODE IV INCOHERENT	0.5	2.3	-3.7	1.7	0.4	5.0	3.2	3.9	-0.8	2.2	-0.1	4.0
RAYMODE X COHERENT*	-0.4	2.9	-3.2	3.8	-2.1	5.4	-2.4	5.5	-0.1	3.6	-1.8	4.5
RAYMODE X INCOHERENT	1.4	2.3	-0.9	1.4	3.0	3.3	0.1	4.1	1.6	3.2	0.9	3.3

*AS SMOOTHED BY POLYNOMIAL FITS

TABLE C-13. SUMS OF THE WEIGHTS* CORRESPONDING TO MEANS AND STANDARD DEVIATIONS** OF DIFFERENCES BETWEEN SMOOTHED FFP AND MODEL RESULTS

	A					B					C				
	CASE 1					CASE 2					CASE 3				
RANGE INTERVAL (KILOYARDS)	0-20	20-40	40-60	60-80	80-100	0-20	20-40	40-60	60-80	80-100	0-20	20-40	40-60	60-80	80-100
CONGRATS V COHERENT	5	2	2	3	2	3	2	2	4	6	2	2	2	2	2
CONGRAT V INCOHERENT	7	2	3	5	3	2	2	3	3	2	2	3	3	3	3
FACT COHERENT	3	2	2	3	2	2	2	2	6	6	3	3	3	3	3
FACT INCOHERENT	4	3	3	5	3	2	2	2	6	4	3	3	3	3	3
NISSM II COHERENT	6	2	2	4	2	4	4	4	7	7	7	6	6	7	6
NISSM II INCOHERENT	8	3	2	5	3	5	4	2	7	5	7	6	6	7	6
RAYMODE IV COHERENT	7	4	5	5	4	3	2	4	5	3	2	4	6	7	8
RAYMODE IV INCOHERENT	9	3	4	7	6	3	3	4	3	4	2	3	4	6	7
RAYMODE X COHERENT	5	2	2	3	2	2	3	4	4	3	2	2	2	2	2
RAYMODE X INCOHERENT	5	3	3	7	2	2	2	3	3	2	2	2	2	2	2

* AS DEFINED IN TABLE 7

** AS GIVEN IN TABLES C-1 THROUGH C-3

TABLE C-13. SUMS OF THE WEIGHTS* CORRESPONDING TO MEANS AND STANDARD DEVIATIONS** OF DIFFERENCES BETWEEN SMOOTHED FFP AND MODEL RESULTS (CONT'D)

	D					E					F				
	CASE 4					CASE 5					CASE 6				
RANGE INTERVAL (KILOYARDS)	0-20-	20-40	40-60	60-80	80-100	0-20	20-40	40-60	60-80	80-100	0-20	20-40	40-60	60-80	80-100
CONGRATS V COHERENT	2	2	3	3	2	2	2	3	4	2	2	2	2	4	2
CONGRAT V INCOHERENT	3	4	5	3	2	2	2	2	3	3	2	2	2	3	3
FACT COHERENT	2	3	4	3	4	2	4	3	3	3	2	2	3	3	3
FACT INCOHERENT	3	4	6	3	3	2	2	2	4	4	2	2	3	3	4
NISSM II COHERENT	2	2	3	5	2	2	2	2	6	3	2	3	3	5	3
NISSM II INCOHERENT	3	4	5	4	3	2	2	2	4	3	2	2	2	5	2
RAYMODE IV COHERENT	4	4	4	5	3	3	2	3	4	5	2	4	5	3	6
RAYMODE IV INCOHERENT	3	3	5	3	2	2	2	3	4	5	2	2	3	3	4
RAYMODE X COHERENT	2	2	2	3	2	2	2	2	3	3	2	2	2	3	3
RAYMODE X INCOHERENT	3	4	5	3	2	2	2	2	3	3	2	2	2	3	2

* AS DEFINED IN TABLE 7

** AS GIVEN IN TABLES C-4 THROUGH C-6

TABLE C-14. SUMS OF THE WEIGHTS* CORRESPONDING TO MEANS AND STANDARD DEVIATIONS** OF DIFFERENCES BETWEEN PARKA DATA AND MODEL RESULTS

	A					B				
	CASE 7					CASE 8				
RANGE INTERVAL (KILOYARDS)	0-20	20-40	40-60	60-80	80-100	0-20	20-40	40-60	60-80	80-100
CONGRATS V COHERENT	3	4	2	4	2	2	2	2	3	2
CONGRATS V INCOHERENT	2	2	3	3	2	2	2	3	3	4
FACT COHERENT	2	4	3	3	5	2	2	2	4	3
FACT COHERENT	2	2	3	3	3	2	2	3	4	5
FFP CW	3	4	4	4	2	2	2	3	5	2
FFP 1/3 - OCTAVE	2	3	3	4	2	3	2	3	4	3
NISSM II COHERENT	2	4	6	6	2	2	3	3	3	3
NISSM II INCOHERENT	2	2	3	4	3	2	2	3	3	4
RAYMODE IV COHERENT	2	6	4	3	3	2	4	3	3	3
RAYMODE IV INCOHERENT	2	3	4	3	2	2	3	2	3	2
RAYMODE X COHERENT	2	4	4	5	3	2	2	2	3	3
RAYMODE X INCOHERENT	2	2	3	3	2	2	2	3	3	3

* AS DEFINED IN TABLE 7

** AS GIVEN IN TABLES C-7 and C-8

APPENDIX D

TABLES OF μ'S AND σ'S OF DIFFERENCES BETWEEN A STANDARD AND THE MODELS, ARRANGED BY MODEL

TABLE D1-A

MEANS AND STANDARD DEVIATIONS OF DIFFERENCES
BETWEEN THE STANDARD* AND CONGRATS V (COHERENT)

RANGE INTERVAL (KILOYARDS)	0-20		20-40		40-60		60-80		80-100		0-100	
CASE	μ	σ	μ	σ	μ	σ	μ	σ	μ	σ	μ	σ
1	3.3	6.3	0.2	0.8	0.5	1.3	1.0	4.2	1.3	1.2	1.2	3.6
2	-3.4	2.5	-0.7	0.5	-1.1	0.7	-2.7	6.7	-9.9	5.0	-3.6	5.2
3	-1.0	1.7	-0.7	0.6	0.1	0.3	-0.2	1.6	-0.1	0.3	-0.4	1.1
4	1.9	1.5	0.7	1.8	2.9	4.0	0.0	6.3	0.8	1.8	1.3	3.7
5	0.5	2.5	-0.6	1.9	0.1	3.1	-0.3	6.7	0.3	2.4	0.0	3.7
6	0.0	2.5	-0.5	1.3	0.4	1.6	-1.8	6.3	1.1	1.7	-0.2	3.4
7	-2.7	3.8	-4.3	4.5	-0.1	2.6	-3.4	4.6	2.0	2.7	-1.9	4.3
8	0.6	2.2	-1.5	1.6	2.6	2.7	2.3	4.1	1.5	2.6	1.2	3.2
1-3	-0.4	4.9	-0.4	0.8	-0.1	1.1	-0.6	4.9	-2.9	5.8	-0.9	4.2
4-6	0.8	2.4	-0.1	1.8	1.1	3.3	-0.7	6.4	0.7	2.0	0.4	3.7
1-6	0.2	3.9	-0.3	1.4	0.5	2.5	-0.6	5.7	-1.1	4.7	-0.3	4.0
7-8	-1.3	3.5	-3.2	3.8	0.9	2.9	0.0	5.1	1.7	2.5	-0.5	4.1

* Smoothed FFP for cases 1-6; PARKA data for cases 7-8

TABLE D1-B

MEANS AND STANDARD DEVIATIONS OF DIFFERENCES
BETWEEN THE STANDARD* AND CONGRATS V (INCOHERENT)

RANGE INTERVAL (KILOYARDS)	0-20		20-40		40-60		60-80		80-100		0-100	
CASE	μ	σ	μ	σ	μ	σ	μ	σ	μ	σ	μ	σ
1	8.0	11.2	-2.6	1.6	3.6	1.4	8.5	5.8	3.7	1.0	4.2	6.9
2	1.0	1.3	2.8	0.8	5.5	0.8	2.4	5.9	2.0	2.5	2.7	3.3
3	-2.7	1.0	-3.6	0.2	-3.6	0.1	-3.0	1.8	-3.6	0.3	-3.3	1.0
4	4.3	2.3	4.0	4.2	5.6	7.3	0.4	5.1	0.7	2.8	3.0	5.1
5	1.4	1.2	1.2	0.6	1.0	1.0	0.9	5.5	2.4	3.5	1.4	3.1
6	1.6	1.2	1.6	1.2	2.4	1.6	0.3	4.2	3.2	1.8	1.8	2.5
7	0.7	2.7	-1.3	1.4	2.5	3.2	-2.0	4.5	2.2	2.8	0.3	3.4
8	1.8	1.4	-0.8	1.3	4.0	2.3	2.7	3.7	4.9	3.8	2.5	3.4
1-3	2.1	7.9	-1.1	3.0	1.8	4.0	2.6	6.8	0.7	3.5	1.2	5.5
4-6	2.4	2.1	2.3	2.8	3.0	4.7	0.5	4.9	2.1	3.0	2.1	3.8
1-6	2.3	5.8	0.6	3.4	2.4	4.4	1.6	6.0	1.4	3.3	1.6	4.7
7-8	1.2	2.2	-1.1	1.4	3.1	2.9	0.9	4.6	3.6	3.5	1.3	3.5

* Smoothed FFP for cases 1-6; PARKA data for cases 7-8

TABLE D2-A

MEANS AND STANDARD DEVIATIONS OF DIFFERENCES BETWEEN THE STANDARD* AND FACT (COHERENT)

RANGE INTERVAL (KILOYARDS)	0-20		20-40		40-60		60-80		80-100		0-100	
CASE	μ	σ	μ	σ	μ	σ	μ	σ	μ	σ	μ	σ
1	2.9	3.7	-0.4	0.6	0.0	1.1	-0.4	5.0	1.6	2.3	0.7	3.2
2	1.0	1.9	-0.5	0.6	-0.9	0.9	-4.9	10.1	-11.0	3.4	-3.3	6.5
3	-3.4	0.3	-3.9	0.3	-4.4	0.2	-4.1	1.9	-5.2	0.3	-4.2	1.1
4	1.8	2.1	0.1	3.8	6.0	3.0	0.1	4.0	5.0	3.6	2.6	4.1
5	-2.1	1.9	-4.0	5.0	-0.6	5.6	1.6	5.2	0.3	5.7	-1.0	5.2
6	0.4	1.5	-2.0	2.3	0.7	3.6	0.2	3.4	2.1	4.8	0.3	3.6
7	-2.8	2.3	-4.8	3.6	2.2	4.0	-1.8	5.1	6.8	3.2	-0.6	5.4
8	-0.3	1.3	-2.4	1.6	1.0	1.5	3.8	3.9	0.6	4.4	0.9	3.7
1-3	0.2	3.6	-1.6	1.7	-1.8	2.1	-3.1	6.8	-4.8	5.7	-2.2	4.7
4-6	0.0	2.4	-2.0	4.1	2.0	5.1	0.6	4.2	2.5	5.1	0.6	4.6
1-6	0.1	3.0	-1.8	3.2	0.1	4.3	-1.3	5.9	-1.2	6.5	-0.8	4.9
7-8	-1.8	2.3	-3.8	3.1	1.7	3.3	1.5	5.2	3.7	4.9	0.1	4.7

* Smoothed FFP for cases 1-6; PARKA data for cases 7-8

TABLE D2-B

MEANS AND STANDARD DEVIATIONS OF DIFFERENCES
BETWEEN THE STANDARD* AND FACT (INCOHERENT)

RANGE INTERVAL (KILOYARDS)	0-20		20-40		40-60		60-80		80-100		0-100	
CASE	μ	σ	μ	σ	μ	σ	μ	σ	μ	σ	μ	σ
1	2.8	8.4	-3.1	2.0	3.6	1.2	5.7	8.7	4.5	2.6	2.7	6.3
2	1.0	1.8	-0.4	0.6	0.3	0.6	-5.9	9.0	-7.6	2.3	-2.5	5.5
3	-3.5	0.5	-3.8	0.2	-4.3	0.2	-4.3	1.7	-5.2	0.2	-4.2	1.0
4	3.7	2.2	4.2	4.2	6.2	6.2	0.5	4.8	1.4	3.3	3.2	4.8
5	1.1	1.5	1.8	0.6	1.9	1.7	1.8	6.0	5.0	4.8	2.3	3.8
6	1.5	1.7	2.3	1.6	3.2	2.6	0.6	3.9	5.5	3.5	2.6	3.2
7	0.4	2.5	-1.1	1.6	3.2	2.2	-2.2	4.2	3.5	2.5	0.6	3.4
8	2.0	1.5	-0.2	1.1	4.9	1.3	3.9	3.4	7.4	3.9	3.6	3.6
1-3	0.1	5.6	-2.4	1.9	-0.1	3.4	-1.5	8.8	-2.7	5.6	-1.3	5.7
4-6	2.1	2.1	2.8	2.8	3.8	4.4	1.0	4.9	4.0	4.3	2.7	4.0
1-6	1.1	4.3	0.2	3.5	1.8	4.3	-0.3	7.2	0.6	6.0	0.7	5.3
7-8	1.1	2.2	-0.8	1.5	3.8	2.1	1.5	4.8	5.4	3.7	2.0	3.8

* Smoothed FFP for cases 1-6; PARKA data for cases 7-8

TABLE D3-A

MEANS AND STANDARD DEVIATIONS OF DIFFERENCES BETWEEN THE STANDARD* AND FFP (CW)

RANGE INTERVAL (KILOYARDS)	0-20		20-40		40-60		60-80		80-100		0-100	
CASE	μ	σ	μ	σ	μ	σ	μ	σ	μ	σ	μ	σ
1	-	-	-	-	-	-	-	-	-	-	-	-
2	-	-	-	-	-	-	-	-	-	-	-	-
3	-	-	-	-	-	-	-	-	-	-	-	-
4	-	-	-	-	-	-	-	-	-	-	-	-
5	-	-	-	-	-	-	-	-	-	-	-	-
6	-	-	-	-	-	-	-	-	-	-	-	-
7	-3.9	1.9	-4.9	4.8	-4.1	5.1	-0.7	8.1	1.2	1.8	-2.9	5.3
8	0.7	1.6	-2.3	1.3	2.7	3.7	3.2	6.1	2.7	2.4	1.5	4.3
1-3	-	-	-	-	-	-	-	-	-	-	-	-
4-6	-	-	-	-	-	-	-	-	-	-	-	-
1-6	-	-	-	-	-	-	-	-	-	-	-	-
7-8	-1.9	2.9	-3.9	4.0	-1.5	5.6	1.6	7.1	2.0	2.2	-0.8	5.3

* Smoothed FFP for cases 1-6; PARKA data for cases 7-8

TABLE D3-B

MEANS AND STANDARD DEVIATIONS OF DIFFERENCES BETWEEN THE STANDARD* AND FFP (1/3-OCTAVE)

RANGE INTERVAL (KILOYARDS)	0-20		20-40		40-60		60-80		80-100		0-100	
CASE	μ	σ	μ	σ	μ	σ	μ	σ	μ	σ	μ	σ
1	-	-	-	-	-	-	-	-	-	-	-	-
2	-	-	-	-	-	-	-	-	-	-	-	-
3	-	-	-	-	-	-	-	-	-	-	-	-
4	-	-	-	-	-	-	-	-	-	-	-	-
5	-	-	-	-	-	-	-	-	-	-	-	-
6	-	-	-	-	-	-	-	-	-	-	-	-
7	-0.1	1.8	-2.5	3.4	-2.3	4.1	-0.5	6.9	0.8	1.5	-1.2	4.1
8	1.0	3.3	-0.8	1.4	4.0	2.8	5.3	5.0	5.2	2.9	3.1	4.2
1-3	-	-	-	-	-	-	-	-	-	-	-	-
4-6	-	-	-	-	-	-	-	-	-	-	-	-
1-6	-	-	-	-	-	-	-	-	-	-	-	-
7-8	0.4	2.5	-1.8	2.9	0.0	4.8	2.9	6.4	3.0	3.1	0.8	4.6

* Smoothed FFP for cases 1-6; PARKA data for cases 7-8

TABLE D4-A

MEANS AND STANDARD DEVIATIONS OF DIFFERENCES
BETWEEN THE STANDARD* AND NISSM II (COHERENT)

RANGE INTERVAL (KILOYARDS)	0-20		20-40		40-60		60-80		80-100		0-100	
CASE	μ	σ	μ	σ	μ	σ	μ	σ	μ	σ	μ	σ
1	6.5	8.1	0.0	0.7	-0.5	1.1	-1.0	7.1	0.4	1.8	1.0	5.6
2	-7.5	2.6	-7.7	1.6	-7.3	1.4	-7.1	9.8	-12.9	4.6	-8.5	5.5
3	-12.7	3.7	-14.8	0.5	-12.7	0.6	-15.0	5.0	-15.1	2.0	-14.1	3.1
4	0.1	0.7	-0.3	1.5	-1.9	3.9	-6.5	8.7	-0.1	2.2	-1.8	5.1
5	-1.0	1.2	-0.3	2.5	0.1	2.6	-5.6	9.0	-0.7	4.9	-1.5	5.3
6	0.4	1.7	-3.3	2.6	0.1	3.3	-4.5	7.2	0.3	5.8	-1.4	5.0
7	-2.5	2.3	-5.2	3.6	-8.3	7.7	-8.5	6.8	1.0	2.6	-5.0	6.0
8	-0.1	2.9	-3.7	2.6	0.8	5.3	-0.3	3.9	1.2	4.7	-0.5	4.1
1-3	-4.5	9.7	-7.5	6.2	-6.8	5.1	-7.7	9.4	-9.2	7.5	-7.2	7.9
4-6	-0.2	1.4	-1.3	2.6	-0.6	3.4	-5.5	8.3	-0.2	4.5	-1.6	5.1
1-6	-2.4	7.3	-4.4	5.7	-3.7	5.4	-6.6	8.9	-4.7	7.7	-4.4	7.2
7-8	-1.5	2.8	-4.6	3.3	-4.9	8.1	-3.6	6.6	1.1	3.7	-2.9	5.7

* Smoothed FFP for cases 1-6; PARKA data for cases 7-8

TABLE D4-B

MEANS AND STANDARD DEVIATIONS OF DIFFERENCES BETWEEN THE STANDARD* AND NISSM II (INCOHERENT)

RANGE INTERVAL (KILOYARDS)	0-20		20-40		40-60		60-80		80-100		0-100	
CASE	μ	σ	μ	σ	μ	σ	μ	σ	μ	σ	μ	σ
1	7.3	12.6	-3.3	1.7	2.9	1.3	3.8	6.7	2.3	1.9	2.6	7.2
2	-6.5	3.2	-6.8	0.8	-2.5	1.4	-7.8	9.2	-9.9	2.5	-6.7	5.1
3	-12.8	3.0	-15.0	0.2	-13.6	0.7	-14.2	4.4	-15.5	1.2	-14.2	2.6
4	3.0	1.8	3.6	4.3	5.1	7.0	-3.5	4.7	-1.0	4.3	1.4	5.6
5	0.4	1.4	1.2	0.7	0.9	1.0	-2.4	7.4	1.8	3.8	0.4	4.1
6	0.4	1.6	1.4	1.0	2.3	1.5	-3.4	6.1	2.3	2.5	0.6	3.8
7	0.0	2.3	-1.5	1.4	1.5	3.1	-5.8	5.8	0.4	4.1	-1.0	4.1
8	1.7	1.5	-0.8	1.3	3.9	2.4	0.1	5.0	4.2	4.4	1.5	3.9
1-3	-4.0	11.4	-8.4	5.0	-4.4	7.0	-6.0	10.3	-7.7	7.7	-6.1	8.7
4-6	1.3	2.0	2.1	2.8	2.8	4.5	-3.1	6.1	1.0	3.8	0.8	4.6
1-6	-1.4	8.6	-3.1	6.6	-0.8	6.9	-4.6	8.5	-3.3	7.5	-2.7	7.8
7-8	0.7	2.1	-1.2	1.4	2.4	3.0	-2.3	5.9	2.3	4.5	0.1	4.2

* Smoothed FFP for cases 1-6; PARKA data for cases 7-8

TABLE D5-A

MEANS AND STANDARD DEVIATIONS OF DIFFERENCES
BETWEEN THE STANDARD* AND RAYMODE IV (COHERENT)

RANGE INTERVAL (KILOYARDS)	0-20		20-40		40-60		60-80		80-100		0-100	
CASE	μ	σ	μ	σ	μ	σ	μ	σ	μ	σ	μ	σ
1	6.3	10.8	-5.5	5.3	-6.6	3.5	6.5	3.9	-5.5	3.7	-0.9	8.5
2	2.5	3.3	0.3	1.6	4.9	3.7	4.2	6.6	-2.2	3.9	2.0	4.8
3	-1.7	1.5	-6.6	0.7	-9.4	3.1	-9.6	7.9	-29.6	6.0	-11.4	10.6
4	3.4	3.2	-4.4	3.7	-0.3	7.8	1.2	9.2	-3.4	2.6	-0.7	6.5
5	-0.3	3.8	-2.8	0.9	-3.1	2.8	0.6	8.1	-7.6	5.6	-2.6	5.6
6	0.2	1.1	-5.0	3.4	-4.3	7.6	1.5	5.4	-7.1	8.3	-2.9	6.5
7	-1.1	2.7	-8.4	6.5	-3.8	5.9	-1.1	5.9	-2.3	3.2	-3.8	5.9
8	-0.9	2.6	-6.0	1.1	-1.7	4.0	3.8	2.5	-1.1	4.3	-0.6	4.5
1-3	2.4	7.3	-3.9	4.4	-3.7	7.1	0.4	9.5	-12.4	13.1	-3.5	10.1
4-6	1.1	3.3	-4.0	3.1	-2.5	6.6	1.1	7.6	-6.0	6.1	-2.1	6.3
1-6	1.7	5.7	-4.0	3.8	-3.1	6.9	0.7	8.6	-9.2	10.7	-2.8	8.4
7-8	-1.0	2.5	-7.4	5.1	-3.0	5.2	1.8	4.7	-1.7	3.7	-2.3	5.5

* Smoothed FFP for cases 1-6; PARKA data for cases 7-8

TABLE D5-B

MEANS AND STANDARD DEVIATIONS OF DIFFERENCES BETWEEN THE STANDARD* AND RAYMODE IV (INCOHERENT)

RANGE INTERVAL (KILOYARDS)	0-20		20-40		40-60		60-80		80-100		0-100	
CASE	μ	σ	μ	σ	μ	σ	μ	σ	μ	σ	μ	σ
1	13.9	10.7	4.8	1.4	7.6	1.6	15.5	4.1	11.7	3.6	10.7	6.7
2	4.4	1.2	5.2	0.7	6.0	0.4	2.7	5.1	-3.0	3.3	3.1	4.2
3	-0.9	1.3	-4.0	1.0	-8.3	1.4	-9.2	4.2	-23.7	3.7	-9.2	8.3
4	4.0	1.9	1.1	4.4	3.1	8.8	2.8	5.7	-2.3	1.3	1.7	5.6
5	1.4	1.1	-2.2	1.1	-2.4	3.3	3.6	5.6	-3.7	6.0	-0.6	4.8
6	1.2	1.9	-1.2	1.2	-1.3	3.5	1.9	4.0	-4.4	5.5	-0.8	4.2
7	0.5	2.7	-3.8	1.8	0.7	6.0	0.2	3.4	-1.3	2.4	-0.9	3.9
8	0.4	2.0	-3.7	1.7	-0.1	2.9	5.3	2.7	-0.3	2.0	0.9	4.0
1-3	5.8	8.7	2.0	4.4	1.8	7.3	3.0	11.1	-5.0	15.1	1.5	10.5
4-6	2.2	2.1	-0.8	3.0	-0.2	6.2	2.8	5.1	-3.4	4.8	0.1	5.0
1-6	4.0	6.6	0.6	4.0	0.8	6.8	2.9	8.6	-4.2	11.2	0.8	8.3
7-8	0.5	2.3	-3.7	1.7	0.4	5.0	3.2	3.9	-0.8	2.2	-0.1	4.0

* Smoothed FFP for cases 1-6; PARKA data for cases 7-8

TABLE D6-A

MEANS AND STANDARD DEVIATIONS OF DIFFERENCES BETWEEN THE STANDARD* AND RAYMODE X (COHERENT)

RANGE INTERVAL (KILOYARDS)	0-20		20-40		40-60		60-80		80-100		0-100	
CASE	μ	σ	μ	σ	μ	σ	μ	σ	μ	σ	μ	σ
1	4.5	7.5	0.1	0.4	-0.5	0.9	-1.1	4.7	-0.6	1.1	0.5	4.5
2	1.1	2.7	4.4	0.8	7.1	0.6	4.5	5.5	4.5	2.4	4.3	3.5
3	2.3	1.0	2.3	0.3	2.1	0.3	2.3	1.0	2.1	0.3	2.2	0.7
4	2.3	2.1	1.0	1.5	-1.1	1.8	-2.8	5.1	-1.7	2.5	-0.5	3.4
5	-0.6	0.9	-0.4	0.8	-0.2	0.9	-1.7	3.9	-1.3	3.3	-0.8	2.4
6	0.1	0.8	0.3	1.2	0.6	2.2	-1.6	3.4	-2.8	3.3	-0.7	2.7
7	-1.8	2.7	-4.2	4.6	-4.9	4.9	-4.7	6.5	-0.9	3.8	-3.5	4.7
8	1.5	1.8	-1.7	1.2	2.6	1.7	-0.9	4.4	0.7	3.6	0.1	3.3
1-3	2.6	4.8	2.3	1.8	2.9	3.2	1.9	4.8	2.0	2.6	2.3	3.7
4-6	0.6	1.9	0.3	1.3	-0.2	1.8	-2.0	4.2	-1.9	3.1	-0.7	2.9
1-6	1.6	3.8	1.3	1.9	1.3	3.0	-0.1	4.9	0.1	3.5	0.8	3.6
7-8	-0.4	2.9	-3.2	3.8	-2.1	5.4	-2.4	5.5	-0.1	3.6	-1.8	4.5

* Smoothed FFP for cases 1-6; PARKA data for cases 7-8

TABLE D6-B

MEANS AND STANDARD DEVIATIONS OF DIFFERENCES
BETWEEN THE STANDARD* AND RAYMODE X (INCOHERENT)

RANGE INTERVAL (KILOYARDS)	0-20		20-40		40-60		60-80		80-100		0-100	
CASE	μ	σ	μ	σ	μ	σ	μ	σ	μ	σ	μ	σ
1	3.5	8.9	-3.1	1.9	3.0	1.6	9.3	6.0	1.2	0.6	2.8	6.3
2	-0.6	1.6	2.4	0.9	5.5	0.8	2.9	5.5	2.4	2.4	2.5	3.4
3	-0.7	1.9	-0.8	1.2	-0.9	1.2	-0.5	1.4	-0.8	1.2	-0.7	1.4
4	4.0	2.7	4.2	4.5	5.6	7.6	-0.1	5.3	-1.5	2.9	2.4	5.6
5	0.7	1.1	1.4	0.6	0.9	1.1	1.0	4.9	0.8	3.8	0.9	2.9
6	1.2	1.1	1.9	1.0	2.3	1.7	0.3	3.8	1.5	1.5	1.4	2.2
7	1.2	2.8	-1.1	1.5	2.6	3.9	-2.2	4.2	-0.1	2.9	0.1	3.4
8	1.7	1.5	-0.7	1.2	3.7	2.2	1.7	3.4	3.3	2.8	1.8	2.8
1-3	0.7	5.6	-0.5	2.7	2.5	2.9	3.9	6.3	1.0	2.1	1.5	4.5
4-6	2.0	2.3	2.5	2.9	2.9	4.9	0.4	4.7	0.3	3.1	1.6	3.9
1-6	1.4	4.4	1.0	3.2	2.7	4.0	2.1	5.8	0.6	2.7	1.6	4.2
7-8	1.4	2.3	-0.9	1.4	3.0	3.3	0.1	4.1	1.6	3.2	0.9	3.3

* Smoothed FFP cases for 1-6; PARKA data for cases 7-8

Appendix E

Current POSSM Membership

The NAVSEA Panel on Sonar System Models (POSSM) is under the general sponsorship of NAVSEA 06H1-4. POSSM functions as a subsidiary of the Mobile Sonar Technology (MOST) Sonar Analysis Committee (SAC) for NAVSEA 06H1. Requests for additional information pertaining to POSSM activities should be directed to any of the following current POSSM members.

Executive Secretary

A. P. Franceschetti, SEA 06H1-4
Naval Sea Systems Command
Washington, D. C. 20362

Commercial (202) 692-3166
Autovon 222-3166

Chairman

F. R. DiNapoli, Code 3123
Naval Underwater Systems Center
New London, CT 06320

Commercial (203) 442-0771, Ext. 2647
Autovon 636-2647

Naval Underwater Systems Center

Commercial (203) 442-0771
Autovon 636-XXXX

H. Weinberg, Code 314, Ext. 2589
H. Newman, Code 315, Ext. 2122
R. Lauer, Code 3123, Ext. 2827

Naval Undersea Center

San Diego, California 92132

Commercial (714) 225-2316
Autovon 933-2316

A. DiLoreto, Code 014, Ext. 2544
R. McGirr, Code 30, Ext. 6501
E. Chaika, Code 304, Ext. 2316

Naval Research Laboratory

Washington, D. C. 20375

Commercial (202) 767-3210
Autovon 297-3210

W. A. Kuperman, Code 8120

Naval Ocean Research and Development Activity

Naval Oceanographic Office
Naval Research Laboratory
4555 Overlook Ave., SW
Washington, D. C. 20375

Commercial (202) 767-2830
Autovon 297-2830

K. V. Mackenzie, Code 9420

Naval Coastal Systems Laboratory

Panama City, Florida 30401

Commercial (904) 234-4366
Autovon 436-4366

T. Watson, Code 732

Arthur D. Little, Inc.

25 Acorn Park
Cambridge, MA 02140

Commercial (617) 864-5770, Ext. 3068

G. E. Miller

Official Mailing Addresses

1. Commanding Officer
Naval Underwater Systems Center
New London, CT 06320

2. Commander
Naval Undersea Center
San Diego, CA 92132

3. Director
Naval Research Laboratory
Washington, D. C. 20375

4. Commander
   Naval Oceanographic Office
   Washington, D. C. 20373

5. Commanding Officer
   Naval Coastal Systems Laboratory
   Panama City, FL 30401

6. Commander
   Naval Sea Systems Command
   Washington, D. C. 20362

INITIAL DISTRIBUTION LIST

Addressee	No. of Copies
ASN(R&D)	1
DDR&E (Environmental and Life Sciences), (Library), (WSEG)	3
CNO (OP-095, -098, -224, -32, -321, -322, -966 (Systems Analysis Division), -981)	8
CNM (MAT-014, -03, -03L, -03T, -030, -031, -0314, -032, -033, -034, -0345, -SP15, PM-1, -4, -200)	15
NAVAIRSYSCOMHQ (NAIR-03, -370, -5330, -604)	4
NAVELECSYSCOMHQ (NELEX-03, -320, PME-124, -124TA)	4
NAVFACENGCOMHQ (NFAC-03)	1
NAVSEASYSCOMHQ (SEA-03B, -03E, -37, -06H, -06H2, -06H1-4, -660G-31, -660G (Cornette, Klisch), -660F-5, PMS-392, -395, -06H1 (per transmittal to National Leaders of TTCP Panel G-TP-9 Australia, New Zealand, United Kingdom, and Canada)	17
ONR (ONR-411, -102-OS, -105, -221, -412, -461, -468, -480, -485, 486 (Bezdek), -AESD)	11
Commander, Air Test and Evaluation Squadron 1 (VX 1)	1
Commander, Oceanographic Development Squadron 8 (VXN 8)	1
Antisubmarine Warfare Systems Project Office (ASW-10, -11, -12, -13, -14, -15)	6
ASW Tactical School, Atlantic Fleet (Library)	1
CINCLANTFLT	1
COMCRUDESLANT	1
COMCRUDESPAC (Code 425)	1
Commander, Destroyer Development Group, Atlantic (Scientific Advisory Team)	1
Fleet ASW School	1
Fleet Numerical Weather Central	1
Fleet Sonar School	1
Naval War College	1
Naval Weapons Center (Code 753)	1
Oceanographer of the Navy	1
COMOPTEVFOR, Atlantic	1
DEPCOMOPTEVFOR, Pacific	1
COMNLONTEVDET	1
CINCPACFLT	1
COMSUBDEVGRUONE	6
COMSUBDEVGRUTWO (Mr. J. Seaton)	3
COMSUBGRU TWO	1
COMSUBLANT	1
COMSUBPAC	1
COMTRALANT	1
COMTRAPAC	1
DDC, Alexandria	12
ARPA	1
U. S. Coast Guard Headquarters, Office of R&D	1
U. S. Coast Guard R&D Center, Groton	1
U. S. Coast Guard Academy, New London	1

INITIAL DISTRIBUTION LIST (Cont'd)

Addressee	No. of Copies
Armed Forces Staff College (Administrative Command)	1
National Academy of Sciences, National Research Council, Committee on Undersea Warfare (Executive Secretary)	1
National Oceanic and Atmospheric Administration	1
National Oceanographic Data Center	1
APL/UW, Seattle	1
ARL/UT (J. Bardin), (G. Bernard), (A. Anderson)	3
ARL/PENN State	1
Atlantic Environmental Group, NMFS	1
Oregon State University, Department of Oceanography	1
Woods Hole Oceanographic Institution	1
AFSPCOMMCEN/SUR, San Antonio, TX 78243	1
British Embassy, Department SCD, Rm 104 (Miss A. P. King)	1
University of Florida (P. Graycar)	1
Library of Congress, Major Issues System	1
Marine Physical Laboratory, University of California, Scripps Institution of Oceanography	1
Johns Hopkins University	1
Texas A & M University	1
University of Miami	1
University of North Carolina	1
University of Rhode Island	1
Gulf Universities Research Consortium	1
NORDA (Code 22) (Dr. R. D. Gaul)	1
TRACOR Inc. (R. Urick)	1
Defence Research Establishment Atlantic (Canada) (H. Merlinger)	1
Defence Research Establishment Pacific (Canada) (D. Thomson)	1
SACLANT ASW Research Centre (J. Jensen) (G. C. Vittori)	2
The Director, Weapons Research Establishment, Australia (G. Gartrell)	2
The Director, Royal Australian Navy Research Laboratory, Australia	1
Fleet Training Center, Newport	1
COMKWESTEVDET	1
NAVAIRDEVCEN, Code 205 (C. Bartbetger)	1
Naval Academy	1
CIVENGRLAB, P. Hueneme	1
NAVCOASTSYSLAB, Panama City (Library, Code 100, 732 (T. Watson), 740, 741)	5
NELC (Library)	1
Naval Missile Center (Library)	1
NAVOCEANO (Library), (Code 00, 02, 3000, 3400, 3410, 3420, 3430, 3440, 5400, 5420, 6100, 6130, 6152)	14
NAVSURFWPNCEN (Library), (Code 050, 221, 730, 880, WR14 (I. Blatstein), WU22 (M. Stripling))	7
Naval Personnel and Training Research Laboratory, San Diego (Library)	1
NAVPGSCOL, Monterey (Library)	1
NRL, (Library, Code 8000, 8100, 8109 (R. Rollins), 8120 (W. Kuperman) (2), 8167 (J. Cybulski), 8170, 8400, 8700, 9420 (K. MacKenzie))	11

INITIAL DISTRIBUTION LIST (Cont'd)

Addressee	No. of Copies
NAVSEC (Code 6034, 6141, 6178C.03)	3
DTNSRDC (Library, Code 194, 731)	3
Naval Space Systems Activity	1
NAVTORPSTA (Library, Code 5122)	2
NAVTRAEQUIPCEN (Code 02)	1
NAVUSEACEN, San Diego (Library, Code 00, 01, 014 (A. DiLoreto), 02, 05, 23, 30 (R. McGirr), 304 (D. Chaika, D. Gordon, L. Arndt, J. Stewart), 307 (3)	15